Fluctuations in a melt of flexible polymers with bond-directed dipolar monomers

by

Henry Emmanuel Amuasi

Thesis presented in partial fulfilment of the

requirements for the degree of MASTER OF SCIENCE

at the University of Stellenbosch.

Supervisor: Dr. K. Müller-Nedebock

October 2006

DECLARATION

I, the undersigned, hereby declare that the work contained in this thesis is my own original work and that I have not previously in its entirety or in part submitted it at any university for a degree.

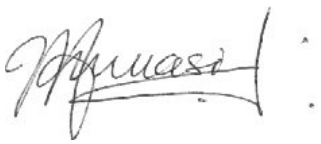

SIGNATURE

4^{th} October, 2006.

DATE

ABSTRACT

We employ the Random Phase Approximation (RPA) method to compute the static density and magnetic structure functions of a melt of flexible polymers whose monomers possess bond-directed dipoles which interact with each other. In order to observe the effect of screening of the dipolar interaction on the structure functions we obtain results for cases with and without steric interactions and also for cases with and without Debye-Hückel screening of the dipole moments. We show that in all these cases the system exhibits criticality at the same critical Bjerrum length, $\lambda_{B*} = 9e_0^2/\left(4\pi\rho_0 c^2 l^2\right)$ where ρ_0 is the monomer concentration, l is the Kuhn length, and c is the ratio of the dipole moment to the length of the bond that constrains it. We also show that in the unscreened cases the dipole-dipole structure function is fairly constant diverging at the critical temperature and over all length scales, whereas with screening the dipole-dipole structure function exhibits a narrow peak at large length scales and a broad peak at length scales comparable to a few Kuhn lengths. Near the critical temperature the dipole-dipole structure function remains finite for all length scales of interest except for a narrow band in the vicinity of the Kuhn length. On the other hand, the density structure function remains finite at all temperatures in both the unscreened and screened cases, but it rather shows a depression in a narrow band in the vicinity of the Kuhn length.

OPSOMMING

Ons gebruik die metode van die toevalsfase-benadering ("Random Phase Approximation" RPA) om die statiese digtheids- en magnetiese struktuurfunksies te bereken vir 'n smelt van hoogsbuigsame polimere, waarvan die monomere dipole langs die verbindings besit wat met mekaar in wisselwerking tree. Om die effek van afskerming op die dipolare wisselwerking en die struktuurfunksies te kan waarneem, bepaal ons resultate vir die gevalle met en sonder steriese wisselwerkings en ook vir gevalle met en sonder die Debye-Hückel afskerming van die dipoolmomente. Ons wys dat in al hierdie gevalle die stelsel kritieke gedrag by dieselfde kritieke Bjerrum-lengte $\lambda_{B*} = 9e_0^2/\left(4\pi\rho_0 c^2 l^2\right)$ toon, waar ρ_0 die monomeerkonsentrasie, l die Kuhn-lengte en c die verhouding van die dipoolmoment tot die lengte van die verbinding is wat dit beperk. Ons wys ook dat, in die onafgeskermde gevalle, die dipool-dipool struktuurfunksie min-of-meer konstant is en by die kritieke temperatuur oor alle lengteskale divergeer; inteenstelling, met afskerming, toon die dipool-dipool struktuurfunksie 'n nou piek by groot lengteskale en 'n wye piek by lengteskale wat met 'n paar Kuhn-lengtes vergelykbaar is. Naby die kritieke temperatuur bly die dipool-dipool struktuurfunksie vir alle lengteskale van belang eindig behalwe vir 'n nou band in die omgewing van die Kuhn-lengte. Andersins bly die digtheidsstruktuurfunksie by alle temperature eindig in beide die onafgeskermde en afgeskermde gevalle, maar dit toon 'n afname in nou band in die omgewing van die Kuhn-lengte.

CONTENTS

1. INTRODUCTION

The purpose of this chapter is to take the reader through a quick tour of the theory of polymers as found in literature published since the latter half of the last century. The treatise here touches only on those aspects of the literature that are essential to understanding the problem at hand and appreciating the solution presented in the subsequent chapters. The aspects of the literature alluded to in this chapter cover the description of polymers and polymer melts, the mathematical models used to abstract them, and the statistical theories used to investigate them. Next, the chapter devotes a section to describing ferrogels and how they motivate the problem that this thesis is concerned with. The last section gives a general layout of the content of the following chapters.

1.1 Polymer Chains and Melts

A polymer is a high molecular weight organic compound (a *macromolecule*), natural or man-made, consisting of many repeating simpler chemical units, or molecules, called *monomers*. Examples of polymers include polyethylene, polystyrene, and poly(oxyethylene). During its fabrication, a polymer molecule is formed when the energy required to add one more chemical unit (monomer) to the macromolecule is almost independent of the size of the macromolecule.

Now consider a closely packed assembly of these polymer molecules. At a sufficiently high temperature, they are in a high state of thermal agitation and form a liquid, called a *polymer melt*. Alternatively, if these polymers are dissolved in another liquid (called a *solvent*) then we have a *polymer solution*. Polymers play a central role in chemical technology and biology. In the latter half of the twenty-first century it has become possible to offer theories which explain the salient features of polymer melts. Our work is concerned with the equilibrium properties of a special type of a polymer melt which we describe in Section 1.6.

The geometry of different polymers can be quite diverse. The simplest geometry that a polymer can possess is that of a line. But by means of branching (see Ref. [1]), polymer molecules can be synthesized with the geometry of stars, combs, tree-like structures, or even cross-linked network structures (see Figure 1.1). In our work we consider polymers with linear geometry called *polymer chains*. The number of monomers, N, in one polymer chain is often called the *index* or *degree of polymerization* of the chain and can be amazingly large. (For example, it is possible to reach $N > 10^5$ with polystyrene.)

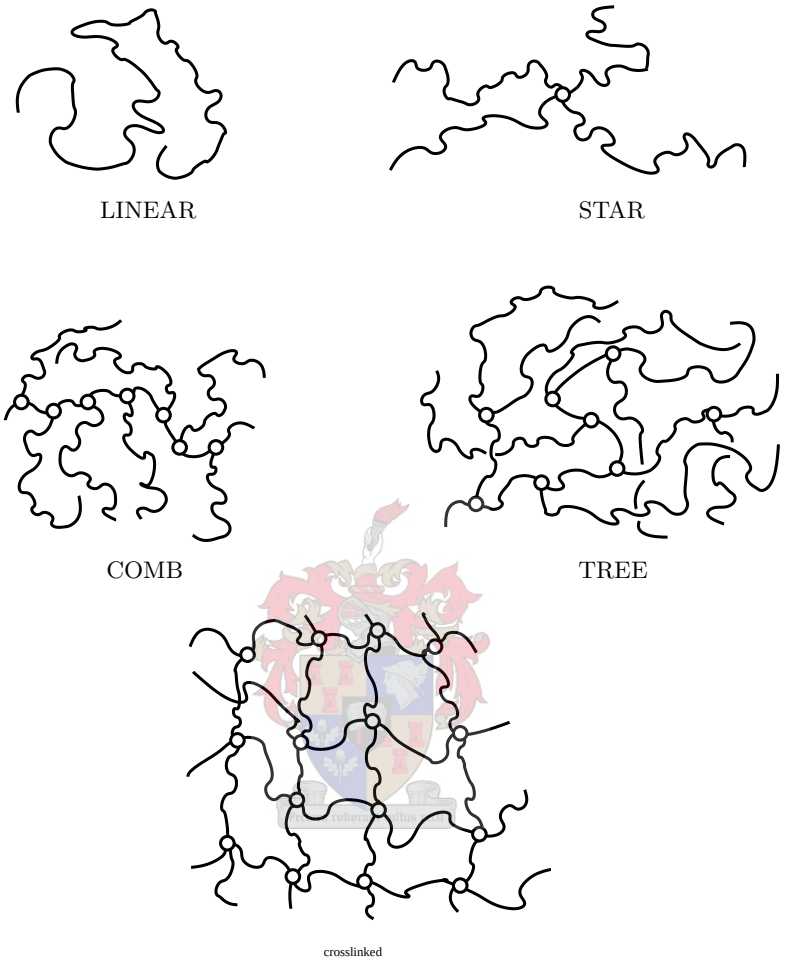

Fig. 1.1: The various geometrical structures that polymer molecules can have.

Quite a number of polymer chain variants are possible. There are two extreme cases: *flexible polymer chains* and *rigid rods* (see Figure 1.2). Flexible chains are characterized by being easily bent and being highly coiled. Rigid rods are straight and cannot be easily bent. There exist intermediate cases synonymously known as *semiflexible*, *semirigid*, or *stiff* polymer chains.

Flexible polymer Rigid polymer

Fig. 1.2: Flexible and rigid polymers.

1.2 Polymer Chain Models: Flexibility

To study the statistical properties of polymer chains, one needs to use a suitable mathematical model to represent a single chain. Many synthetic and biological processable polymers, particularly DNA, are semirigid and have been described in literature [2, 3, 4, 5, 6, 7, 8] using the so-called *wormlike polymer chain model*.

In the wormlike polymer chain model, the polymer chain backbone is abstracted as an (at least) twice-differentiable geometric curve $\mathbf{R}(s)$ in space. This curve is of finite length L and is parametrized by its arc length s. The tangent vector to this curve at a point s on the curve is constructed as $\dot{\mathbf{R}}(s) = \mathrm{d}\mathbf{R}(s)/\mathrm{d}s$ and can be shown to be always of unit length (the reason being that the variable parameterizing the curve is the arc length s itself), this is known as the condition of *local inextensibility*. The crucial feature of the wormlike polymer chain model, however, is that the Hamiltonian of the polymer chain is a functional $H[\mathbf{R}(s)]$ built on the assumption that it costs energy to bend the polymer chain (since it is semirigid). If the tangent vector is constant along the curve then it does not bend. Thus the energy should depend on the derivatives of the unit tangent vector $\dot{\mathbf{R}}(s)$. We call the the magnitude of $\ddot{\mathbf{R}}(s) = \mathrm{d}\dot{\mathbf{R}}(s)/\mathrm{d}s$ the *curvature* of the curve. The bending energy is also taken to be directly proportional to the temperature T, so that the Boltzmann factor $e^{-\beta H[\mathbf{R}(s)]}$ (where $\beta = 1/k_B T$, k_B being the Boltzmann constant) is temperature independent:

$$H[\mathbf{R}(s)] = \frac{\varepsilon}{2} \int_0^L \mathrm{d}s \big[\ddot{\mathbf{R}}(s)\big]^2. \tag{1.1}$$

Hence the partition function for a stiff polymer chain at constant temperature is a functional integral given by

$$\mathscr{Z} = \int \mathscr{D}\big[\dot{\mathbf{R}}(s)\big]\, e^{-\beta H[\mathbf{R}(s)]}\, \delta^3\big[\big(\dot{\mathbf{R}}(s)\big)^2 - 1\big], \tag{1.2}$$

where the integral should be understood as being taken over all chain conformations specified by $\dot{\mathbf{R}}$. Note that the delta function in the integrand embodies the

constraint of local inextensibility. It can be shown (see Ref. [2]) that at a sufficiently large length scale, that is, at a scale of the order of the *persistence length parameter*, $l_p = \beta\varepsilon$, the wormlike polymer chain behaves as a random walk. One advantage of the wormlike polymer chain model is that by varying the persistence length parameter between the limits $l_p \ll L$ and $l_p \gg L$, one may easily scuttle between the extreme limits of flexibility and rigidity respectively. The above model is solvable in principle, but it has been noted [3] that in practice the mathematical difficulties associated with equations governing the states of the wormlike polymer chain model can be formidable. Therefore the wormlike polymer chain model is often considered with auxiliary simplifying assumptions and approximations, such as relaxing the constraint of local inextensibility for instance (see Refs. [3, 7]).

Although a fully realistic theory of polymer solutions will involve considerable technical complexity in such matters as the precise flexibility of the molecular linkages and the molecular forces, and the nature of the interaction of the molecules with those of the solvent, there remain a core of general functional relationships in, for example the equation of state [9], which can be reduced to problems which are easily posed, but which can only be resolved by fairly powerful mathematical tools. In this dissertation it is hoped to derive the skeleton theory in which the dependence of the thermodynamic functions upon the parameters specifying the solution will be demonstrated. For this reason, we avoid the use of the wormlike polymer chain model altogether and employ the discrete version of Edwards' Hamiltonian [10], a Hamiltonian which has proven to be a useful and simpler tool in the study of diverse polymer problems [11, 12, 13, 14]. Edwards' Hamiltonian is, nevertheless, better suited to highly flexible polymer chains. We defer the full description of this model until Section 2.3. It suffices for now to say that in this model, the polymer is abstracted as essentially a discrete random walk in space.

1.3 Long Range Interactions

Note that in the preceding discussion on single chain models we implicitly limited interactions among monomers to within a few neighbours along the chain. It is these interactions that are responsible for the flexibility (or rigidity) of the chain. In reality, however, monomers distant along the chain do interact if they come close to each other in space (see Figure 1.3). Following Doi and Edwards [10], we use the term '*long range interactions*' to refer to interactions between monomers which are far apart along the chain. This term is used in contrast to '*short range interactions*' which represents the interaction among a few neighbouring monomers and is responsible for the local structure of the polymer chain.

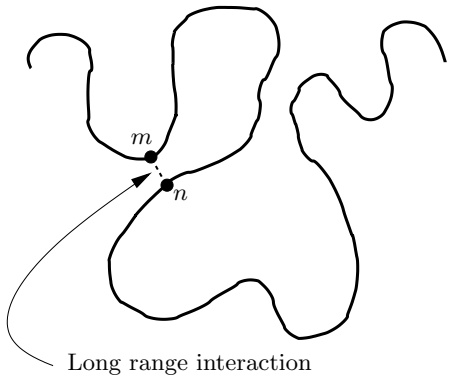

Fig. 1.3: Long range interactions (for example the excluded volume interactions) are those interactions that occur between monomers that are far apart along the polymer chain. Note that the term 'long' represents the distance along the chain not the spatial separation

An obvious long range interaction is the *steric effect*: since the monomer has finite volume, other monomers cannot come into its own region. This interaction is non-trivial and reveals itself in the *swelling* of the polymer; the coil size of a polymer chain with such an interaction is significantly larger than that of the *ideal* chain which has no such interaction. This effect is known as the *excluded volume effect* [15].

The type of polymer chains which we deal with in this dissertation consists of monomers which also possess dipole moments. Consequently, another long range interaction appears: the *dipolar interactions*. This interaction is fully described in Section 2.3.

In polymer melts, or solutions, interactions also exist between different polymers. These inter-polymer interactions are comprised of those interactions (also classified as long range interactions) between monomers on different polymer chains. In the second chapter of this dissertation we investigate the flexible chain model with such dipolar interactions included but without the excluded volume effect, and in the third chapter we include the excluded volume interactions.

1.4 Classification of Polymer solutions

A polymer melt may most generally be described as a system of a large number, say N_p, of polymer chains assembled together in a finite region of space of volume Ω. If this space is also mediated by a liquid (called a solvent), then we have a *polymer solution*. Naturally such systems, because of the large number of particles (the monomers) constituting its polymer chains, lend themselves to useful study by means of equilibrium statistical methods. Edwards [9, 10] in 1966, put forward a simple description of such systems, classifying them

into three broad regimes determined by the parameters of the solution: N the number of monomers per polymer chain (also called the *index of polymerization*), N_p the number of polymer chains, l the effective length of a polymer bond, v the *excluded volume per monomer* which may also be viewed as the effective volume per monomer (the definition of v is given in Section 3.4), and Ω the total volume. The regimes Edwards identified are the (a) dilute, (b) semidilute, and (c) concentrated regimes of polymer solutions.

A dilute solution is defined as one of sufficiently low concentration that the polymer chains are separated from one another; each polymer on the average occupying a spherical region of radius R_g (called the *radius of gyration*). Now if we assume each polymer chain to be a random walk of N steps, then $R_g \sim \sqrt{N}l$ and this regime may be described by the following relation:

$$\left(\sqrt{N}\, l\right)^3 \ll \Omega/N_p. \tag{1.3}$$

A dilute solution is characterized by a small mean density (or concentration) of monomers NN_p/Ω and by large spatial fluctuations localized over regions of size comparable to that of a polymer chain. These fluctuations are illustrated in Figure 1.4. In such solutions the polymer–polymer interaction is very small.

As the concentration of polymers is increased (that is as N_p is increased) we enter the semidilute solution regime in which

$$\left(\sqrt{N}\, l\right)^3 \gtrsim \Omega/N_p. \tag{1.4}$$

In this regime, though the mean concentration of polymers, N_p/Ω, (or their volume fraction NN_pv/Ω) is still small, the polymer chains are long enough (Nl large) to cause strong overlapping among themselves. A semidilute solution is characterized by a mean density with large and strongly correlated spatial fluctuations in the local monomer concentration as illustrated in Figure 1.4.

A concentrated solution is one of sufficiently high concentration that

$$\Omega/N\, N_p \leq v. \tag{1.5}$$

In this case, the mean concentration of monomers becomes large, and the fluctuations become small compared to the mean concentration of monomers (as illustrated in Figure 1.4). Hence this regime becomes amenable to treatment by a mean field theory including small spatial fluctuations (up to quadratic order approximation). This mean field theory is variously known as the *Random Phase Approximation* (RPA) or the *Gaussian Approximation*. Such is the nature of our concerns in this dissertation.

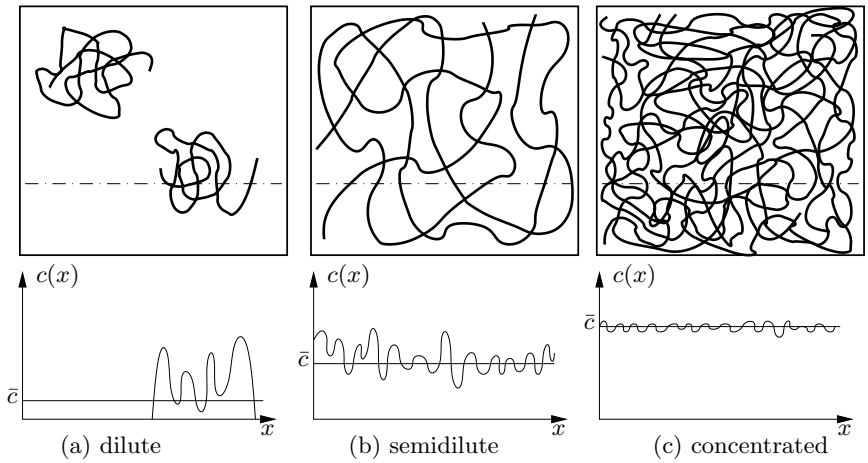

Fig. 1.4: Three concentration regimes of polymer solutions. $c(x)$ denotes the concentration profile along the dot-dashed lines.

1.5 The Random Phase Approximation

It was de Gennes [16] who pointed out that the mean-field theory is rather good for high molecular mass (large N) polymer melts, in contrast to low molecular mass polymer melts, for which the mean-field theory breaks down close to the critical point. His argument was based on the *Ginzburg criterion* [14, 16, 17, 18] which states that the mean-field approach is quantitatively correct if the fluctuations of the monomer concentration are small compared to the mean concentration near the critical point. He found that for large N the mean-field theory breaks down very close to the critical temperature T_c, that is for $(T - T_c)/T_c \sim 1/N$. Thus in the limit of $N \to \infty$, the mean-field theory is correct in the whole region around the critical point.

The random phase approximation is a term that has been used to describe various approaches to calculating the fluctuations in the mean field theory of polymers. Some authors [4] derive the theory by applying a special form of the fluctuation-dissipation theorem [17] in which the fluctuations of the local concentration field of monomers, $\langle \delta\rho(\mathbf{r}) \rangle = \langle \rho(\mathbf{r}) - \rho_0 \rangle$ (or some other chosen order parameter such as the local magnetization field $\mathbf{u}(\mathbf{r})$), may be written using two different expressions. In the first relation, $\langle \delta\rho(\mathbf{r}) \rangle$ is written as being modified in response to a spatially-varying external field, $h(\mathbf{r})$, plus a spatially-varying molecular field, $w_m(\mathbf{r})$, written in the mean field approximation and representing the mean interaction of all the other monomers in the system with any single monomer:

$$\langle \delta\rho(\mathbf{r}) \rangle = -\int \mathrm{d}^3 r \, \chi_0(r, r')[h(\mathbf{r}) + w_m(\mathbf{r})], \tag{1.6}$$

where

$$w_m(\mathbf{r}) = -\int \mathrm{d}^3 r\, w(r,\, r')\langle\rho(\mathbf{r})\rangle \;=\; -\int \mathrm{d}^3 r\, w(r,\, r')\langle\delta\rho(\mathbf{r}) + \rho_0\rangle, \tag{1.7}$$

and $w(r,\, r')$ represents the interaction potential between the monomers. The fluctuation-dissipation theorem then states that the response function, $\chi_0(r,\, r')$, of such a relation is directly proportional to the density-density pair correlation function, $\langle\delta\rho(\mathbf{r})\,\delta\rho(\mathbf{r}')\rangle_0$ of non-interacting polymers, which can be readily computed. In the second relation, $\langle\delta\rho(\mathbf{r})\rangle$ is written as being modified in response to the spatially-varying external field, $h(\mathbf{r})$ alone:

$$\langle\delta\rho(\mathbf{r})\rangle = -\int \mathrm{d}^3 r\, \chi(r,\, r')\, h(\mathbf{r}), \tag{1.8}$$

and hence the response function, $\chi(r,\, r')$, in such a relation is directly proportional the true density-density pair correlation function, $\langle\delta\rho(\mathbf{r})\,\delta\rho(\mathbf{r}')\rangle$, of the melt. Thus these two equations ((1.6) and (1.8)) are equated and the resulting integral equation is solved self-consistently for the true response function (or density-density correlation function) of the melt. In our work, however, we do not employ this method.

Our approach to the RPA instead employs a Gaussian approximation in which an attempt is made to obtain a Hamiltonian written as a functional of the order parameter $\rho(\mathbf{r})$ the local density field (or $\mathbf{u}(\mathbf{r})$ the local magnetization field). Technically, one is able to do so successfully only up to quadratic order in these parameters. Vilgis, Weyersberg, Jarkova, and Brereton [12, 11] also employ this method. However, unlike Vilgis and Jarkova [13], we do not approximate the dipolar interaction by an approximate short-range function, but we apply the exact unscreened dipolar interaction [19] (see equation (2.13)) between pairs of dipoles. We later also apply Debye-Hückel [17] screening to the dipolar interaction.

One surprising result of our calculations for the density fluctuations for the unscreened case is that we do not observe any of the usual indications of microdomain structure as put forward by Leibler [20], that is, the density structure function obtained does not show any peaks or singularities anywhere within the domain of length scales comparable to the length scale of the size of a polymer (the radius of gyration R_g). Neither does the density structure function indicate a phase transition at any temperature. However, our investigations into the magnetization fluctuations made us to rediscover the fluctuation-induced long-range orientational correlations mentioned by Vilgis, Weyersberg and Brereton [11]. These correlations appear to increase over all length scales as the temperature is lowered towards a certain critical temperature where the isotropic phase breaks down. This temperature also signals the breakdown of the Gaussian approximation.

1.6 Introducing the Problem: Ferrogels and Polyelectrolytes

In this work, we consider in particular the fluctuations in a concentrated polymer melt of fixed volume at a constant temperature, and whose polymer chains are made up of dipolar monomers whose dipole moments are constrained to lie along the polymer chain backbone; all dipoles on a polymer having the same sense of direction along the chain. The description of such a polymer is illustrated in Figure 2.3 on page 25. Thus the monomers interact with each other via the dipolar potential energy of interaction. We investigate not only fluctuations of the local monomer concentration field (or density order parameter), but also the fluctuations of the local dipole moment vector field (or magnetization order parameter).

The reader may wonder why we investigate a melt of this peculiar type of polymer. There are at least two reasons. One reason is that this type of polymer melt is a very simplified model that has been proposed in recent literature [13] as a first attempt to understand the thermodynamic properties of magnetic field sensitive polymer gels called *ferrogels*. The other reason is because this model can be understood as a limit of certain polyampholytes [21], which are polymers in solution with alternating charges distributed along their backbone. Recently both ferrogels and polyelectrolytes have been of considerable research interest because of their various applications in soft matter physics.

1.6.1 Ferrogels

A ferrogel is a chemically cross-linked polymer network swollen by (or dissolved in) a ferrofluid [22, 23, 24, 25]. A ferrofluid, or a magnetic fluid, is a colloidal dispersion of monodomain magnetic particles. Their typical size is about 10 nm and they have superparamagnetic[1]behaviour. In the ferrogel, the finely distributed magnetic particles are located in the swelling liquid and attached to the crosslinked network chains by adhesive forces. These solid particles of colloidal size are the elementary carriers of a magnetic moment. In the absence of an applied magnetic field the moments are randomly oriented, and thus the gel has no net magnetization. As soon as an external field is applied, the magnetic moments tend to align with the field to produce a bulk magnetic moment. With ordinary field strengths, the tendency of the dipole moments to align with the applied field is partially overcome by thermal agitation, such as the molecules of a paramagnetic gas. As the strength of the magnetic field increases, all the particles eventually align their moments along the direction of the field, and as a result, the magnetization saturates. If the field is turned off, the magnetic dipole

[1] Superparamagnetism occurs when the material is composed of very small crystallites (1-10 nm). In this case, even though the temperature is below the Curie or Neel temperature and the thermal energy is not sufficient to overcome the coupling forces between neighboring atoms, the thermal energy is sufficient to change the direction of magnetization of the entire crystallite. The resulting fluctuations in the direction of magnetization cause the magnetic field to average to zero. The material behaves in a manner similar to paramagnetism, except that instead of each individual atom being independently influenced by an external magnetic field, the magnetic moment of the entire crystallite tends to align with the magnetic field.

moments quickly randomize and thus the bulk magnetization is again reduced to zero. In a zero magnetic field a ferrogel presents a mechanical behaviour very close to that of a swollen network filled with non-magnetic colloidal particles.

Some ferrogels belong to a larger class of adaptive (smart, intelligent) materials called *polymer gels* [26]. These materials can actuate, or alter their properties in response to a changing environment. Among them mechanical actuators have been the subject of much investigation in recent years. They undergo a controllable change of shape due to some external physical effects and can convert energy (electrical, thermal, chemical) directly to mechanical energy. This can be used to do work against load.

Certain polymer gels represent one class of actuators that have the unique ability to change elastic and swelling properties in a reversible manner. These wet and soft materials offer lifelike capabilities for the future direction of technological development. Volume phase transition in response to infinitesimal change of external stimuli like pH, temperature, solvent composition, electric field, and light has been observed in various gels. Their application in devices such as actuators, controlled delivery systems, sensors, separators and artificial muscles has been suggested and are in progress.

Attempts at developing stimuli-responsive gels for technological purposes are complicated by the fact that structural changes, like shape and swelling degree changes that occur, are kinetically restricted by the collective diffusion of chains and the friction between the polymer network and the swelling agent. This disadvantage often hinders the effort of designing optimal gels for different applications. In order to accelerate the response of an adaptive gel to stimuli, the use of magnetic field sensitive gels as a new type of actuator has been developed [24]. Magnetic field sensitive gels, or as we call them "ferrogels", are typical representatives of smart materials.

Naturally, a theory for ferrogels is very difficult and suffers from many different length scales. The development of a single theory that takes into account all the aspects of ferrogels seems to be too difficult. Therefore we aim here for a much simpler model, which might not be capable of describing the experimental results in detail, but give first hints of methods and solutions. Following Vilgis and Jarkova [13] we assume that the magnetic moments are placed along the contour of the chains. In the light of the foregoing discussion, this assumption seems to be rather unrealistic. Nevertheless it enables some calculations to be performed and the prediction of results for polymer melts that involve magnetic interactions. Therefore we assume that each monomer carries a dipole moment whose main axis points in the direction of the tangent vector. This assumption is made only to ease calculations. The magnetic particles couple somehow to the polymer chains but no one so far has resolved this mechanism.

We also neglect the cross-links between polymer chains thus releasing the chains to move freely with respect to each other. This situation is completely changed when the chains are crossed-linked to each other to form a network. The cross-links restrict the chain motion significantly and the phase depends naturally on the cross-linking state. (See Ref. [13] for a treatment of both the uncross-linked case and the cross-links using quenched variables.)

Our point of departure from the work of Vilgis and Jarkova [13] is that we utilize the exact expression for the dipolar interaction between a pair of dipoles $\mathbf{p}_1$ and $\mathbf{p}_2$ separated by a vector $\mathbf{r}$:

$$U(\mathbf{p}_1, \mathbf{p}_2, \mathbf{r}) = \frac{\lambda_B}{\beta}\left(\frac{\mathbf{p}_1 \cdot \mathbf{p}_2 - 3\,(\hat{\mathbf{r}} \cdot \mathbf{p}_1)\,(\hat{\mathbf{r}} \cdot \mathbf{p}_2)}{|\mathbf{r}|^3}\right), \tag{1.9}$$

instead of the short-ranged isotropic function given as an approximation to the expression above

$$U'(\mathbf{p}_1, \mathbf{p}_2, \mathbf{r}) = J_0\delta(\mathbf{r})\mathbf{p}_1 \cdot \mathbf{p}_2, \tag{1.10}$$

where J_0 is a constant. Our reasons for investigating the true form of the dipolar function are that, as Zhang and Widom [27, 28] have pointed out, two characteristics of dipoles lead to unusual difficulties in analyzing these systems: long range and anisotropy. The r^{-3} falloff leads to conditional convergence of the local field due to a distribution of dipoles at remote locations. The anisotropy in the numerator of equation (1.9) leads to frustration in aligning favourably with nearby dipoles.

1.6.2 Polyelectrolytes

Polyelectrolytes may widely be defined as highly charged macromolecules or aggregates formed in aqueous solution by dissociation of charged units of these macromolecules. Many important biological macromolecules are polyelectrolytes. The most important example is DNA and RNA molecules, which dissociate in solution forming a strongly negatively charged polyion surrounded by atmosphere of small mobile counterions. Protein molecules in solution usually contain polar groups of the both signs. There exists also many synthetical polyelectrolytes with important technological applications.

By a process known as adsorption mobile charges from the bathing solution and fixed charges along the polyelectrolyte can combine, leading to the emergence of higher multipoles along the polyelectrolyte chain, the first one being a dipole stemming from the association of a negative fixed charge on the polyelectrolyte and a specifically adsorbed mobile charge from the bathing solution.

Muthukumar [21] and Podgornik [7] have worked on dipolar flexible and dipolar semiflexible single chains respectively. Muthukumar, by using the Edwards Hamiltonian, discovered the formation of localized aggregated structures along the chain that dominate the statistical behaviour of the flexible polyelectrolyte chain, while Podgornik , by means of the wormlike chain model, discovered how screening of the dipolar interaction modifies the persistence length of an otherwise bare neutral polymer.

1.7 Layout of the Calculations and Results

The content of the following chapters is structured along the following lines: in Chapter 2 we aim to introduce the Random Phase Approximation (RPA) by

calculating the Hamiltonian (or the partition function) and the dipole-dipole structure function for a melt of unscreened dipolar polymers whose monomers do not have any volume, and hence they do not exclude each other.

In Chapter 3 we perform RPA computations again for the same melt, but this time with the excluded volume interaction included between its monomers. We obtain results for the Hamiltonian in terms of monomer and bond vector concentrations.

Next, Chapter 4 presents and analyzes the results of Chapter 3. It shows some plots of the dipole-dipole structure function and of the density structure function and proposes that the reason for their shape is due to the long-range character of the unscreened dipole potential.

Then Chapter 5 gives the RPA results for the case of Debye-Hückel-screened dipolar interactions.

Lastly Chapter 6 concludes by highlighting all the results obtained in this dissertation and also offers possible further directions for future investigation.

2. THE RANDOM PHASE APPROXIMATION

Our quest is to obtain, in as closed form as possible, the *partition function* of a melt or solution of polymer chains with dipole moments directed along the chains and which is in thermal equilibrium with its surroundings at a constant temperature. This thermodynamic system offers itself to simple mathematical treatment while capturing most of the essential features of polymer solutions that an experimentalist may encounter in practice. The traditional recipe to obtaining the partition function is as follows:

1. Identify, or define, the different *microstate variables* of the system. (We have some freedom in fulfilling this requirement. As we will see later, the particular set of microstate variables one chooses depends on the observer of the system.)

2. Construct the *Hamiltonian* of the system. The Hamiltonian may be seen to be a function over microstate-space, assigning to each state a scalar value known as the 'energy' or 'cost' of the system being in that state. The Hamiltonian is also parametrized by the *macrostate* variables (such as the temperature, volume, etc.) of the system. These macrostate variables represent the constraints imposed on the system by its environment.

3. Determine the 'probability' associated with the energy of each state. This probability is known as the *Boltzmann factor* of the state.

4. Sum the Boltzmann factors over all the states to obtain the *partition function*.

Once the partition function has been obtained, various equilibrium statistical properties of the system can be extracted from it by applying their corresponding operators on the partition function.

In favour of the simplicity of the mathematical treatment we shall assume in this chapter that the monomers of our polymer chains do not possess any volume and hence do not exclude each other in space. In the next chapter we shall treat also the excluded volume interactions.

2.1 Defining the Microstates

Upon first consideration, the different microstates of our system depend on the different conformations in space that each polymer can take. It is not

difficult to describe the different conformations of a single polymer chain: we simply use a sequence of the three-dimensional position vectors of the monomers along the chain, for example, for a polymer with $N+1$ monomers we may use $\{\mathbf{r}_n\}_{n=0,\ldots,N}$ or $\{\mathbf{r}_0, \mathbf{b}_n\}_{n=1,\ldots,N}$ where $\mathbf{r}_n$ denotes the position vector of the n-th monomer along the polymer chain and $\mathbf{b}_n = \mathbf{r}_n - \mathbf{r}_{n-1}$ is the bond vector directed from $\mathbf{r}_{n-1}$ to $\mathbf{r}_n$. For a melt of polymer chains we need, in addition, to label each polymer. Let us use the index α to label each polymer. Thus supposing we have in our melt N_p polymers, then a state of our system is sufficiently identified by the sequence $\{\mathbf{r}_n^\alpha\}_{n=0,\ldots,N_\alpha}^{\alpha=1,\ldots,N_p}$ or $\{\mathbf{r}_0^\alpha, \mathbf{b}_n^\alpha\}_{n=1,\ldots,N_\alpha}^{\alpha=1,\ldots,N_p}$. We will assume for simplicity that all polymers in the melt have the same number, N, of monomers. It is common practice in polymer physics to define the so-called mesoscopic Hamiltonian, $H(\{\mathbf{r}_n\})$, over conformations of the polymer chain as described as above. It turns out however that for the problem at hand we need a different set of variables to describe the states for our system.

Remembering that our system has dipoles attached to the monomers, we thus anticipate that at low temperatures the dipolar interactions between the monomers in the melt win over their thermal agitations, and hence will give rise to *micro-domain structure*, a phase in which long-range order of the dipoles appears. Consequently, spatial fluctuations in the local magnetization field, $m(\mathbf{r})$ (and possibly the local density field $\rho(\mathbf{r})$), become significant on a scale which is large compared with the typical bond-length of the polymer chains. The fluctuations in density may be characterized by a density-density correlation function [20, 4]:

$$S(\mathbf{r}_1 - \mathbf{r}_2) = \beta \langle \rho(\mathbf{r}_1)\, \rho(\mathbf{r}_2) \rangle, \tag{2.1}$$

where $\beta = 1/k_B T$, T being the temperature, and k_B is the Boltzmann constant. Here $\langle \ldots \rangle$ denotes the thermal average. The Fourier transform, $S(\mathbf{k})$, of $S(\mathbf{r})$ can be studied by means of elastic radiation scattering experiments: light, X-ray, or neutron scattering. (Here $\mathbf{k}$ denotes the *scattering wave-vector*, which may be roughly viewed as the reciprocal distance between planes of monomers in the melt.) In such experiments, the intensity, or more precisely, the differential cross-section [17], of radiation detected at a given $\mathbf{k}$ is directly proportional to $S(\mathbf{k})$. The *scattering power*, $S(\mathbf{k})$, can be calculated with the Random Phase Approximation (RPA) method, which will be this chapter's main focus.

So we imagine a beam of 'neutrons' incident on our melt of polymers with dipoles directed along the polymer bonds. These 'neutrons' (which possess intrinsic dipole moments) will interact with, and hence be scattered off, the scattering units of the system, which we will assume to be only the dipolar monomers directed along the polymer chains. Hence the 'camera', or detector, recording these scattering events will 'see' only the spatial distribution, or *field* of dipolar monomers of the system: the observer is, to some extent, oblivious to the particular conformations of the polymer chains that presented a particular spatial distribution of dipolar monomers (see Figure 2.1). In fact, there may be many different conformations of the polymer chains (or microstates of the system) that conform to the same dipole distribution.

Our task therefore, is to 'collect' all polymer conformations corresponding

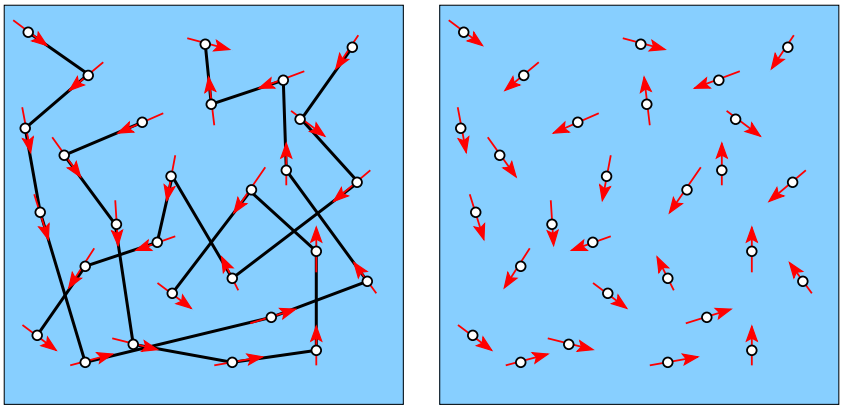

Fig. 2.1: (a) The medium being investigated as perceived in the mind of the observer. (b) The same medium being investigated, but as seen by the detector of the scattering experiment: the detector is oblivious to the particular conformation that presented this dipole distribution.

to a particular dipole distribution and label them all as one microstate which we will call the 'collective microstate'. This task will amount to transforming the mesoscopic Hamiltonian, defined over polymer conformations, into a new Hamiltonian defined instead over dipole distributions. We hereby introduce the so-called '*collective coordinates*' so that whereas '*microstate coordinates*' label the microstates of the mesoscopic Hamiltonian, collective coordinates label the collective microstates of the '*collective Hamiltonian*'.

2.2 Collective Coordinates

We introduce the following definitions for collective coordinates [12]:

1. The monomer density (or concentration) collective coordinate:

$$\rho(\mathbf{r}) \equiv \sum_{\alpha,\, n} \delta^{(3)}(\mathbf{r} - \mathbf{r}_n^\alpha), \tag{2.2}$$

   and

2. the bond-vector density collective coordinate:

$$\mathbf{u}(\mathbf{r}) \equiv \sum_{\alpha,\, n} \delta^{(3)}(\mathbf{r} - \mathbf{r}_n^\alpha)\mathbf{b}_n^\alpha, \tag{2.3}$$

   where we have set $\mathbf{b}_0^\alpha = 0$ for all α.

These new fields, $\rho(\mathbf{r})$ and $\mathbf{u}(\mathbf{r})$, may each be considered to be a superposition of a large number of plane-wave-like fluctuations of different wavelengths, so that these new fields can each be rewritten as [1]

$$\begin{aligned}\rho(\mathbf{r}) = \quad & \sum_{\mathbf{k}} \rho_{\mathbf{k}}\, e^{-i\mathbf{k}\cdot\mathbf{r}} = \quad & \frac{\Omega}{(2\pi)^3}\int \mathrm{d}^3k\; \rho_{\mathbf{k}}\, e^{-i\mathbf{k}\cdot\mathbf{r}},\\ \mathbf{u}(\mathbf{r}) = \quad & \sum_{\mathbf{k}} \mathbf{u}_{\mathbf{k}}\, e^{-i\mathbf{k}\cdot\mathbf{r}} = \quad & \frac{\Omega}{(2\pi)^3}\int \mathrm{d}^3k\; \mathbf{u}_{\mathbf{k}}\, e^{-i\mathbf{k}\cdot\mathbf{r}},\end{aligned} \tag{2.5}$$

where the amplitudes $\rho_{\mathbf{k}}$ and $\mathbf{u}_{\mathbf{k}}$ are, respectively, the Fourier transforms for

1. the density collective coordinate:

$$\begin{aligned}\rho_{\mathbf{k}} \equiv \mathscr{F}\big[\rho(\mathbf{r})\big] &= \int \frac{\mathrm{d}^3r}{\Omega}\, e^{i\mathbf{k}\cdot\mathbf{r}}\, \rho(\mathbf{r})\\ &= \int_{\Omega} \frac{\mathrm{d}^3r}{\Omega}\, e^{i\mathbf{k}\cdot\mathbf{r}} \sum_{\alpha,\,n} \delta^{(3)}(\mathbf{r}-\mathbf{r}_n^{\alpha})\\ &= \frac{1}{\Omega}\sum_{\alpha,\,n} e^{i\mathbf{k}\cdot\mathbf{r}_n^{\alpha}},\end{aligned} \tag{2.6}$$

and for

2. the bond-vector density collective coordinate:

$$\begin{aligned}\mathbf{u}_{\mathbf{k}} \equiv \mathscr{F}\big[\mathbf{u}(\mathbf{r})\big] &= \int \frac{\mathrm{d}^3r}{\Omega}\, e^{i\mathbf{k}\cdot\mathbf{r}}\, \mathbf{u}(\mathbf{r})\\ &= \int \frac{\mathrm{d}^3r}{\Omega}\, e^{i\mathbf{k}\cdot\mathbf{r}} \sum_{\alpha,\,n} \delta^{(3)}(\mathbf{r}-\mathbf{r}_n^{\alpha})\mathbf{b}_n^{\alpha}\\ &= \frac{1}{\Omega}\sum_{\alpha,\,n} e^{i\mathbf{k}\cdot\mathbf{r}_n^{\alpha}}\, \mathbf{b}_n^{\alpha}.\end{aligned} \tag{2.7}$$

The amplitudes, $\rho_{\mathbf{k}}$ and $\mathbf{u}_{\mathbf{k}}$, represent the spatial fluctuations of $\rho(\mathbf{r})$ and $\mathbf{u}(\mathbf{r})$ on a scale given by $\mathbf{k}$. It is clear from their representations that $\rho_{\mathbf{k}}$ and $\mathbf{u}_{\mathbf{k}}$ are, in general, complex except for ρ_0 and $\mathbf{u}_0$, which are real. Moreover notice that not all $\rho_{\mathbf{k}}$ and $\mathbf{u}_{\mathbf{k}}$ are independent of each other since

$$\rho_{-\mathbf{k}} = {\rho_{\mathbf{k}}}^* \quad \text{and} \quad \mathbf{u}_{-\mathbf{k}} = {\mathbf{u}_{\mathbf{k}}}^*. \tag{2.8}$$

[1] Notice that in equation (2.5) we presented, on purpose, two formally distinct ways of representing the fields $\mathbf{u}(\mathbf{r})$ and $\rho(\mathbf{r})$: the *series* and the *integral* representations. We point out here that each representation furnishes its own expression for the three-dimensional Dirac delta function, as shown in the following equation:

$$\delta^{(3)}(\mathbf{r}-\mathbf{r}') = \frac{1}{\Omega}\sum_{\mathbf{k}} e^{-i\mathbf{k}\cdot(\mathbf{r}-\mathbf{r}')} = \frac{1}{(2\pi)^3}\int \mathrm{d}^3k\, e^{-i\mathbf{k}\cdot(\mathbf{r}-\mathbf{r}')}. \tag{2.4}$$

In the rest of this document, we chose to use the more succinct series representation.

In the rest of this document, the reader will encounter such abbreviated notation as "$\mathbf{k} > 0$", "$\mathbf{k} \geq 0$", or "$\mathbf{k} \neq 0$": "$\mathbf{k} > 0$" refers to the region in three-dimensional $\mathbf{k}$ -space described by $\{k_x, k_y, k_z > 0\}$ (the upper half-space) where k_x, k_y, and k_z are the x, y, z-components of $\mathbf{k}$; "$\mathbf{k} \geq 0$" is "$\mathbf{k} > 0$" and $\mathbf{k} = 0$; and "$\mathbf{k} \neq 0$" means all of $\mathbf{k}$ -space excluding the origin. As we shall see later, there is an advantage to working in $\mathbf{k}$-space, namely, it eventually enables us to compute the partition function, after a suitable approximation, by performing a Gaussian integral with an already diagonalized quadratic form over the phase amplitudes.

2.3 The Mesoscopic Hamiltonian

The mesoscopic Hamiltonian gives the energy of polymer chains modeled by *Gaussian chains* whose bonds (such as $\mathbf{b}_n^\alpha$) follow the three-dimensional Gaussian distribution:

$$p(\mathbf{b}_n^\alpha) = \left(\frac{3}{2\pi l^2}\right)^{\frac{3}{2}} \exp\left[-\frac{3(\mathbf{b}_n^\alpha)^2}{2l^2}\right]. \tag{2.9}$$

where the constant l is called the *Kuhn length* or the *effective* bond length of the polymer (and not the actual bond length, for reasons soon to be given). So

$$\left\langle (\mathbf{b}_n^\alpha)^2 \right\rangle = l^2. \tag{2.10}$$

The conformational distribution function of a melt of Gaussian chains is therefore

$$\begin{aligned} P(\{\mathbf{b}_n^\alpha\}) &= \prod_{\alpha,\,n} \left(\frac{3}{2\pi l^2}\right)^{\frac{3}{2}} \exp\left[-\frac{3(\mathbf{b}_n^\alpha)^2}{2l^2}\right] \\ &= \left(\frac{3}{2\pi l^2}\right)^{\frac{3NN_p}{2}} \exp\left[-\sum_{\alpha,\,n} \frac{3(\mathbf{b}_n^\alpha)^2}{2l^2}\right] \end{aligned} \tag{2.11}$$

The Gaussian chain *does not* describe correctly the local structure of the polymer because the Gaussian chain assumes statistical independence of adjacent bonds, which is generally not true for most polymers because of short-range interactions between neighbouring monomers along the chain. But the Gaussian chain *does* correctly describe the structure on a *large enough scale* (i.e., the mesoscopic scale) because for most types of polymers (and polymer models) bond-to-bond correlation decreases rapidly (roughly exponentially) with increasing separation between the bonds along the polymer. Hence any type of polymer chain may be subdivided into, say, N submolecules each consisting of, say, λ bonds, so that $\mathbf{b}_n^\alpha$ is actually the end-to-end vector of one of these submolecules, and l is the root-mean-square length of one of these submolecules, hence its name: *effective* bond length. The parameter, λ, can be taken to be large enough so that the vectors $\mathbf{b}_n^\alpha$ become independent of each other. The advantage of the Gaussian

chain is that it is mathematically much easier to handle than other models. The Gaussian chain is also referred to as the *ideal chain*.

The Gaussian chain is often represented by a mechanical model in which $(N+1)$ "monomers" are considered to be interconnected by harmonic springs whose total potential energy is

$$H_0(\{\mathbf{b}_n\}) = \frac{1}{\beta}\frac{3}{2l^2}\sum_n (\mathbf{b}_n)^2. \tag{2.12}$$

Thus the spring constant of each bond is $3/\beta l^2$ which is temperature-dependent. Using the above expression for our Hamiltonian of a melt of polymers, we see that at equilibrium, the Boltzmann factor, $\exp\left(-\beta\, H_0(\{\mathbf{b}_n^\alpha\})\right)$ for a melt of polymers is exactly the same as the exponential factor in equation (2.11).

While the Gaussian chain effectively describes polymer chains with interactions existing between neighbouring monomers along the same polymer chain, it fails to account for interactions that may exist between monomers separated far apart on the polymer chain, such as dipolar interactions (since the monomers are assumed to possess dipole moments) and excluded volume interactions. Therefore such interactions should be added to the mesoscopic Hamiltonian by hand. In this chapter we shall treat only the dipolar interactions, then in the following chapter we shall also include the excluded volume interaction.

The interaction energy between two dipoles with dipole moments, say, $\mathbf{p}_1$ and $\mathbf{p}_2$ separated by a separation vector, say, $\mathbf{r}$ directed from $\mathbf{p}_1$ to $\mathbf{p}_2$ is

$$U(\mathbf{p}_1,\, \mathbf{p}_2,\, \mathbf{r}) = \frac{\lambda_B}{\beta e_0^2}\left(\frac{\mathbf{p}_1\cdot\mathbf{p}_2 - 3\,(\hat{\mathbf{r}}\cdot\mathbf{p}_1)\,(\hat{\mathbf{r}}\cdot\mathbf{p}_2)}{|\mathbf{r}|^3}\right), \tag{2.13}$$

where $\hat{\mathbf{r}} = \mathbf{r}/|\mathbf{r}|$, λ_B is the *Bjerrum length* [7], and e_0 is the electron charge. Note that implicitly the Bjerrum length is directly proportional to β (see Appendix A) so that $U(\mathbf{p}_1,\, \mathbf{p}_2,\, \mathbf{r})$ is temperature-independent, but the Boltzmann factor $\exp\left(-\beta\, U\right)$ is temperature-dependent. Figure 2.2 illustrates the essential features of the dipolar interaction.

The total dipolar energy of interaction in a melt of polymers includes interactions between monomers on different polymer chains, and is therefore

$$\begin{aligned} U(\{\mathbf{p}_n^\alpha,\, \mathbf{r}_n^\alpha\}) &= \frac{\lambda_B}{\beta e_0^2}\sum_{\substack{\alpha,\,\beta\\ n>m}} \frac{\mathbf{p}_n^\alpha\cdot\mathbf{p}_m^\beta - 3\left(\hat{\mathbf{r}}_{n\,m}^{\alpha\,\beta}\cdot\mathbf{p}_n^\alpha\right)\left(\hat{\mathbf{r}}_{n\,m}^{\alpha\,\beta}\cdot\mathbf{p}_m^\beta\right)}{\left|\mathbf{r}_m^\beta - \mathbf{r}_n^\alpha\right|^3} \\ &= \frac{\lambda_B}{\beta e_0^2}\sum_{\substack{\alpha,\,\beta\\ n>m}} \mathbf{p}_n^\alpha\cdot\frac{\mathbb{1} - 3\,\hat{\mathbf{r}}_{n\,m}^{\alpha\,\beta}\,\hat{\mathbf{r}}_{n\,m}^{\alpha\,\beta}}{\left|\mathbf{r}_m^\beta - \mathbf{r}_n^\alpha\right|^3}\cdot\mathbf{p}_m^\beta, \end{aligned} \tag{2.14}$$

where $\hat{\mathbf{r}}_{n\,m}^{\alpha\,\beta} = \left(\mathbf{r}_m^\beta - \mathbf{r}_n^\alpha\right)/\left|\mathbf{r}_m^\beta - \mathbf{r}_n^\alpha\right|$. If furthermore the dipoles are constrained to align themselves with the bonds along the polymer chain to which they belong, that is,

$$\mathbf{p}_n^\alpha = c\,\mathbf{b}_n^\alpha \tag{2.15}$$

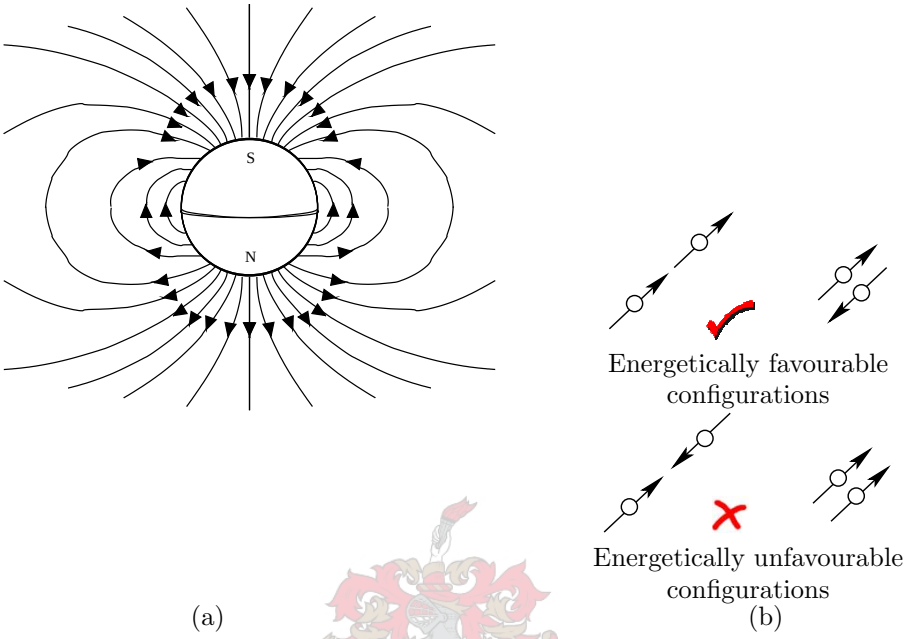

Fig. 2.2: (a) The field in a vertical plane through a dipole depicted as a sphere; each field line in the diagram shows the direction that another dipole is most likely to point at if placed at a point along that field line. (b) Energetically favourable and energetically unfavourable configurations of a pair of dipoles.

where c is a dimensionful constant, then

$$U(\{\mathbf{r}_n^\alpha\}) = \frac{\lambda_B\, C}{\beta} \sum_{\substack{\alpha,\,\beta \\ n>m}} \mathbf{b}_n^\alpha \cdot \frac{\mathbb{1} - 3\,\hat{\mathbf{r}}_{n\,m}^{\alpha\,\beta}\,\hat{\mathbf{r}}_{n\,m}^{\alpha\,\beta}}{\left|\mathbf{r}_m^\beta - \mathbf{r}_n^\alpha\right|^3} \cdot \mathbf{b}_m^\beta, \tag{2.16}$$

where

$$C = c^2/e_0^2 \tag{2.17}$$

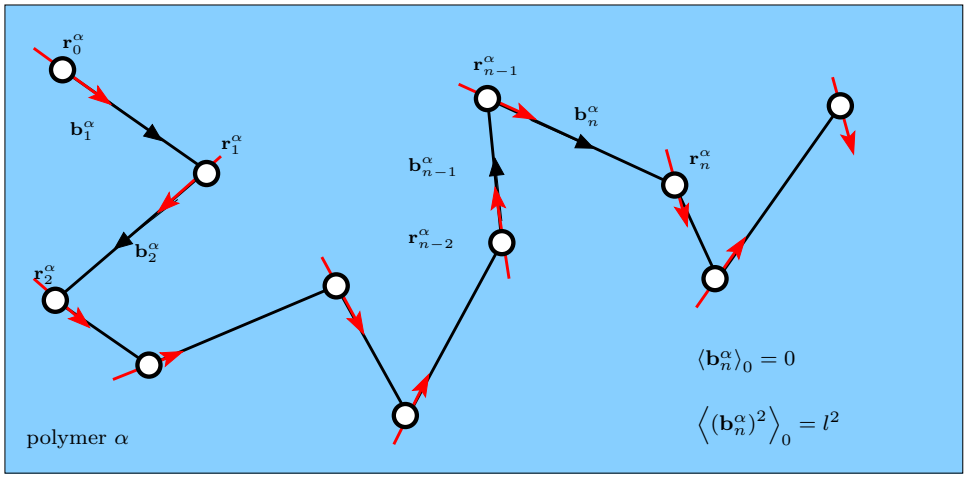

Fig. 2.3: A diagram showing a section of a typical polymer chain of our model with dipoles (represented by the arrows) directed along the chain.

Hence, finally, our mesoscopic Hamiltonian is

$$H(\{\mathbf{r}_n^\alpha\}) = \frac{1}{\beta}\frac{3}{2\,l^2}\sum_{\alpha,\,n}(\mathbf{b}_n^\alpha)^2 + \frac{\lambda_B\,C}{\beta}\sum_{\substack{\alpha,\,\beta\\ n>m}}\mathbf{b}_n^\alpha\cdot\frac{\mathbb{1}-3\,\hat{\mathbf{r}}_{n\,m}^{\alpha\,\beta}\,\hat{\mathbf{r}}_{n\,m}^{\alpha\,\beta}}{\left|\mathbf{r}_m^\beta-\mathbf{r}_n^\alpha\right|^3}\cdot\mathbf{b}_m^\beta, \qquad (2.18)$$

and we may now proceed with the transformation of this Hamiltonian into another Hamiltonian defined over collective variables.

2.4 The Transformation

We point out here that, in principle, when we consider the microstates of a physical system we should take into account not only the positions of the particles in the system but also their momenta. This consideration, however, leads to an (uninteresting) additional term in the Hamiltonian, namely the *kinetic energy*. Hence the full partition function, $\mathscr{Z}$, is an integral over momentum-space and position-space (collectively called *phase-space*). Moreover, after integrating over momentum-space alone, the kinetic energy term in the Hamiltonian only leads to an uninteresting dimensionful factor, $\mathscr{Z}_m$, in the full partition function. The remaining factor is the *conformational partition function*, $\mathscr{Z}_c$, since it is an integral over position-space variables alone, that is, over conformations in position-space. Thus

$$\mathscr{Z} = \mathscr{Z}_m\,\mathscr{Z}_c. \qquad (2.19)$$

The dimensions of $\mathscr{Z}_m$ are $1/\left[\mathrm{L}^d\right]$ where [L] denotes the dimensions of length and d is the number of degrees of freedom of the system $\mathscr{Z}$ describes. Since $\mathscr{Z}$ is dimensionless, then $\mathscr{Z}_c$ has dimensions of $\left[\mathrm{L}^d\right]$. For our system of a melt of

polymers we have

$$\mathscr{Z}_c = \int \mathscr{D}\mathbf{b}\, e^{-\beta\, H_0(\{\mathbf{r}_n^\alpha\})}\, e^{-\beta\, U(\{\mathbf{r}_n^\alpha\})} \tag{2.20}$$

where $\mathscr{D}\mathbf{b}$ is a measure which must have the same dimensions as $\mathscr{Z}_c$.

The integrand of equation (2.20) may be considered to be a probability density function of random variables $\{\mathbf{r}_n^\alpha\}$. Then our crossing-over to collective variables will amount to finding the probability density function of a new random variable, such as $\{\mathbf{u_k}\}$, which is itself a function of $\{\mathbf{r}_n^\alpha\}$. The standard technique to finding this new probability density function is to first treat $\{\mathbf{u_k}\}$ and $\{\mathbf{r}_n^\alpha\}$ as independent variables. Next, introduce as a new factor into the integrand of equation (2.20), the Dirac delta containing the functional dependency between $\{\mathbf{u_k}\}$ and $\{\mathbf{r}_n^\alpha\}$. Finally, integrate over $\{\mathbf{r}_n^\alpha\}$. As a result, the conformational partition function transforms into an integral over the $\{\mathbf{u_k}\}$. This technique is summed up in the following equation: we need to find a $H_0(\{\mathbf{u_k}\})$ and $U(\{\mathbf{u_k}\})$ such that the following equation holds

$$\begin{aligned}\mathscr{Z}_c &= \int \mathscr{D}\mathbf{u}\, e^{-\beta\, H_0(\{\mathbf{u_k}\})}\, e^{-\beta\, U(\{\mathbf{u_k}\})} \\ &= \int \mathscr{D}\mathbf{u} \left[\int \mathscr{D}\mathbf{b} \prod_{\mathbf{k}\geq 0} \delta\left(\mathbf{u_k} - \frac{1}{\Omega} \sum_{\alpha,\, n} e^{i\mathbf{k}\cdot\mathbf{r}_n^\alpha}\, \mathbf{b}_n^\alpha \right) e^{-\beta\, H_0(\{\mathbf{r}_n^\alpha\})}\, e^{-\beta\, U(\{\mathbf{r}_n^\alpha\})} \right].\end{aligned} \tag{2.21}$$

2.5 Transforming the Potential Energy of Interaction

Incidentally it is much easier to transform $U(\{\mathbf{r}_n^\alpha\})$: in fact, as we now show, $U(\{\mathbf{r}_n^\alpha\})$ may simply be rewritten in terms of $\{\mathbf{u_k}\}$. First, we find that $U(\{\mathbf{r}_n^\alpha\})$, as given in equation (2.16), may be written as

$$U(\{\mathbf{r}_n^\alpha\}) = \frac{1}{2} \sum_{\substack{\alpha,\,\beta \\ n,\,m}} \mathbf{b}_n^\alpha \cdot \mathbf{J}'\big(\mathbf{r}_n^\alpha - \mathbf{r}_m^\beta\big) \cdot \mathbf{b}_m^\beta\, (1 - \delta_{\alpha\,\beta}\, \delta_{n\,m}), \tag{2.22}$$

the pre-factor of $\frac{1}{2}$ having been included to ensure summation over *distinct pairs of monomers*, while the trailing factor of $(1 - \delta_{\alpha\,\beta}\, \delta_{n\,m})$ has been included to ensure summation over *distinct monomers*. We label $\mathbf{J}'(\mathbf{r})$ as an *exchange interaction* and it has the form

$$\mathbf{J}'(\mathbf{r}) = \frac{\lambda_B C}{\beta}\, \frac{\mathbb{1} - 3\,\hat{\mathbf{r}}\,\hat{\mathbf{r}}}{|\mathbf{r}|^3}. \tag{2.23}$$

To avoid having to carry these factors around all the time, we simply define a slightly modified exchange interaction, $\mathbf{J}(\mathbf{r})$, as

$$\mathbf{J}(\mathbf{r}) \equiv \frac{\lambda_B C}{2\beta}\, \frac{\mathbb{1} - 3\,\hat{\mathbf{r}}\,\hat{\mathbf{r}}}{|\mathbf{r}|^3}\, (1 - \delta_{r,\,0}). \tag{2.24}$$

Now let $\mathbf{J_k}$ be the Fourier transform of $\mathbf{J}(\mathbf{r})$, that is,

$$\mathbf{J}(\mathbf{r}) = \sum_{\mathbf{k}} \mathbf{J_k}\, e^{-i\mathbf{k}\cdot\mathbf{r}}. \tag{2.25}$$

Therefore equation (2.22) may be rewritten as

$$\begin{aligned} U(\{\mathbf{r}_n^\alpha\}) &= \sum_{\substack{\alpha,\,\beta\\ n,\,m}} \mathbf{b}_n^\alpha \cdot \left[\sum_{\mathbf{k}} \mathbf{J_k}\, e^{-i\mathbf{k}\cdot\left(\mathbf{r}_n^\alpha - \mathbf{r}_m^\beta\right)}\right] \cdot \mathbf{b}_m^\beta \\ &= \sum_{\mathbf{k}} \sum_{\substack{\alpha,\,\beta\\ n,\,m}} \left[e^{-i\mathbf{k}\cdot\mathbf{r}_n^\alpha}\mathbf{b}_n^\alpha\right] \cdot \mathbf{J_k} \cdot \left[e^{i\mathbf{k}\cdot\mathbf{r}_m^\beta}\mathbf{b}_m^\beta\right] \\ &= \Omega^2 \sum_{\mathbf{k}} \mathbf{u}_{-\mathbf{k}} \cdot \mathbf{J_k} \cdot \mathbf{u_k} \quad \equiv \quad U(\{\mathbf{u_k}\}). \end{aligned} \tag{2.26}$$

We shall postpone the calculation of $\mathbf{J_k}$ till after the next section.

2.6 Transforming the Gaussian Chain Energy: the RPA method

Now that we have successfully transformed the potential energy of interaction, all that remains is to transform the Gaussian chain energy:

$$H_0(\{\mathbf{b}_n^\alpha\}) = \frac{a}{\beta} \sum_{\alpha,\,n} (\mathbf{b}_n^\alpha)^2 \tag{2.27}$$

where $a = \frac{3}{2\,l^2}$. We want to find a new Hamiltonian, $H_0(\{\mathbf{u_k}\})$, defined over states determined by the sets $\{\mathbf{u_k}\}$. Referring to equation (2.21) we see that this new Hamiltonian is given by [2]

$$\begin{aligned} e^{-\beta\, H_0(\{\mathbf{u_k}\})} = \int \mathscr{D}\mathbf{b} \prod_{\mathbf{k}>0} &\delta^{(2)(3)}\left(\mathbf{u_k} - \frac{1}{\Omega}\sum_{\alpha,\,n} e^{i\mathbf{k}\cdot\mathbf{r}_n^\alpha}\,\mathbf{b}_n^\alpha\right) \\ &\times \delta^{(3)}\left(\mathbf{u}_0 - \frac{1}{\Omega}\sum_{\alpha,\,n}\mathbf{b}_n^\alpha\right) e^{-\beta\, H_0(\{\mathbf{b}_n^\alpha\})}, \end{aligned} \tag{2.31}$$

[2] The Dirac delta, $\delta^{(2)}(z)$ (where $z = x+iy\,;\quad x,\,y \in \mathbb{R}$), over the complex-plane is defined, as

$$\delta^{(2)}(z) \;=\; \delta(x)\delta(y) \;=\; \int \frac{\mathrm{d}k_x}{2\pi}\, e^{ik_x\cdot x} \int \frac{\mathrm{d}k_y}{2\pi}\, e^{ik_y\cdot y}. \tag{2.28}$$

Let $k = \frac{k_x+ik_y}{2}$ and $\int \mathrm{d}^2k \equiv \iint \frac{\mathrm{d}k_x}{2}\frac{\mathrm{d}k_y}{2}$. Then

$$k_x x + k_y y = k^* z + k z^* \tag{2.29}$$

so that

$$\delta^{(2)}(z) = \int \frac{\mathrm{d}^2k}{\pi^2} e^{i(k^* z + k z^*)}. \tag{2.30}$$

where $\int \mathscr{D}\mathbf{b} = \frac{1}{N_p!}\int \prod_{\alpha} \mathrm{d}^3 r_0^{\alpha} \prod_{\alpha,\, n} \mathrm{d}^3 b_n^{\alpha}$. The factor of $\frac{1}{N_p!}$ has been included because the chains are indistinguishable from each other and hence a correction to the partition function is required in order to resolve Gibbs paradox.
The integral expressions for the delta functions are

$$\begin{aligned}
&\prod_{\mathbf{k}>0} \delta^{(2)(3)}\left(\mathbf{u}_{\mathbf{k}} - \frac{1}{\Omega}\sum_{\alpha,\, n} e^{i\mathbf{k}\cdot\mathbf{r}_n^{\alpha}}\, \mathbf{b}_n^{\alpha}\right) \\
&\quad = \prod_{\mathbf{k}>0} \int \frac{\mathrm{d}^6\psi_{\mathbf{k}}}{\pi^6}\, \exp\left[i\left\{ \boldsymbol{\psi}_{\mathbf{k}}^{*}\cdot\left(\mathbf{u}_{\mathbf{k}} - \frac{1}{\Omega}\sum_{\alpha,\, n} e^{i\mathbf{k}\cdot\mathbf{r}_n^{\alpha}}\, \mathbf{b}_n^{\alpha}\right)\right.\right. \\
&\qquad\qquad \left.\left. +\ \boldsymbol{\psi}_{\mathbf{k}}\cdot\left(\mathbf{u}_{\mathbf{k}}^{*} - \frac{1}{\Omega}\sum_{\alpha,\, n} e^{-i\mathbf{k}\cdot\mathbf{r}_n^{\alpha}}\, \mathbf{b}_n^{\alpha}\right)\right\}\right] \\
&\quad = \int \left[\prod_{\mathbf{k}>0} \frac{\mathrm{d}^6\psi_{\mathbf{k}}}{\pi^6}\right] \exp\left[i\sum_{\mathbf{k}\neq 0}\left(\boldsymbol{\psi}_{\mathbf{k}}\cdot\mathbf{u}_{-\mathbf{k}} - \frac{1}{\Omega}\sum_{\alpha,\, n} e^{-i\mathbf{k}\cdot\mathbf{r}_n^{\alpha}}\, \boldsymbol{\psi}_{\mathbf{k}}\cdot\mathbf{b}_n^{\alpha}\right)\right]
\end{aligned} \tag{2.32}$$

and

$$\delta^{(3)}\left(\mathbf{u}_0 - \frac{1}{\Omega}\sum_{\alpha,\, n}\mathbf{b}_n^{\alpha}\right) = \int \frac{\mathrm{d}^3\psi_0}{(2\pi)^3}\, \exp\left[i\left(\psi_0\cdot\mathbf{u}_0 - \frac{1}{\Omega}\sum_{\alpha,\, n}\psi_0\cdot\mathbf{b}_n^{\alpha}\right)\right] \tag{2.33}$$

where the $\boldsymbol{\psi}_{\mathbf{k}}$ may be considered to be the amplitudes of a new field conjugate to $\mathbf{u}(\mathbf{r})$. More on this later. Let

$$\int \mathscr{D}\boldsymbol{\psi} = \int \left[\prod_{\mathbf{k}>0} \frac{\mathrm{d}^6\psi_{\mathbf{k}}}{\pi^6}\right] \int \frac{\mathrm{d}^3\psi_0}{(2\pi)^3}, \tag{2.34}$$

then

$$\begin{aligned}
e^{-\beta H_0(\{\mathbf{u}_{\mathbf{k}}\})} &= \int \mathscr{D}\boldsymbol{\psi} \exp\left[i\sum_{\mathbf{k}} \boldsymbol{\psi}_{\mathbf{k}}\cdot\mathbf{u}_{-\mathbf{k}}\right] \\
&\quad \times \int \mathscr{D}\mathbf{b} \exp\left[-\frac{i}{\Omega}\sum_{\mathbf{k}}\sum_{\alpha,\, n} e^{-i\mathbf{k}\cdot\mathbf{r}_n^{\alpha}}\, \boldsymbol{\psi}_{\mathbf{k}}\cdot\mathbf{b}_n^{\alpha}\right] e^{-\beta H_0(\{\mathbf{b}_n^{\alpha}\})}
\end{aligned} \tag{2.35}$$

But for the complicated argument of the second exponential we would have proceeded straightaway to carry out the $\mathbf{b}$ integration. So here is where we make an approximation. First of all, if we look closely at the integral over $\mathbf{b}$ in equation (2.35), we discover that its mathematical form is similar to that of a partition function of *a melt of Gaussian chains in the presence of an external vector field*,[3] $\boldsymbol{\psi}(\mathbf{r})$, defined by:

$$\boldsymbol{\psi}(\mathbf{r}) = \frac{1}{\beta} \times \frac{i}{\Omega}\sum_{\mathbf{k}} e^{-i\mathbf{k}\cdot\mathbf{r}}\, \boldsymbol{\psi}_{\mathbf{k}}. \tag{2.38}$$

[3] If there is an external vector field, $\mathbf{E}(\mathbf{r})$, acting on each segment, $\mathbf{b}_n^{\alpha}$, of any Gaussian

Let us call this field a *phase vector field* because of its apparent imaginary character. Note that this field is not actually present but it is purely an artifact of the transformation process (from microstate variables to collective variables). Our approximation involves the assumption that this phase vector field, $\boldsymbol{\psi}(\mathbf{r})$, is itself small and in addition its spatial fluctuations are small (that is, all the $\boldsymbol{\psi}_{\mathbf{k}}$ are small). In other words, we assume that the most important contributions of the $\boldsymbol{\psi}_{\mathbf{k}}$ to the $\boldsymbol{\psi}$ integral in equation (2.35) come from a small region in $\boldsymbol{\psi}(\mathbf{r})$-space covering the origin. It is this assumption which forms the basis of the so-called Random Phase Approximation (RPA). Hence we may expand the second exponential in (2.35) to quadratic order in its argument: [4]

$$\exp\left[-\frac{i}{\Omega}\sum_{\mathbf{k},\,\alpha,\,n} e^{-i\mathbf{k}\cdot\mathbf{r}_n^\alpha}\,\boldsymbol{\psi}_{\mathbf{k}}\cdot\mathbf{b}_n^\alpha\right] \approx 1-\frac{i}{\Omega}\sum_{\mathbf{k},\,\alpha,\,n} e^{-i\mathbf{k}\cdot\mathbf{r}_n^\alpha}\,\boldsymbol{\psi}_{\mathbf{k}}\cdot\mathbf{b}_n^\alpha - \frac{1}{2\Omega^2}\sum_{\substack{\mathbf{k},\,\alpha,\,n\\ \mathbf{q},\,\beta,\,m}} e^{-i\left(\mathbf{k}\cdot\mathbf{r}_n^\alpha+\mathbf{q}\cdot\mathbf{r}_m^\beta\right)}\,(\boldsymbol{\psi}_{\mathbf{k}}\cdot\mathbf{b}_n^\alpha)(\boldsymbol{\psi}_{\mathbf{q}}\cdot\mathbf{b}_m^\beta) \tag{2.39}$$

so that after applying the expression for $H_0\big(\{\mathbf{b}_n^\alpha\}\big)$ (equation (2.27)) to equation (2.35) we have

$$\begin{aligned} e^{-\beta H_0(\{\mathbf{u}_{\mathbf{k}}\})} \approx \int\mathscr{D}\boldsymbol{\psi}\exp\left[i\sum_{\mathbf{k}}\boldsymbol{\psi}_{\mathbf{k}}\cdot\mathbf{u}_{\mathbf{k}}\right]\Bigg(\int\mathscr{D}\mathbf{b}\,\exp\left[-a\sum_{\alpha,\,n}(\mathbf{b}_n^\alpha)^2\right] \\ -\frac{i}{\Omega}\int\mathscr{D}\mathbf{b}\sum_{\mathbf{k},\,\alpha,\,n}\boldsymbol{\psi}_{\mathbf{k}}\cdot\mathbf{b}_n^\alpha\,\exp\left[-i\mathbf{k}\cdot\mathbf{r}_n^\alpha - a\sum_{\alpha,\,n}(\mathbf{b}_n^\alpha)^2\right] \\ -\frac{1}{2\Omega^2}\int\mathscr{D}\mathbf{b}\sum_{\substack{\mathbf{k},\,\alpha,\,n\\ \mathbf{q},\,\beta,\,m}}(\boldsymbol{\psi}_{\mathbf{k}}\cdot\mathbf{b}_n^\alpha)(\boldsymbol{\psi}_{\mathbf{q}}\cdot\mathbf{b}_m^\beta) \\ \times\exp\left[-i\left(\mathbf{k}\cdot\mathbf{r}_n^\alpha+\mathbf{q}\cdot\mathbf{r}_m^\beta\right)-a\sum_{\alpha,\,n}(\mathbf{b}_n^\alpha)^2\right]\Bigg). \end{aligned} \tag{2.40}$$

chain, then the energy of interaction between $\mathbf{E}(\mathbf{r})$ and the melt is

$$U_0(\{\mathbf{r}_n^\alpha\}) = \sum_{\alpha,\,n}\mathbf{E}(\mathbf{r}_n^\alpha)\cdot\mathbf{b}_n^\alpha \tag{2.36}$$

so that the partition function becomes

$$\mathscr{Z}[\mathbf{E}(\mathbf{r})] = \int\mathscr{D}\mathbf{b}\,e^{-\beta H_0(\{\mathbf{r}_n^\alpha\})}\,e^{-\beta\sum_{\alpha,\,n}\mathbf{E}(\mathbf{r}_n^\alpha)\cdot\mathbf{b}_n^\alpha}. \tag{2.37}$$

[4] Higher-order expansions will give rise to more accurate approximations. This is somewhat equivalent to the perturbation expansions encountered in Quantum Field Theory during the calculation of, for example, the evolution operator

The first $\mathbf{b}$ integral gives

$$\begin{aligned}\int\mathscr{D}\mathbf{b}\,\exp\left[-a\sum_{\alpha,\,n}(\mathbf{b}_n^\alpha)^2\right] &= \frac{1}{N_p!}\int\left[\prod_\alpha \mathrm{d}^3 r_0^\alpha\right]\int\left[\prod_{\alpha,\,n}\mathrm{d}^3 b_n^\alpha\right]\exp\left[-a\sum_{\alpha,\,n}(\mathbf{b}_n^\alpha)^2\right]\\ &= \frac{1}{N_p!}\left[\int \mathrm{d}^3 r_0\int\prod_n \mathrm{d}^3 b_n\,\exp\Big[-a\sum_n(\mathbf{b}_n)^2\Big]\right]^{N_p}\\ &= \frac{1}{N_p!}[\mathscr{Z}_0]^{N_p},\end{aligned} \tag{2.41}$$

where we have recognized that $\mathscr{Z}_0$ is the conformational partition function of a single Gaussian chain (without any interactions):

$$\begin{aligned}\mathscr{Z}_0 &= \int \mathrm{d}^3 r_0\int\prod_n \mathrm{d}^3 b_n\,\exp\left[-a\sum_n(\mathbf{b}_n)^2\right]\\ &= \Omega\left[\int_{-\infty}^{\infty}\mathrm{d}b\exp\left(-ab^2\right)\right]^{3N} = \quad \Omega\Big(\frac{\pi}{a}\Big)^{\frac{3N}{2}}.\end{aligned} \tag{2.42}$$

Just before tackling the second $\mathbf{b}$ integral in equation (2.40) let us define the Gaussian chain average:

$$\begin{aligned}\langle\ldots\rangle_0 &= \frac{\int\mathscr{D}\mathbf{b}\,(\ldots)\,\exp\left[-a\sum_{\alpha,\,n}(\mathbf{b}_n^\alpha)^2\right]}{\int\mathscr{D}\mathbf{b}\,\exp\left[-a\sum_{\alpha,\,n}(\mathbf{b}_n^\alpha)^2\right]}\\ &= N_p!\,[\mathscr{Z}_0]^{-N_p}\int\mathscr{D}\mathbf{b}\,(\ldots)\,\exp\left[-a\sum_{\alpha,\,n}(\mathbf{b}_n^\alpha)^2\right].\end{aligned} \tag{2.43}$$

Hence the second $\mathbf{b}$ integral in equation (2.40) gives

$$\begin{aligned}&\int\mathscr{D}\mathbf{b}\sum_{\mathbf{k},\,\alpha,\,n}\boldsymbol{\psi}_{\mathbf{k}}\cdot\mathbf{b}_n^\alpha\,\exp\left[-i\mathbf{k}\cdot\mathbf{r}_n^\alpha - a\sum_{\alpha,\,n}(\mathbf{b}_n^\alpha)^2\right]\\ &\quad= [N_p!]^{-1}[\mathscr{Z}_0]^{N_p}\sum_{\mathbf{k}}\boldsymbol{\psi}_{\mathbf{k}}\cdot\sum_{\alpha,\,n}\left\langle\mathbf{b}_n^\alpha\,e^{-i\mathbf{k}\cdot\mathbf{r}_n^\alpha}\right\rangle_0\\ &\quad= [N_p!]^{-1}[\mathscr{Z}_0]^{N_p}\sum_{\mathbf{k}}\boldsymbol{\psi}_{\mathbf{k}}\cdot\sum_{\alpha,\,n}\left\langle\mathbf{b}_n^\alpha\,e^{-i\mathbf{k}\cdot\left(\mathbf{r}_0^\alpha+\sum_i^n\mathbf{b}_i^\alpha\right)}\right\rangle_0.\end{aligned} \tag{2.44}$$

Since all the $\mathbf{b}_n^\alpha$'s and $\mathbf{r}_0^\alpha$'s are statistically independent, the quantity being averaged on the last line of the equation above is a mere product of averages. So that we have, continuing from the last equation,

$$[N_p!]^{-1}[\mathscr{Z}_0]^{N_p}\sum_{\mathbf{k}}\boldsymbol{\psi}_{\mathbf{k}}\cdot\sum_{\alpha,\,n}\left\langle e^{-i\mathbf{k}\cdot\mathbf{r}_0^\alpha}\right\rangle_0\left\langle\mathbf{b}_n^\alpha\,e^{-i\mathbf{k}\cdot\mathbf{b}_n^\alpha}\right\rangle_0\left\langle e^{-i\mathbf{k}\cdot\sum_i^{n-1}\mathbf{b}_i^\alpha}\right\rangle_0. \tag{2.45}$$

Computing the first average (of a function of $\mathbf{r}_0^\alpha$) yields a "Kronecker delta": [5]

$$[N_p!]^{-1}[\mathscr{Z}_0]^{N_p}\sum_{\mathbf{k}}\boldsymbol{\psi}_{\mathbf{k}}\cdot\sum_{\alpha,\,n}\delta_{\mathbf{k},\,0}\left\langle \mathbf{b}_n^\alpha\, e^{-i\mathbf{k}\cdot\mathbf{b}_n^\alpha}\right\rangle_0\left\langle e^{-i\mathbf{k}\cdot\sum_i^{n-1}\mathbf{b}_i^\alpha}\right\rangle_0, \tag{2.48}$$

and then summing over $\mathbf{k}$ gives

$$[N_p!]^{-1}[\mathscr{Z}_0]^{N_p}\boldsymbol{\psi}_0\cdot\sum_{\alpha,\,n}\langle\mathbf{b}_n^\alpha\rangle_0=0, \tag{2.49}$$

since $\langle\mathbf{b}_n^\alpha\rangle_0$ vanishes. The third $\mathbf{b}$ integral in equation (2.40) gives

$$\begin{aligned}
&\int\mathscr{D}\mathbf{b}\sum_{\substack{\mathbf{k},\,\alpha,\,n\\ \mathbf{q},\,\beta,\,m}}(\boldsymbol{\psi}_{\mathbf{k}}\cdot\mathbf{b}_n^\alpha)(\boldsymbol{\psi}_{\mathbf{q}}\cdot\mathbf{b}_m^\beta)\exp\left[-i\big(\mathbf{k}\cdot\mathbf{r}_n^\alpha+\mathbf{q}\cdot\mathbf{r}_m^\beta\big)-a\sum_{\alpha,\,i}(\mathbf{b}_i^\alpha)^2\right]\\
&\quad=[N_p!]^{-1}[\mathscr{Z}_0]^{N_p}\sum_{\mathbf{k},\,\mathbf{q}}\boldsymbol{\psi}_{\mathbf{k}}\cdot\sum_{\substack{\alpha,\,n\\ \beta,\,m}}\left\langle\mathbf{b}_n^\alpha\,\mathbf{b}_m^\beta\, e^{-i\left(\mathbf{k}\cdot\mathbf{r}_n^\alpha+\mathbf{q}\cdot\mathbf{r}_m^\beta\right)}\right\rangle_0\cdot\boldsymbol{\psi}_{\mathbf{q}}\\
&\quad=[N_p!]^{-1}[\mathscr{Z}_0]^{N_p}\sum_{\mathbf{k},\,\mathbf{q}}\boldsymbol{\psi}_{\mathbf{k}}\cdot\\
&\qquad\sum_{\substack{\alpha,\,n\\ \beta,\,m}}\left\langle e^{-i\left(\mathbf{k}\cdot\mathbf{r}_0^\alpha+\mathbf{q}\cdot\mathbf{r}_0^\beta\right)}\right\rangle_0\left\langle\mathbf{b}_n^\alpha\,\mathbf{b}_m^\beta\, e^{-i\left(\mathbf{k}\cdot\sum_i^n\mathbf{b}_i^\alpha+\mathbf{q}\cdot\sum_j^m\mathbf{b}_j^\beta\right)}\right\rangle_0\cdot\boldsymbol{\psi}_{\mathbf{q}}.
\end{aligned} \tag{2.50}$$

We then break the second sum into two sums: one sum to cater for those summation terms in which $\alpha=\beta$, and the other sum to cater for all other

[5] We can obtain the expression for the Kronecker-delta in the following manner: the Fourier transform of a function, say $f(\mathbf{r})$, is

$$f_{\mathbf{k}}\;=\;\int\frac{\mathrm{d}^3r}{\Omega}\,e^{i\mathbf{k}\cdot\mathbf{r}}\,f(\mathbf{r})\;=\;\int\frac{\mathrm{d}^3r}{\Omega}\,e^{i\mathbf{k}\cdot\mathbf{r}}\sum_{\mathbf{q}}f_{\mathbf{q}}\,e^{-i\mathbf{q}\cdot\mathbf{r}}\;=\;\sum_{\mathbf{q}}f_{\mathbf{q}}\Big(\int\frac{\mathrm{d}^3r}{\Omega}\,e^{i(\mathbf{k}-\mathbf{q})\cdot\mathbf{r}}\Big), \tag{2.46}$$

which implies the form of the Kronecker-delta must be given by

$$\delta_{\mathbf{k},\,\mathbf{q}}=\int\frac{\mathrm{d}^3r}{\Omega}\,e^{i(\mathbf{k}-\mathbf{q})\cdot\mathbf{r}}. \tag{2.47}$$

summation terms. The right-hand side of the above equation then becomes

$$
\begin{aligned}
&[N_p!]^{-1}[\mathscr{Z}_0]^{N_p}\sum_{\mathbf{k},\,\mathbf{q}}\Bigg[\boldsymbol{\psi}_{\mathbf{k}}\cdot\sum_{\substack{\alpha\\ n,\,m}}\Big\langle e^{-i(\mathbf{k}+\mathbf{q})\cdot\mathbf{r}_0^{\alpha}}\Big\rangle_0\Big\langle\mathbf{b}_n^{\alpha}\,\mathbf{b}_m^{\alpha}\,e^{-i\left(\mathbf{k}\cdot\sum_i^n\mathbf{b}_i^{\alpha}+\mathbf{q}\cdot\sum_j^m\mathbf{b}_j^{\alpha}\right)}\Big\rangle_0\cdot\boldsymbol{\psi}_{\mathbf{q}}\\
&\qquad+\boldsymbol{\psi}_{\mathbf{k}}\cdot\sum_{\substack{\alpha\neq\beta\\ n,\,m}}\Big\langle e^{-i\left(\mathbf{k}\cdot\mathbf{r}_0^{\alpha}+\mathbf{q}\cdot\mathbf{r}_0^{\beta}\right)}\Big\rangle_0\Big\langle\mathbf{b}_n^{\alpha}\,\mathbf{b}_m^{\beta}\,e^{-i\left(\mathbf{k}\cdot\sum_i^n\mathbf{b}_i^{\alpha}+\mathbf{q}\cdot\sum_j^m\mathbf{b}_j^{\beta}\right)}\Big\rangle_0\cdot\boldsymbol{\psi}_{\mathbf{q}}\Bigg]\\
&=[N_p!]^{-1}[\mathscr{Z}_0]^{N_p}\sum_{\mathbf{k},\,\mathbf{q}}\Bigg[\boldsymbol{\psi}_{\mathbf{k}}\cdot\sum_{\substack{\alpha\\ n,\,m}}\delta_{\mathbf{k},\,\text{-}\mathbf{q}}\Big\langle\mathbf{b}_n^{\alpha}\,\mathbf{b}_m^{\alpha}\,e^{-i\left(\mathbf{k}\cdot\sum_i^n\mathbf{b}_i^{\alpha}+\mathbf{q}\cdot\sum_j^m\mathbf{b}_j^{\alpha}\right)}\Big\rangle_0\cdot\boldsymbol{\psi}_{\mathbf{q}}\\
&\qquad+\boldsymbol{\psi}_{\mathbf{k}}\cdot\sum_{\substack{\alpha\neq\beta\\ n,\,m}}\delta_{\mathbf{k},\,0}\,\delta_{\mathbf{q},\,0}\Big\langle\mathbf{b}_n^{\alpha}\,\mathbf{b}_m^{\beta}\,e^{-i\left(\mathbf{k}\cdot\sum_i^n\mathbf{b}_i^{\alpha}+\mathbf{q}\cdot\sum_j^m\mathbf{b}_j^{\beta}\right)}\Big\rangle_0\cdot\boldsymbol{\psi}_{\mathbf{q}}\Bigg].
\end{aligned}
\tag{2.51}
$$

Summation over $\mathbf{q}$ (and $\mathbf{k}$ in the second sum) gives

$$
\begin{aligned}
&[N_p!]^{-1}[\mathscr{Z}_0]^{N_p}\Bigg[\sum_{\mathbf{k}}\boldsymbol{\psi}_{\mathbf{k}}\cdot\sum_{\substack{\alpha\\ n,\,m}}\Big\langle\mathbf{b}_n^{\alpha}\,\mathbf{b}_m^{\alpha}\,e^{-i\mathbf{k}\cdot\left(\sum_i^n\mathbf{b}_i^{\alpha}-\sum_j^m\mathbf{b}_j^{\alpha}\right)}\Big\rangle_0\cdot\boldsymbol{\psi}_{\text{-}\mathbf{k}}\\
&\qquad+\boldsymbol{\psi}_0\cdot\sum_{\substack{\alpha\neq\beta\\ n,\,m}}\big\langle\mathbf{b}_n^{\alpha}\,\mathbf{b}_m^{\beta}\big\rangle_0\cdot\boldsymbol{\psi}_0\Bigg].
\end{aligned}
\tag{2.52}
$$

All the terms in the first sum over α are identical, and since α runs from 1 to N_p, we can replace the sum over α by a multiplicative factor N_p:

$$
\begin{aligned}
&[N_p!]^{-1}[\mathscr{Z}_0]^{N_p}\Bigg[\sum_{\mathbf{k}}\boldsymbol{\psi}_{\mathbf{k}}\cdot N_p\sum_{n,\,m}\Big\langle\mathbf{b}_n\,\mathbf{b}_m\,e^{-i\mathbf{k}\cdot(\mathbf{r}_n-\mathbf{r}_m)}\Big\rangle_0\cdot\boldsymbol{\psi}_{\text{-}\mathbf{k}}\\
&\qquad+\boldsymbol{\psi}_0\cdot\sum_{\substack{\alpha\neq\beta\\ n,\,m}}\big\langle\mathbf{b}_n^{\alpha}\big\rangle_0\big\langle\mathbf{b}_m^{\beta}\big\rangle_0\cdot\boldsymbol{\psi}_0\Bigg].
\end{aligned}
\tag{2.53}
$$

The last term vanishes since $\langle\mathbf{b}_n^{\alpha}\rangle_0=0$. We also define a new quantity called the *bond-matrix structure function* for the Gaussian chain,

$$
\mathbf{G}^0(\mathbf{k})=\sum_{n,\,m}\Big\langle\mathbf{b}_n\mathbf{b}_m\,e^{-i\mathbf{k}\cdot(\mathbf{r}_n-\mathbf{r}_m)}\Big\rangle_0\,. \tag{2.54}
$$

Thus finally the third $\mathbf{b}$ integral in equation (2.40) gives

$$
[N_p!]^{-1}[\mathscr{Z}_0]^{N_p}N_p\sum_{\mathbf{k}}\boldsymbol{\psi}_{\mathbf{k}}\cdot\mathbf{G}^0(\mathbf{k})\cdot\boldsymbol{\psi}_{\text{-}\mathbf{k}}, \tag{2.55}
$$

and equation (2.40) becomes

$$\begin{aligned} e^{-\beta H_0(\{\mathbf{u_k}\})} &\approx [N_p!]^{-1}[\mathscr{Z}_0]^{N_p} \int \mathscr{D}\boldsymbol{\psi} \exp\left[i \sum_{\mathbf{k}} \boldsymbol{\psi}_{\mathbf{k}} \cdot \mathbf{u}_{-\mathbf{k}} \right] \\ &\qquad \times \left(1 - \frac{N_p}{2\Omega^2} \sum_{\mathbf{k}} \boldsymbol{\psi}_{\mathbf{k}} \cdot \mathbf{G}^0(\mathbf{k}) \cdot \boldsymbol{\psi}_{-\mathbf{k}} \right) \\ &\approx [N_p!]^{-1}[\mathscr{Z}_0]^{N_p} \int \mathscr{D}\boldsymbol{\psi} \exp\left[i \sum_{\mathbf{k}} \boldsymbol{\psi}_{\mathbf{k}} \cdot \mathbf{u}_{-\mathbf{k}} \right. \\ &\qquad \left. - \frac{N_p}{2\Omega^2} \sum_{\mathbf{k}} \boldsymbol{\psi}_{\mathbf{k}} \cdot \mathbf{G}^0(\mathbf{k}) \cdot \boldsymbol{\psi}_{-\mathbf{k}} \right]. \end{aligned} \tag{2.56}$$

In the second approximation above we have remembered our previous assumption that fluctuations of the auxiliary field, $\boldsymbol{\psi}_{\mathbf{k}}$, are small. Before proceeding to do the integral over $\boldsymbol{\psi}_{\mathbf{k}}$, let us take note of the following properties of the matrix $\mathbf{G}^0(\mathbf{k})$: we first observe from the sum in equation (2.54) that

$$\mathbf{G}^0(-\mathbf{k}) = \left[\mathbf{G}^0(\mathbf{k})\right]^*, \tag{2.57}$$

and second, if $\left[\mathbf{G}^0(\mathbf{k})\right]^{i\,j}$ denotes the ij-th matrix element of $\mathbf{G}^0(\mathbf{k})$ then

$$\left[\mathbf{G}^0(\mathbf{k})\right]^{i\,j} = \sum_{n,\,m} \left\langle {b_n}^i \, {b_m}^j \, e^{-i\mathbf{k}\cdot(\mathbf{r}_n - \mathbf{r}_m)} \right\rangle_0. \tag{2.58}$$

Since n and m are dummy indices we might as well swap them. This swapping is tantamount to a reordering of the summation terms and yields

$$\begin{aligned} \left[\mathbf{G}^0(\mathbf{k})\right]^{i\,j} &= \sum_{n,\,m} \left\langle {b_m}^i \, {b_n}^j \, e^{i\mathbf{k}\cdot(\mathbf{r}_n - \mathbf{r}_m)} \right\rangle_0 \\ &= \left(\sum_{n,\,m} \left\langle {b_n}^j \, {b_m}^i \, e^{-i\mathbf{k}\cdot(\mathbf{r}_n - \mathbf{r}_m)} \right\rangle_0 \right)^* \\ &= \left(\left[\mathbf{G}^0(\mathbf{k})\right]^{j\,i} \right)^*. \end{aligned} \tag{2.59}$$

So $\mathbf{G}^0(\mathbf{k})$ is an hermitian matrix, and we conclude from equations (2.57) and (2.59) that

$$\mathbf{G}^0(\mathbf{k}) = \left[\mathbf{G}^0(-\mathbf{k})\right]^{\mathrm{T}}. \tag{2.60}$$

Hence the the second sum in equation (2.56) may be rewritten as

$$\begin{aligned}
&\sum_{\mathbf{k}} \boldsymbol{\psi}_{\mathbf{k}} \cdot \mathbf{G}^0(\mathbf{k}) \cdot \boldsymbol{\psi}_{\text{-}\mathbf{k}} \\
&\quad = \mathbf{u}_0 \cdot \mathbf{G}^0(0) \cdot \mathbf{u}_0 + \sum_{\mathbf{k}>0} \left(\boldsymbol{\psi}_{\mathbf{k}} \cdot \mathbf{G}^0(\mathbf{k}) \cdot \boldsymbol{\psi}_{\text{-}\mathbf{k}} + \boldsymbol{\psi}_{\text{-}\mathbf{k}} \cdot \mathbf{G}^0(\text{-}\mathbf{k}) \cdot \boldsymbol{\psi}_{\mathbf{k}} \right) \\
&\quad = \mathbf{u}_0 \cdot \mathbf{G}^0(0) \cdot \mathbf{u}_0 + \sum_{\mathbf{k}>0} \left(\boldsymbol{\psi}_{\mathbf{k}} \cdot \mathbf{G}^0(\mathbf{k}) \cdot \boldsymbol{\psi}_{\text{-}\mathbf{k}} + \boldsymbol{\psi}_{\mathbf{k}} \cdot \left[\mathbf{G}^0(\text{-}\mathbf{k}) \right]^{\mathrm{T}} \cdot \boldsymbol{\psi}_{\text{-}\mathbf{k}} \right) \\
&\quad = \mathbf{u}_0 \cdot \mathbf{G}^0(0) \cdot \mathbf{u}_0 + 2 \sum_{\mathbf{k}>0} \boldsymbol{\psi}_{\mathbf{k}} \cdot \mathbf{G}^0(\mathbf{k}) \cdot \boldsymbol{\psi}_{\text{-}\mathbf{k}}.
\end{aligned} \tag{2.61}$$

Using the rewritten sum in equation (2.61), equation (2.56) becomes

$$\begin{aligned}
e^{\text{-}\beta H_0(\{\mathbf{u_k}\})} \approx [N_p!]^{\text{-}1} [\mathscr{Z}_0]^{N_p} & \\
\times \int \frac{\mathrm{d}^3\psi_0}{(2\pi)^3} \exp \left[\text{-}\boldsymbol{\psi}_0 \cdot \left\{ \frac{N_p}{2\Omega^2} \, \mathbf{G}^0(0) \right\} \cdot \boldsymbol{\psi}_0 + i\boldsymbol{\psi}_0 \cdot \mathbf{u}_0 \right] & \\
\times \int \left[\prod_{\mathbf{k}>0} \frac{\mathrm{d}^6\psi_{\mathbf{k}}}{\pi^6} \right] \exp \left[\text{-} \sum_{\mathbf{k}>0} \boldsymbol{\psi}_{\mathbf{k}} \cdot \left\{ \frac{N_p}{\Omega^2} \, \mathbf{G}^0(\mathbf{k}) \right\} \cdot \boldsymbol{\psi}_{\text{-}\mathbf{k}} \right. & \\
\left. + \sum_{\mathbf{k}>0} (i\boldsymbol{\psi}_{\mathbf{k}} \cdot \mathbf{u}_{\text{-}\mathbf{k}} + i\boldsymbol{\psi}_{\text{-}\mathbf{k}} \cdot \mathbf{u}_{\mathbf{k}}) \right], &
\end{aligned} \tag{2.62}$$

enabling us to perform the integral over $\{\boldsymbol{\psi}_{\mathbf{k}}\}$:

$$\begin{aligned}
&e^{\text{-}\beta H_0(\{\mathbf{u_k}\})} \approx [N_p!]^{\text{-}1} [\mathscr{Z}_0]^{N_p} \\
&\times \left\{ \frac{1}{(2\pi)^3} \sqrt{\frac{(2\pi)^3}{\det \mathbf{G}^0(0)} \left(\frac{\Omega^2}{N_p} \right)^3} \exp \left[\text{-}\frac{1}{2} \mathbf{u}_0 \cdot \frac{\Omega^2}{N_p} \left[\mathbf{G}^0(0) \right]^{\text{-}1} \cdot \mathbf{u}_0 \right] \right\} \\
&\times \left\{ \left[\prod_{\mathbf{k}>0} \frac{1}{\pi^6} \frac{\pi^3}{\det \mathbf{G}^0(\mathbf{k})} \left(\frac{\Omega^2}{N_p} \right)^3 \right] \exp \left[\text{-} \sum_{\mathbf{k}>0} \mathbf{u}_{\mathbf{k}} \cdot \left\{ \frac{\Omega^2}{N_p} \left[\mathbf{G}^0(\mathbf{k}) \right]^{\text{-}1} \right\} \cdot \mathbf{u}_{\text{-}\mathbf{k}} \right] \right\}
\end{aligned} \tag{2.63}$$

where $\left[\mathbf{G}^0(\mathbf{k}) \right]^{\text{-}1}$ denotes the inverse of $\mathbf{G}^0(\mathbf{k})$. Since the inverse of an hermitian matrix is also hermitian, we finally have:

$$e^{\text{-}\beta H_0(\{\mathbf{u_k}\})} = \text{a constant} \times \exp \left[\text{-}\frac{\Omega^2}{2N_p} \sum_{\mathbf{k}} \mathbf{u}_{\mathbf{k}} \cdot \left[\mathbf{G}^0(\mathbf{k}) \right]^{\text{-}1} \cdot \mathbf{u}_{\text{-}\mathbf{k}} \right]. \tag{2.64}$$

We point out here that because we were forced to introduce an approximation in the course of this derivation, even though we started out with a melt of Gaussian chains, the above result then applies to polymer chains that are only *nearly* Gaussian.

2.7 The Gaussian Chain's Bond-Matrix Structure Function

From equation (2.54) we have

$$\begin{aligned}
\mathbf{G}^0(\mathbf{k}) &= \sum_{n,\,m} \Big\langle \mathbf{b}_n\, \mathbf{b}_m\, e^{-i\mathbf{k}\cdot(\mathbf{r}_n-\mathbf{r}_m)} \Big\rangle_0 \\
&= \sum_{n,\,m} \Big\langle \mathbf{b}_n\, \mathbf{b}_m\, e^{-i\mathbf{k}\cdot\left(\sum_{i=1}^{n}\mathbf{b}_i-\sum_{j=1}^{m}\mathbf{b}_j\right)} \Big\rangle_0 \\
&= \left(\sum_{n>m}+\sum_{n<m}+\sum_{n=m}\right) \Big\langle \mathbf{b}_n\, \mathbf{b}_m\, e^{-i\mathbf{k}\cdot\left(\sum_{i=1}^{n}\mathbf{b}_i-\sum_{j=1}^{m}\mathbf{b}_j\right)} \Big\rangle_0 \\
&= \sum_{n>m} \Big\langle \mathbf{b}_n\, \mathbf{b}_m\, e^{-i\mathbf{k}\cdot\sum_{i=m+1}^{n}\mathbf{b}_i} \Big\rangle_0 \\
&\quad + \sum_{n<m} \Big\langle \mathbf{b}_n\, \mathbf{b}_m\, e^{i\mathbf{k}\cdot\sum_{i=n+1}^{m}\mathbf{b}_i} \Big\rangle_0 + \sum_{n=m} \langle \mathbf{b}_n\, \mathbf{b}_m \rangle_0
\end{aligned} \tag{2.65}$$

Since for the Gaussian chain, the $\mathbf{b}_i$'s are independent of each other, the terms of the first sum has such factors as

$$\sum_{n>m} \big\langle \mathbf{b}_n\, e^{-i\mathbf{k}\cdot\mathbf{b}_n} \big\rangle_0 \langle \mathbf{b}_m \rangle_0 \prod_{i=m+1}^{n-1} \big\langle e^{-i\mathbf{k}\cdot\mathbf{b}_i} \big\rangle_0 \tag{2.66}$$

which vanishes because $\langle \mathbf{b}_m \rangle_0 = 0$. Similarly the second sum vanishes because the factor $\langle \mathbf{b}_n \rangle_0 = 0$. Thus from the definition of $\langle \ldots \rangle_0$ given in equation (2.43)

$$\begin{aligned}
\mathbf{G}^0(\mathbf{k}) &= \sum_n \langle \mathbf{b}_n\, \mathbf{b}_n \rangle_0 \\
&= N \left[\int \mathrm{d}^3 b\, \mathbf{b}\, \mathbf{b}\, \exp\left[-a\mathbf{b}^2\right]\right] \left[\int \mathrm{d}^3 b\, \exp\left[-a\mathbf{b}^2\right]\right]^{N-1} \\
&\quad \times \left[\int \mathrm{d}^3 b\, \exp\left[-a\mathbf{b}^2\right]\right]^{-\frac{3N}{2}} \\
&= N \left(\frac{\pi}{a}\right)^{-\frac{3}{2}} \left[\int \mathrm{d}^3 b\, \mathbf{b}\, \mathbf{b}\, \exp\left[-a\mathbf{b}^2\right]\right].
\end{aligned} \tag{2.67}$$

Thus an element of the matrix $\mathbf{G}^0(\mathbf{k})$ is

$$\begin{aligned}
\left[\mathbf{G}^0(\mathbf{k})\right]^{i\,j} &= N \left(\frac{\pi}{a}\right)^{-\frac{3}{2}} \left[\int \mathrm{d}^3 b\, b^i\, b^j\, \exp\left[-a\mathbf{b}^2\right]\right] \\
&= N \left(\frac{\pi}{a}\right)^{-\frac{3}{2}} \left[\int_{-\infty}^{\infty} \mathrm{d}b\, \exp\left[-ab^2\right]\right]^2 \left[\int_{-\infty}^{\infty} \mathrm{d}b\, b^2\, \exp\left[-ab^2\right]\right] \delta^{i\,j} \\
&= N \left(\frac{\pi}{a}\right)^{-\frac{1}{2}} \left[-\frac{\mathrm{d}}{\mathrm{d}a}\left(\sqrt{\frac{\pi}{a}}\right)\right] \delta^{i\,j} \\
&= \frac{N\,\delta^{i\,j}}{2a} \quad = \quad \frac{N\,l^2\,\delta^{i\,j}}{3}.
\end{aligned} \tag{2.68}$$

The bond-matrix structure function for the Gaussian chain is therefore

$$\mathbf{G}^0(\mathbf{k}) = G^0(\mathbf{k})\,\mathbb{1}, \tag{2.69}$$

where

$$G^0(\mathbf{k}) = \frac{N\,l^2}{3}. \tag{2.70}$$

2.8 The Fourier Transform of the Exchange Interaction

From equations (2.23) and (2.24) we have

$$\mathbf{J}(\mathbf{r}) \equiv \frac{\lambda_B\,C}{2\,\beta}\,\frac{\mathbb{1} - 3\,\hat{\mathbf{r}}\,\hat{\mathbf{r}}}{|\mathbf{r}|^3}\,(1 - \delta_{r,\,0}). \tag{2.71}$$

Its Fourier transform is

$$\mathbf{J}_{\mathbf{k}} = \frac{\lambda_B\,C}{2\,\beta}\int_{\Omega}\frac{\mathrm{d}^3 r}{\Omega}\,e^{i\mathbf{k}\cdot\mathbf{r}}\,\frac{\mathbb{1} - 3\,\hat{\mathbf{r}}\,\hat{\mathbf{r}}}{|\mathbf{r}|^3}\,(1 - \delta_{r,\,0}). \tag{2.72}$$

It is difficult to evaluate this integral directly. However we may obtain $\mathbf{J}_{\mathbf{k}}$ by first choosing a suitable basis for expressing its matrix elements. We choose the following orthonormal basis: $\left\{\hat{\mathbf{k}},\ \hat{\mathbf{k}}_{\perp}^{(1)},\ \hat{\mathbf{k}}_{\perp}^{(2)}\right\}$ where $\hat{\mathbf{k}}$ is the unit vector along the $\mathbf{k}$-direction. Since $\mathbf{r}$ in the integral above is a dummy variable, we are at liberty to choose the $\mathbf{r}$-space reference axes, and we choose these axes so that the z-axis in $\mathbf{r}$-space always coincides with $\mathbf{k}$. Then using spherical-polar coordinates (r, θ, φ), we have

$$\hat{\mathbf{k}}\cdot\hat{\mathbf{r}} = \cos\theta, \qquad \hat{\mathbf{k}}_{\perp}^{(1)}\cdot\hat{\mathbf{r}} = \sin\varphi\,\sin\theta, \qquad \hat{\mathbf{k}}_{\perp}^{(2)}\cdot\hat{\mathbf{r}} = \cos\varphi\,\sin\theta. \tag{2.73}$$

The diagonal terms of $\mathbf{J}_{\mathbf{k}}$ are then

$$\begin{aligned}
\hat{\mathbf{k}}\cdot\mathbf{J}_{\mathbf{k}}\cdot\hat{\mathbf{k}} &= \frac{\lambda_B\,C}{2\,\beta}\int_{\Omega}\frac{\mathrm{d}^3 r}{\Omega}\,e^{ikr\cos\theta}\,\frac{1 - 3\cos^2\theta}{r^3}\,(1 - \delta_{r,\,0}),\\
\hat{\mathbf{k}}_{\perp}^{(1)}\cdot\mathbf{J}_{\mathbf{k}}\cdot\hat{\mathbf{k}}_{\perp}^{(1)} &= \frac{\lambda_B\,C}{2\,\beta}\int_{\Omega}\frac{\mathrm{d}^3 r}{\Omega}\,e^{ikr\cos\theta}\,\frac{1 - 3\sin^2\varphi\,\sin^2\theta}{r^3}\,(1 - \delta_{r,\,0}),\\
\hat{\mathbf{k}}_{\perp}^{(2)}\cdot\mathbf{J}_{\mathbf{k}}\cdot\hat{\mathbf{k}}_{\perp}^{(2)} &= \frac{\lambda_B\,C}{2\,\beta}\int_{\Omega}\frac{\mathrm{d}^3 r}{\Omega}\,e^{ikr\cos\theta}\,\frac{1 - 3\cos^2\varphi\,\sin^2\theta}{r^3}\,(1 - \delta_{r,\,0}).
\end{aligned} \tag{2.74}$$

It is easy to see that

$$\hat{\mathbf{k}}\cdot\mathbf{J}_{\mathbf{k}}\cdot\hat{\mathbf{k}} \;+\; \hat{\mathbf{k}}_{\perp}^{(1)}\cdot\mathbf{J}_{\mathbf{k}}\cdot\hat{\mathbf{k}}_{\perp}^{(1)} \;+\; \hat{\mathbf{k}}_{\perp}^{(2)}\cdot\mathbf{J}_{\mathbf{k}}\cdot\hat{\mathbf{k}}_{\perp}^{(2)} = 0. \tag{2.75}$$

Moreover, integration over φ is sufficient to establish that

$$\hat{\mathbf{k}}_{\perp}^{(1)}\cdot\mathbf{J}_{\mathbf{k}}\cdot\hat{\mathbf{k}}_{\perp}^{(1)} = \hat{\mathbf{k}}_{\perp}^{(2)}\cdot\mathbf{J}_{\mathbf{k}}\cdot\hat{\mathbf{k}}_{\perp}^{(2)}. \tag{2.76}$$

The off-diagonal matrix element (of $\mathbf{J_k}$):

$$\hat{\mathbf{k}} \cdot \mathbf{J_k} \cdot \hat{\mathbf{k}}_{\perp}^{(1)} = \frac{\lambda_B\, C}{2\,\beta} \int_{\Omega} \frac{\mathrm{d}^3 r}{\Omega}\, e^{ikr\cos\theta}\, \frac{\text{-}3\sin\varphi\, \sin\theta\, \cos\theta}{r^3}\, (1-\delta_{r,\,0}). \tag{2.77}$$

vanishes after integration over φ. Similarly all other off-diagonal elements vanish.

The aforementioned properties (see equations (2.75) and (2.76)) of the remaining diagonal structure are immediately incorporated in an expression of the form:

$$\mathbf{J_k} = A(\mathbf{k}) \left(\mathbb{1} - 3\,\hat{\mathbf{k}}\,\hat{\mathbf{k}} \right), \tag{2.78}$$

where $A(\mathbf{k})$ is a scalar function of $\mathbf{k}$ that can be determined as follows. From equations (2.74) and (2.78)

$$\hat{\mathbf{k}} \cdot \mathbf{J_k} \cdot \hat{\mathbf{k}} = -2\,A(\mathbf{k}) = \frac{\lambda_B\, C}{2\,\beta} \int_{\Omega} \frac{\mathrm{d}^3 r}{\Omega}\, e^{ikr\cos\theta}\, \frac{1-3\cos^2\theta}{r^3}\, (1-\delta_{r,\,0}). \tag{2.79}$$

Therefore,

$$\begin{aligned} A(\mathbf{k}) &= \frac{\text{-}\lambda_B\, C}{4\,\beta} \int_{\Omega} \frac{\mathrm{d}^3 r}{\Omega}\, e^{ikr\cos\theta}\, \frac{1-3\cos^2\theta}{r^3}\, (1-\delta_{r,\,0}) \\ &= \frac{\text{-}2\pi\lambda_B\, C}{4\,\beta\,\Omega} \int_{r=0}^{\infty} \mathrm{d}r \int_{\cos\theta=\text{-}1}^{1} \mathrm{d}(\cos\theta)\, r^2\, e^{ikr\cos\theta}\, \frac{1-3\cos^2\theta}{r^3}\, (1-\delta_{r,\,0}) \end{aligned} \tag{2.80}$$

To perform the θ integral, let us first consider the function

$$I(g) = \int_{x=\text{-}1}^{1} \mathrm{d}x\, x^2\, e^{igx}. \tag{2.81}$$

Successive integration by parts yields for non-zero g:

$$I(g) = \left(\frac{x^2\, e^{igx}}{ig} + \frac{2x\, e^{igx}}{g^2} - \frac{2e^{igx}}{ig^3} \right) \Bigg|_{x=\text{-}1}^{1} = \frac{2\sin g}{g} \left(1 - \frac{2}{g^2} \right) + \frac{4\cos g}{g^2}, \tag{2.82}$$

while $I(0) = 2/3$. Applying this result to equation (2.80) (by effecting the substitutions $g \to kr$ and $x \to \cos\theta$) yields for $k \neq 0$

$$A(\mathbf{k}) = \frac{2\pi\lambda_B\, C}{\beta\,\Omega} \int_{r=0}^{\infty} \mathrm{d}r \left[\frac{\sin(kr)}{kr^2} \left(1 - \frac{3}{k^2 r^2} \right) + \frac{3\cos(kr)}{k^2 r^3} \right] (1-\delta_{r,\,0}), \tag{2.83}$$

and

$$A(0) = 0. \tag{2.84}$$

We may use integration by parts to solve the remaining integral in equation (2.83):

$$\begin{aligned}
\int_{r=0}^{\infty} \mathrm{d}r \frac{\sin(kr)}{kr^2}\,(1-\delta_{r,0}) &= \lim_{r\to 0}\left[\int_r^{\infty}\mathrm{d}p\,\frac{\cos(kp)}{p} - \frac{\sin(kp)}{kp}\Big|_{p=r}^{\infty}\right] \\
-\int_{r=0}^{\infty} \mathrm{d}r \frac{3\sin(kr)}{k^3r^4}\,(1-\delta_{r,0}) &= \lim_{r\to 0}\frac{1}{2}\left[\int_r^{\infty}\mathrm{d}p\,\frac{\cos(kp)}{p}\right. \\
&\qquad \left. - \frac{\sin(kp)}{kp} + \frac{\cos(kp)}{k^2p^2} + \frac{2\sin(kp)}{k^3p^3}\Big|_{p=r}^{\infty}\right] \qquad (2.85)\\
\int_{r=0}^{\infty} \mathrm{d}r \frac{3\cos(kr)}{k^2r^3}\,(1-\delta_{r,0}) &= \lim_{r\to 0}\frac{3}{2}\left[-\int_r^{\infty}\mathrm{d}p\,\frac{\cos(kp)}{p}\right. \\
&\qquad \left. + \frac{\sin(kp)}{kp} - \frac{\cos(kp)}{k^2p^2}\Big|_{p=r}^{\infty}\right].
\end{aligned}$$

Adding up these results yields

$$\lim_{r\to 0}\left[\frac{\cos(kr)}{k^2r^2} - \frac{\sin(kr)}{k^3r^3}\right] = \lim_{r\to 0}\left[\frac{1-\frac{k^2r^2}{2}}{k^2r^2} - \frac{kr-\frac{k^3r^3}{3!}}{k^3r^3}\right] = \frac{-1}{3}. \qquad (2.86)$$

Thus from equations (2.83) and (2.84), we have

$$A(\mathbf{k}) = \frac{-2\pi\lambda_B\, C}{3\beta\,\Omega}, \quad \text{for } \mathbf{k}\neq 0 \quad \text{and} \quad A(0)=0, \qquad (2.87)$$

and finally from equation (2.78) we have the result

$$\boxed{\mathbf{J}_{\mathbf{k}} = \frac{-2\pi\lambda_B\, C}{3\beta\,\Omega}\left(\mathbb{1} - 3\,\hat{\mathbf{k}}\,\hat{\mathbf{k}}\right), \quad \text{for } \mathbf{k}\neq 0 \quad \text{and} \quad \mathbf{J}_0 = 0.} \qquad (2.88)$$

2.9 Analyzing the Collective Hamiltonian

Gathering the results obtained from equations (2.21), (2.26), and (2.64), our partition function is

$$\begin{aligned}
\mathscr{Z}_c &= \int \mathscr{D}\mathbf{u}\; e^{-\beta[H_0(\{\mathbf{u_k}\})+U(\{\mathbf{u_k}\})]} \\
&\propto \int \mathscr{D}\mathbf{u}\; e^{-\Omega^2\sum_{\mathbf{k}}\mathbf{u_k}\cdot\left[\frac{1}{2N_p}\left[\mathbf{G}^0(\mathbf{k})\right]^{-1}+\beta\mathbf{J_k}\right]\cdot\mathbf{u_{-k}}+\mathrm{O}\left(\mathbf{u_k}^3\right)}.
\end{aligned} \qquad (2.89)$$

Therefore the bond-vector structure function is the matrix

$$\langle \mathbf{u_{-k}}\,\mathbf{u_k}\rangle = \Omega^{-2}\left[\frac{1}{N_p}\left[\mathbf{G}^0(\mathbf{k})\right]^{-1} + 2\beta\mathbf{J_k}\right]^{-1}, \qquad (2.90)$$

which is valid for those values of the melt parameters and for those values of $\mathbf{k}$ that make the matrix positive definite and hence keep the Gaussian integral in equation (2.89) from diverging. Substituting the expression for $\mathbf{G}^0(\mathbf{k})$ (equation (2.69)) and for $\mathbf{J}_\mathbf{k}$ (equation (2.88)) into the equation above we obtain

$$\langle \mathbf{u}_{\text{-}\mathbf{k}}\, \mathbf{u}_\mathbf{k} \rangle = \Omega^{\text{-}2} \left[\frac{3}{N_p N l^2} - \frac{4\pi\lambda_B C}{3\Omega} + \frac{4\pi\lambda_B C}{\Omega} \hat{\mathbf{k}}\,\hat{\mathbf{k}} \right]^{\text{-}1}. \tag{2.91}$$

We may apply the result of Appendix B to find the inverse of the matrix above which is of the form $\left(a\mathbb{1} + b\hat{\mathbf{k}}\,\hat{\mathbf{k}} \right)$ and we obtain

$$\frac{1}{a}\left(\mathbb{1} - \frac{b}{a+b} \hat{\mathbf{k}}\,\hat{\mathbf{k}} \right) \tag{2.92}$$

where

$$\begin{aligned} a &= \frac{\Omega(9\Omega - 4\pi\lambda_B C N N_p l^2)}{3 N N_p l^2}, \\ b &= 4\pi\lambda_B C \Omega. \end{aligned} \tag{2.93}$$

Thus we have found that the RPA bond-vector structure factor of our melt of dipolar polymers without excluded volume is independent of the value of k. Physically this means that correlations between dipoles are distributed equally over all length scales.

In the orthonormal basis, $\left\{ \hat{\mathbf{k}}, \hat{\mathbf{k}}_\perp^{(1)}, \hat{\mathbf{k}}_\perp^{(2)} \right\}$, first introduced in Section 2.8, $\langle \mathbf{u}_\mathbf{k}\, \mathbf{u}_{\text{-}\mathbf{k}} \rangle$ is a diagonal matrix

$$\langle \mathbf{u}_\mathbf{k}\, \mathbf{u}_{\text{-}\mathbf{k}} \rangle = \begin{pmatrix} (a+b)^{\text{-}1} & 0 & 0 \\ 0 & a^{\text{-}1} & 0 \\ 0 & 0 & a^{\text{-}1} \end{pmatrix} \tag{2.94}$$

where, using equations (2.93),

$$\begin{aligned} (a+b)^{\text{-}1} &= \frac{3 N N_p l^2}{\Omega(9\Omega + 8\pi\lambda_B C N N_p l^2)} \\ a^{\text{-}1} &= \frac{3 N N_p l^2}{\Omega(9\Omega - 4\pi\lambda_B C N N_p l^2)}. \end{aligned} \tag{2.95}$$

The positive definite property of $\langle \mathbf{u}_{\text{-}\mathbf{k}} \mathbf{u}_\mathbf{k} \rangle$ requires that each of the eigenvalues of $\langle \mathbf{u}_\mathbf{k} \mathbf{u}_{\text{-}\mathbf{k}} \rangle$ be positive. But

$$a^{-1} > 0 \quad \Longleftrightarrow \quad 9\Omega - 4\pi\lambda_B\, C\, N_p N l^2 > 0. \tag{2.96}$$

The above inequality specifies an upper limit for the average concentration of monomers, $\rho_0 = N N_p/\Omega$, at a temperature given by the Bjerrum length λ_B:

$$\rho_0 < \frac{9}{4\pi(\lambda_B\, C\, l^2)} \;=\; \rho_*. \tag{2.97}$$

We may regard ρ_* as a *critical concentration* above which the melt has a different phase which is not described by our model. Alternatively, given the average concentration of monomers, ρ_0, we can specify a 'critical temperature' given by

$$\lambda_{B*} = \frac{9}{4\pi(\rho_0 \, C \, l^2)}, \tag{2.98}$$

below which the phase of the melt described by our model breaks down. (Remember that λ_B is inversely proportional to the temperature of the melt.)

Note that for a given concentration of monomers, as the Bjerrum length λ_B approaches the critical Bjerrum length λ_{B*} from below, the eigenvalue a^{-1} diverges and hence correlations between the dipoles of the monomers in the melt also diverge at all length-scales (that is, all values of k). We suspect that this behaviour is due to the long-range character of the dipolar interaction potential. We shall investigate this idea in Chapter 5 by considering a screened dipolar interaction potential which reduces the long-range character of the original potential. Meanwhile, in the next chapter we investigate the effect of excluded volume on these results.

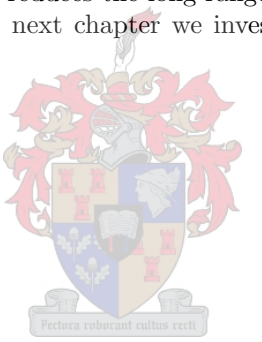

3. RPA WITH EXCLUDED-VOLUME INTERACTION

The treatment of the last chapter applies to a melt of so-called 'ghost' polymers since we neglected the fact that in real polymers long range interactions (interactions between non-neighbouring monomers) invariably include *steric effects*, that is, since a monomer has finite volume, other monomers cannot come into its own region. Without bothering about the details of this interaction now, let the interaction energy between two monomers at positions $\mathbf{r}_n^\alpha$ and $\mathbf{r}_m^\beta$ be represented by the function

$$\widetilde{V}\big(\mathbf{r}_n^\alpha - \mathbf{r}_m^\beta\big), \tag{3.1}$$

which we expect to be short-ranged, that is, $\widetilde{V}(\mathbf{r})$ has large positive values for small $\mathbf{r}$, but has very small values for large $\mathbf{r}$. Thus the total energy of steric interaction within the melt is

$$E(\{\mathbf{r}_n^\alpha\}) = \sum_{\substack{\alpha,\,\beta\\ n,\,m}} V\big(\mathbf{r}_n^\alpha - \mathbf{r}_m^\beta\big). \tag{3.2}$$

where

$$V\big(\mathbf{r}_n^\alpha - \mathbf{r}_m^\beta\big) = \frac{1}{2}\widetilde{V}\big(\mathbf{r}_n^\alpha - \mathbf{r}_m^\beta\big)\,(1 - \delta_{\alpha\,\beta}\,\delta_{n\,m}) \tag{3.3}$$

Proceeding in a manner analogous to the calculations of the last chapter, we shall continue to use the Fourier-space representation. Thus

$$V(\mathbf{r}) = \sum_{\mathbf{k}} V_{\mathbf{k}}\; e^{-i\mathbf{k}\cdot\mathbf{r}}, \tag{3.4}$$

where

$$V_{\mathbf{k}} = \int \frac{\mathrm{d}^3 r}{\Omega}\; e^{i\mathbf{k}\cdot\mathbf{r}}\; V(\mathbf{r}). \tag{3.5}$$

Now equation (3.2) may be rewritten as

$$\begin{aligned} E(\{\mathbf{r}_n^\alpha\}) &= \sum_{\substack{\alpha,\,\beta\\ n,\,m}} \sum_{\mathbf{k}} V_{\mathbf{k}}\; e^{-i\mathbf{k}\cdot\left(\mathbf{r}_n^\alpha - \mathbf{r}_m^\beta\right)} \\ &= \sum_{\mathbf{k}} V_{\mathbf{k}} \left[\sum_{\alpha,\,n} e^{-i\mathbf{k}\cdot\mathbf{r}_n^\alpha}\right]\left[\sum_{\beta,\,m} e^{i\mathbf{k}\cdot\mathbf{r}_m^\beta}\right] \\ &= \Omega^2 \sum_{\mathbf{k}} V_{\mathbf{k}}\,\rho_{\mathbf{k}}\,\rho_{-\mathbf{k}} \;\equiv\; E(\{\rho_{\mathbf{k}}\}). \end{aligned} \tag{3.6}$$

3.1 The Transformation

After including the excluded-volume interaction, the conformational partition function therefore becomes

$$\begin{aligned}\mathscr{Z}_c &= \int\mathscr{D}\mathbf{u}\int\mathscr{D}\rho\, e^{-\beta\, H_0(\{\rho_{\mathbf{k}},\,\mathbf{u}_{\mathbf{k}}\})}\, e^{-\beta\, U(\{\mathbf{u}_{\mathbf{k}}\})}\, e^{-\beta\, E(\{\rho_{\mathbf{k}}\})} \\ &= \int\mathscr{D}\mathbf{u}\int\mathscr{D}\rho\,\left[\int\mathscr{D}\mathbf{b}\prod_{\mathbf{k}>0}\delta\left(\rho_{\mathbf{k}}-\frac{1}{\Omega}\sum_{\alpha,\,n}e^{i\mathbf{k}\cdot\mathbf{r}_n^{\alpha}}\right)\times\right. \\ &\qquad\left.\prod_{\mathbf{k}\geq 0}\delta\left(\mathbf{u}_{\mathbf{k}}-\frac{1}{\Omega}\sum_{\alpha,\,n}e^{i\mathbf{k}\cdot\mathbf{r}_n^{\alpha}}\,\mathbf{b}_n^{\alpha}\right)\, e^{-\beta\, H_0(\{\mathbf{r}_n^{\alpha}\})}\, e^{-\beta\, U(\{\mathbf{r}_n^{\alpha}\})}\, e^{-\beta\, E(\{\mathbf{r}_n^{\alpha}\})}\right].\end{aligned} \tag{3.7}$$

Note that in the expression above a delta function over ρ_0-space has not been included because $\rho_0 = NN_p/\Omega$ (the mean concentration of monomers) does not fluctuate and hence it is not a microstate variable.

Since $E(\{\mathbf{r}_n^{\alpha}\})$ and $U(\{\mathbf{r}_n^{\alpha}\})$ are readily transformed into functions over collective state variables (see equations (3.6) and (2.26)). We need to transform the Gaussian chain energy, $H_0(\{\mathbf{b}_n^{\alpha}\})$, into a function $H_0(\{\rho_{\mathbf{k}},\,\mathbf{u}_{\mathbf{k}}\})$ over collective state variables:

$$\begin{aligned}e^{-\beta\, H_0(\{\rho_{\mathbf{k}},\,\mathbf{u}_{\mathbf{k}}\})} = \int\mathscr{D}\mathbf{b}\prod_{\mathbf{k}>0}\delta\left(\rho_{\mathbf{k}}-\frac{1}{\Omega}\sum_{\alpha,\,n}e^{i\mathbf{k}\cdot\mathbf{r}_n^{\alpha}}\right) \\ \times\prod_{\mathbf{k}>0}\delta^{(2)(3)}\left(\mathbf{u}_{\mathbf{k}}-\frac{1}{\Omega}\sum_{\alpha,\,n}e^{i\mathbf{k}\cdot\mathbf{r}_n^{\alpha}}\,\mathbf{b}_n^{\alpha}\right) \\ \times\,\delta^{(3)}\left(\mathbf{u}_0-\frac{1}{\Omega}\sum_{\alpha,\,n}\mathbf{b}_n^{\alpha}\right)\, e^{-\beta\, H_0(\{\mathbf{b}_n^{\alpha}\})}.\end{aligned} \tag{3.8}$$

The Fourier representation of the delta function over $\rho_{\mathbf{k}}$-space is as follows:

$$\begin{aligned}&\prod_{\mathbf{k}>0}\delta\left(\rho_{\mathbf{k}}-\frac{1}{\Omega}\sum_{\alpha,\,n}e^{i\mathbf{k}\cdot\mathbf{r}_n^{\alpha}}\right) \\ &\quad=\prod_{\mathbf{k}>0}\int\frac{\mathrm{d}^2\phi_{\mathbf{k}}}{\pi^2}\,\exp\left[i\left\{\phi_{\mathbf{k}}^{*}\left(\rho_{\mathbf{k}}-\frac{1}{\Omega}\sum_{\alpha,\,n}e^{i\mathbf{k}\cdot\mathbf{r}_n^{\alpha}}\right)\right.\right. \\ &\qquad\qquad\left.\left.+\;\phi_{\mathbf{k}}\left(\rho_{\mathbf{k}}^{*}-\frac{1}{\Omega}\sum_{\alpha,\,n}e^{-i\mathbf{k}\cdot\mathbf{r}_n^{\alpha}}\right)\right\}\right] \\ &\quad=\int\left[\prod_{\mathbf{k}>0}\frac{\mathrm{d}^2\phi_{\mathbf{k}}}{\pi^2}\right]\exp\left[i\sum_{\mathbf{k}\neq 0}\left(\phi_{\mathbf{k}}\,\rho_{\text{-}\mathbf{k}}-\frac{1}{\Omega}\sum_{\alpha,\,n}e^{-i\mathbf{k}\cdot\mathbf{r}_n^{\alpha}}\,\phi_{\mathbf{k}}\right)\right].\end{aligned} \tag{3.9}$$

Let us introduce the shorthand notation:

$$\int\mathscr{D}\phi\equiv\int\left[\prod_{\mathbf{k}>0}\frac{\mathrm{d}^2\phi_{\mathbf{k}}}{\pi^2}\right]. \tag{3.10}$$

Thus equation (3.8) becomes

$$e^{-\beta H_0(\{\rho_{\mathbf{k}},\,\mathbf{u}_{\mathbf{k}}\})} = \int\mathscr{D}\phi \int\mathscr{D}\boldsymbol{\psi}\ \exp\left[i\sum_{\mathbf{k}}\boldsymbol{\psi}_{\mathbf{k}}\cdot\mathbf{u}_{\text{-}\mathbf{k}} + i\sum_{\mathbf{k}\neq 0}\phi_{\mathbf{k}}\,\rho_{\text{-}\mathbf{k}}\right]$$
$$\times\int\mathscr{D}\mathbf{b}\exp\left[-\frac{i}{\Omega}\sum_{\mathbf{k}}\sum_{\alpha,\,n}e^{-i\mathbf{k}\cdot\mathbf{r}_n^{\alpha}}\,\boldsymbol{\psi}_{\mathbf{k}}\cdot\mathbf{b}_n^{\alpha} - \frac{i}{\Omega}\sum_{\mathbf{k}\neq 0}\sum_{\alpha,\,n}e^{-i\mathbf{k}\cdot\mathbf{r}_n^{\alpha}}\,\phi_{\mathbf{k}}\right]e^{-\beta H_0(\{\mathbf{b}_n^{\alpha}\})}. \tag{3.11}$$

Let us assume that the members of the sets $\{\phi_{\mathbf{k}}\}$ and $\{\boldsymbol{\psi}_{\mathbf{k}}\}$ are all very small so that we can expand the second exponential in the expression above to quadratic order in its argument:

$$\begin{aligned}
&\exp\left[-\frac{i}{\Omega}\sum_{\mathbf{k}}\sum_{\alpha,\,n}e^{-i\mathbf{k}\cdot\mathbf{r}_n^{\alpha}}\,\boldsymbol{\psi}_{\mathbf{k}}\cdot\mathbf{b}_n^{\alpha} - \frac{i}{\Omega}\sum_{\mathbf{k}\neq 0}\sum_{\alpha,\,n}e^{-i\mathbf{k}\cdot\mathbf{r}_n^{\alpha}}\,\phi_{\mathbf{k}}\right]\\
&\qquad\approx 1 - \left[\frac{i}{\Omega}\sum_{\mathbf{k},\,\alpha,\,n}e^{-i\mathbf{k}\cdot\mathbf{r}_n^{\alpha}}\,\boldsymbol{\psi}_{\mathbf{k}}\cdot\mathbf{b}_n^{\alpha} + \frac{i}{\Omega}\sum_{\mathbf{k}\neq 0}\sum_{\alpha,\,n}e^{-i\mathbf{k}\cdot\mathbf{r}_n^{\alpha}}\,\phi_{\mathbf{k}}\right]\\
&\qquad\quad - \frac{1}{2\Omega^2}\left[\sum_{\substack{\mathbf{k},\,\alpha,\,n\\ \mathbf{q},\,\beta,\,m}}e^{-i\left(\mathbf{k}\cdot\mathbf{r}_n^{\alpha}+\mathbf{q}\cdot\mathbf{r}_m^{\beta}\right)}\left(\boldsymbol{\psi}_{\mathbf{k}}\cdot\mathbf{b}_n^{\alpha}\right)\left(\boldsymbol{\psi}_{\mathbf{q}}\cdot\mathbf{b}_m^{\beta}\right)\right.\\
&\qquad\qquad + \sum_{\substack{\mathbf{k}\neq 0,\,\alpha,\,n\\ \mathbf{q}\neq 0,\,\beta,\,m}}e^{-i\left(\mathbf{k}\cdot\mathbf{r}_n^{\alpha}+\mathbf{q}\cdot\mathbf{r}_m^{\beta}\right)}\,\phi_{\mathbf{k}}\,\phi_{\mathbf{q}}\\
&\qquad\qquad\left. + \sum_{\substack{\mathbf{k},\,\alpha,\,n\\ \mathbf{q}\neq 0,\,\beta,\,m}}2e^{-i\left(\mathbf{k}\cdot\mathbf{r}_n^{\alpha}+\mathbf{q}\cdot\mathbf{r}_m^{\beta}\right)}\left(\boldsymbol{\psi}_{\mathbf{k}}\cdot\mathbf{b}_n^{\alpha}\right)\phi_{\mathbf{q}}\right]
\end{aligned} \tag{3.12}$$

The **b** integrals of the first, second, and fourth terms on the right-hand side of the equation above have been computed in the previous chapter. Thus we need tackle only the third, fifth and sixth terms. The third term gives the **b** integral:

$$\begin{aligned}
&\int\mathscr{D}\mathbf{b}\sum_{\mathbf{k}\neq 0,\,\alpha,\,n}\phi_{\mathbf{k}}\,\exp\left[-i\mathbf{k}\cdot\mathbf{r}_n^{\alpha} - a\sum_{\alpha,\,n}\left(\mathbf{b}_n^{\alpha}\right)^2\right]\\
&\qquad = [N_p!]^{-1}[\mathscr{Z}_0]^{N_p}\sum_{\mathbf{k}\neq 0}\phi_{\mathbf{k}}\sum_{\alpha,\,n}\left\langle e^{-i\mathbf{k}\cdot\mathbf{r}_n^{\alpha}}\right\rangle_0\\
&\qquad = [N_p!]^{-1}[\mathscr{Z}_0]^{N_p}\sum_{\mathbf{k}\neq 0}\phi_{\mathbf{k}}\sum_{\alpha,\,n}\left\langle e^{-i\mathbf{k}\cdot\mathbf{r}_0^{\alpha}}\right\rangle_0\left\langle e^{-i\mathbf{k}\cdot\sum_i^n\mathbf{b}_i^{\alpha}}\right\rangle_0\\
&\qquad = [N_p!]^{-1}[\mathscr{Z}_0]^{N_p}\sum_{\mathbf{k}\neq 0}\phi_{\mathbf{k}}\sum_{\alpha,\,n}\delta_{\mathbf{k},0}\left\langle e^{-i\mathbf{k}\cdot\sum_i^n\mathbf{b}_i^{\alpha}}\right\rangle_0 \;=\; 0.
\end{aligned} \tag{3.13}$$

The result of the last integral vanishes because the summation over $\mathbf{k}$ does not include $\mathbf{k} = 0$.

The fifth term in the right-hand side of equation (3.12) gives

$$\begin{aligned}
&\int \mathscr{D}\mathbf{b} \sum_{\substack{\mathbf{k}\neq 0,\,\alpha,\,n\\ \mathbf{q}\neq 0,\,\beta,\,m}} \phi_{\mathbf{k}}\,\phi_{\mathbf{q}} \exp\left[-i\big(\mathbf{k}\cdot\mathbf{r}_n^{\alpha}+\mathbf{q}\cdot\mathbf{r}_m^{\beta}\big) - a\sum_{\alpha,\,i}(\mathbf{b}_i^{\alpha})^2\right] \\
&\quad = [N_p!]^{-1}[\mathscr{Z}_0]^{N_p} \sum_{\substack{\mathbf{k}\neq 0\\ \mathbf{q}\neq 0}} \phi_{\mathbf{k}}\,\phi_{\mathbf{q}} \sum_{\substack{\alpha,\,n\\ \beta,\,m}} \left\langle e^{-i\left(\mathbf{k}\cdot\mathbf{r}_n^{\alpha}+\mathbf{q}\cdot\mathbf{r}_m^{\beta}\right)}\right\rangle_0 \\
&\quad = [N_p!]^{-1}[\mathscr{Z}_0]^{N_p} \sum_{\substack{\mathbf{k}\neq 0\\ \mathbf{q}\neq 0}} \phi_{\mathbf{k}}\,\phi_{\mathbf{q}} \\
&\qquad \sum_{\substack{\alpha,\,n\\ \beta,\,m}} \left\langle e^{-i\left(\mathbf{k}\cdot\mathbf{r}_0^{\alpha}+\mathbf{q}\cdot\mathbf{r}_0^{\beta}\right)}\right\rangle_0 \left\langle e^{-i\left(\mathbf{k}\cdot\sum_i^n \mathbf{b}_i^{\alpha}+\mathbf{q}\cdot\sum_j^m \mathbf{b}_j^{\beta}\right)}\right\rangle_0 .
\end{aligned} \tag{3.14}$$

To evaluate the ideal chain averages above we first split the summation over α and β into two sums: one sum over those terms in which $\alpha = \beta$ and the other sum over all the other terms:

$$\begin{aligned}
&[N_p!]^{-1}[\mathscr{Z}_0]^{N_p} \sum_{\substack{\mathbf{k}\neq 0\\ \mathbf{q}\neq 0}} \Bigg[\phi_{\mathbf{k}}\,\phi_{\mathbf{q}} \sum_{\substack{\alpha\\ n,\,m}} \left\langle e^{-i(\mathbf{k}+\mathbf{q})\cdot\mathbf{r}_0^{\alpha}}\right\rangle_0 \left\langle e^{-i\left(\mathbf{k}\cdot\sum_i^n \mathbf{b}_i^{\alpha}+\mathbf{q}\cdot\sum_j^m \mathbf{b}_j^{\alpha}\right)}\right\rangle_0 \\
&\qquad + \phi_{\mathbf{k}}\,\phi_{\mathbf{q}} \sum_{\substack{\alpha\neq\beta\\ n,\,m}} \left\langle e^{-i\left(\mathbf{k}\cdot\mathbf{r}_0^{\alpha}+\mathbf{q}\cdot\mathbf{r}_0^{\beta}\right)}\right\rangle_0 \left\langle e^{-i\left(\mathbf{k}\cdot\sum_i^n \mathbf{b}_i^{\alpha}+\mathbf{q}\cdot\sum_j^m \mathbf{b}_j^{\beta}\right)}\right\rangle_0\Bigg] \\
&= [N_p!]^{-1}[\mathscr{Z}_0]^{N_p} \sum_{\substack{\mathbf{k}\neq 0\\ \mathbf{q}\neq 0}} \Bigg[\phi_{\mathbf{k}}\,\phi_{\mathbf{q}} \sum_{\substack{\alpha\\ n,\,m}} \delta_{\mathbf{k},\,-\mathbf{q}} \left\langle e^{-i\left(\mathbf{k}\cdot\sum_i^n \mathbf{b}_i^{\alpha}+\mathbf{q}\cdot\sum_j^m \mathbf{b}_j^{\alpha}\right)}\right\rangle_0 \\
&\qquad + \phi_{\mathbf{k}}\,\phi_{\mathbf{q}} \sum_{\substack{\alpha\neq\beta\\ n,\,m}} \delta_{\mathbf{k},\,0}\,\delta_{\mathbf{q},\,0} \left\langle e^{-i\left(\mathbf{k}\cdot\sum_i^n \mathbf{b}_i^{\alpha}+\mathbf{q}\cdot\sum_j^m \mathbf{b}_j^{\beta}\right)}\right\rangle_0\Bigg].
\end{aligned} \tag{3.15}$$

All the terms in the first sum over α are identical, and since α runs from 1 to N_p, we can replace the sum over α by a multiplicative factor N_p:

$$[N_p!]^{-1}[\mathscr{Z}_0]^{N_p}\left[\sum_{\mathbf{k}\neq 0} \phi_{\mathbf{k}}\,\phi_{-\mathbf{k}} N_p \sum_{n,\,m} \left\langle e^{-i\mathbf{k}\cdot(\mathbf{r}_n-\mathbf{r}_m)}\right\rangle_0 + 0\right]. \tag{3.16}$$

Once again, the last term vanished since the summation over $\mathbf{k}$ and $\mathbf{q}$ does not include $\mathbf{k} = 0$ nor $\mathbf{q} = 0$. We also define a quantity called the *structure function* for the Gaussian chain,

$$g^0(\mathbf{k}) = \sum_{n,\,m} \left\langle e^{-i\mathbf{k}\cdot(\mathbf{r}_n-\mathbf{r}_m)}\right\rangle_0 . \tag{3.17}$$

Thus the **b** integral in equation (3.14) gives

$$[N_p!]^{-1}[\mathscr{Z}_0]^{N_p} N_p \sum_{\mathbf{k}\neq 0} g^0(\mathbf{k})\phi_{\mathbf{k}}\,\phi_{\text{-}\mathbf{k}}. \tag{3.18}$$

We will postpone the computation of $g^0(\mathbf{k})$ till the next section.

We are now left with the computation of the sixth term on the right-hand side of equation (3.12). The procedure is completely analogous to the preceding calculation and gives a **b** integral:

$$\begin{aligned}
&\int \mathscr{D}\mathbf{b} \sum_{\substack{\mathbf{k},\,\alpha,\,n\\ \mathbf{q}\neq 0,\,\beta,\,m}} (\boldsymbol{\psi}_{\mathbf{k}}\cdot\mathbf{b}_n^{\alpha})\,\phi_{\mathbf{q}} \exp\left[\text{-}i\big(\mathbf{k}\cdot\mathbf{r}_n^{\alpha}+\mathbf{q}\cdot\mathbf{r}_m^{\beta}\big) - a\sum_{\alpha,\,i}(\mathbf{b}_i^{\alpha})^2\right]\\
&\quad = [N_p!]^{-1}[\mathscr{Z}_0]^{N_p} \sum_{\mathbf{k},\,\mathbf{q}\neq 0} \phi_{\mathbf{q}}\,\boldsymbol{\psi}_{\mathbf{k}}\cdot \sum_{\substack{\alpha,\,n\\ \beta,\,m}} \Big\langle \mathbf{b}_n^{\alpha} e^{\text{-}i\left(\mathbf{k}\cdot\mathbf{r}_n^{\alpha}+\mathbf{q}\cdot\mathbf{r}_m^{\beta}\right)}\Big\rangle_0\\
&\quad = [N_p!]^{-1}[\mathscr{Z}_0]^{N_p} \sum_{\mathbf{k},\,\mathbf{q}\neq 0} \phi_{\mathbf{q}}\,\psi_{\mathbf{k}}\cdot\\
&\qquad \sum_{\substack{\alpha,\,n\\ \beta,\,m}} \Big\langle e^{\text{-}i\left(\mathbf{k}\cdot\mathbf{r}_0^{\alpha}+\mathbf{q}\cdot\mathbf{r}_0^{\beta}\right)}\Big\rangle_0 \Big\langle \mathbf{b}_n^{\alpha} e^{\text{-}i\left(\mathbf{k}\cdot\sum_i^n \mathbf{b}_i^{\alpha}+\mathbf{q}\cdot\sum_j^m \mathbf{b}_j^{\beta}\right)}\Big\rangle_0 .
\end{aligned} \tag{3.19}$$

The usual split of the summation over α and β follows, yielding

$$\begin{aligned}
&[N_p!]^{-1}[\mathscr{Z}_0]^{N_p} \sum_{\mathbf{k},\,\mathbf{q}\neq 0}\Bigg[\phi_{\mathbf{q}}\,\boldsymbol{\psi}_{\mathbf{k}}\cdot \sum_{\substack{\alpha\\ n,\,m}} \Big\langle e^{\text{-}i(\mathbf{k}+\mathbf{q})\cdot\mathbf{r}_0^{\alpha}}\Big\rangle_0 \Big\langle \mathbf{b}_n^{\alpha}\, e^{\text{-}i\left(\mathbf{k}\cdot\sum_i^n \mathbf{b}_i^{\alpha}+\mathbf{q}\cdot\sum_j^m \mathbf{b}_j^{\alpha}\right)}\Big\rangle_0\\
&\qquad + \phi_{\mathbf{q}}\,\boldsymbol{\psi}_{\mathbf{k}}\cdot \sum_{\substack{\alpha\neq\beta\\ n,\,m}} \Big\langle e^{\text{-}i\left(\mathbf{k}\cdot\mathbf{r}_0^{\alpha}+\mathbf{q}\cdot\mathbf{r}_0^{\beta}\right)}\Big\rangle_0 \Big\langle \mathbf{b}_n^{\alpha}\, e^{\text{-}i\left(\mathbf{k}\cdot\sum_i^n \mathbf{b}_i^{\alpha}+\mathbf{q}\cdot\sum_j^m \mathbf{b}_j^{\beta}\right)}\Big\rangle_0\Bigg]\\
&= [N_p!]^{-1}[\mathscr{Z}_0]^{N_p} \sum_{\mathbf{k},\,\mathbf{q}\neq 0}\Bigg[\phi_{\mathbf{q}}\,\boldsymbol{\psi}_{\mathbf{k}}\cdot \sum_{\substack{\alpha\\ n,\,m}} \delta_{\mathbf{k},\,\text{-}\mathbf{q}} \Big\langle \mathbf{b}_n^{\alpha}\, e^{\text{-}i\left(\mathbf{k}\cdot\sum_i^n \mathbf{b}_i^{\alpha}+\mathbf{q}\cdot\sum_j^m \mathbf{b}_j^{\alpha}\right)}\Big\rangle_0\\
&\qquad + \phi_{\mathbf{q}}\,\boldsymbol{\psi}_{\mathbf{k}}\cdot \sum_{\substack{\alpha\neq\beta\\ n,\,m}} \delta_{\mathbf{k},\,0}\,\delta_{\mathbf{q},\,0} \Big\langle \mathbf{b}_n^{\alpha}\, e^{\text{-}i\left(\mathbf{k}\cdot\sum_i^n \mathbf{b}_i^{\alpha}+\mathbf{q}\cdot\sum_j^m \mathbf{b}_j^{\beta}\right)}\Big\rangle_0\Bigg].
\end{aligned} \tag{3.20}$$

We once more sum over N_p identical terms in the first term while the second term vanishes because the summation over $\mathbf{q}$ does not include $\mathbf{q}=0$:

$$[N_p!]^{-1}[\mathscr{Z}_0]^{N_p}\left[\sum_{\mathbf{k}\neq 0} N_p\,\phi_{\text{-}\mathbf{k}}\,\boldsymbol{\psi}_{\mathbf{k}}\cdot\sum_{n,\,m}\Big\langle \mathbf{b}_n\, e^{\text{-}i\mathbf{k}\cdot(\mathbf{r}_n-\mathbf{r}_m)}\Big\rangle_0 + 0\right]. \tag{3.21}$$

We again define a new quantity called the *bond-vector structure function* for the Gaussian chain,

$$\mathbf{D}^0(\mathbf{k}) = \sum_{n,\,m}\Big\langle \mathbf{b}_n e^{\text{-}i\mathbf{k}\cdot(\mathbf{r}_n-\mathbf{r}_m)}\Big\rangle_0, \tag{3.22}$$

which will be computed in the next two sections. So the **b** integral in equation (3.19) gives

$$[N_p!]^{-1}[\mathscr{Z}_0]^{N_p} N_p \sum_{\mathbf{k}\neq 0} \phi_{\text{-}\mathbf{k}}\, \mathbf{D}^0(\mathbf{k}) \cdot \boldsymbol{\psi}_{\mathbf{k}}. \tag{3.23}$$

After collecting all six results (equations (2.41), (2.49), (2.55), (3.13), (3.18), (3.23)) computed thus far and which correspond to the six terms in equation (3.12), equation (3.11) becomes

$$\begin{aligned}
&e^{-\beta H_0(\{\rho_{\mathbf{k}},\, \mathbf{u}_{\mathbf{k}}\})} \\
&\approx [N_p!]^{-1}[\mathscr{Z}_0]^{N_p} \int\mathscr{D}\phi \int\mathscr{D}\boldsymbol{\psi}\ \exp\left[i\sum_{\mathbf{k}} \boldsymbol{\psi}_{\mathbf{k}} \cdot \mathbf{u}_{\text{-}\mathbf{k}} + i\sum_{\mathbf{k}\neq 0} \phi_{\mathbf{k}}\, \rho_{\text{-}\mathbf{k}} \right] \\
&\times \left(1 - \frac{N_p}{2\Omega^2} \left[\sum_{\mathbf{k}} \boldsymbol{\psi}_{\mathbf{k}} \cdot \mathbf{G}^0(\mathbf{k}) \cdot \boldsymbol{\psi}_{\text{-}\mathbf{k}} + \sum_{\mathbf{k}\neq 0} \left[g^0(\mathbf{k}) \phi_{\mathbf{k}}\, \phi_{\text{-}\mathbf{k}} + 2\phi_{\text{-}\mathbf{k}}\, \mathbf{D}^0(\mathbf{k}) \cdot \boldsymbol{\psi}_{\mathbf{k}} \right] \right] \right) \\
&\approx [N_p!]^{-1}[\mathscr{Z}_0]^{N_p} \int\mathscr{D}\phi \int\mathscr{D}\boldsymbol{\psi}\ \exp\left[i\sum_{\mathbf{k}} \boldsymbol{\psi}_{\mathbf{k}} \cdot \mathbf{u}_{\text{-}\mathbf{k}} + i\sum_{\mathbf{k}\neq 0} \phi_{\mathbf{k}}\, \rho_{\text{-}\mathbf{k}} \right. \\
&\quad \left. - \frac{N_p}{2\Omega^2} \left[\sum_{\mathbf{k}} \boldsymbol{\psi}_{\mathbf{k}} \cdot \mathbf{G}^0(\mathbf{k}) \cdot \boldsymbol{\psi}_{\text{-}\mathbf{k}} + \sum_{\mathbf{k}\neq 0} \left[g^0(\mathbf{k}) \phi_{\mathbf{k}}\, \phi_{\text{-}\mathbf{k}} + 2\phi_{\text{-}\mathbf{k}}\, \mathbf{D}^0(\mathbf{k}) \cdot \boldsymbol{\psi}_{\mathbf{k}} \right] \right] \right],
\end{aligned} \tag{3.24}$$

where we have reused our assumption that $\phi_{\mathbf{k}}$ and $\boldsymbol{\psi}_{\mathbf{k}}$ are small in the second approximation above.

Now it remains for us to do the Gaussian integrations over $\boldsymbol{\psi}_{\mathbf{k}}$ and $\phi_{\mathbf{k}}$. To do this we first note that

$$g^0(\text{-}\mathbf{k}) = \left[g^0(\mathbf{k}) \right]^* \quad \text{and} \quad \mathbf{D}^0(\text{-}\mathbf{k}) = \left[\mathbf{D}^0(\mathbf{k}) \right]^*. \tag{3.25}$$

To prepare for integration over $\boldsymbol{\psi}_{\mathbf{k}}$, we first rearrange the terms containing $\boldsymbol{\psi}_{\mathbf{k}}$ to obtain

$$\begin{aligned}
\text{constant} \times \int\mathscr{D}\phi\ \exp\left[i\sum_{\mathbf{k}\neq 0} \phi_{\mathbf{k}}\, \rho_{\text{-}\mathbf{k}} - \frac{N_p}{2\Omega^2} \sum_{\mathbf{k}\neq 0} g^0(\mathbf{k}) \phi_{\mathbf{k}}\, \phi_{\text{-}\mathbf{k}} \right] \times \\
\int\mathscr{D}\boldsymbol{\psi}\ \exp\left[\sum_{\mathbf{k}>0} \left(\text{-}\boldsymbol{\psi}_{\mathbf{k}} \cdot \frac{N_p}{\Omega^2} \mathbf{G}^0(\mathbf{k}) \cdot \boldsymbol{\psi}_{\text{-}\mathbf{k}} + \right. \right. \\
\left. \left. i\boldsymbol{\psi}_{\mathbf{k}} \cdot \left[\mathbf{u}_{\text{-}\mathbf{k}} + \frac{iN_p}{\Omega^2} \phi_{\text{-}\mathbf{k}}\, \mathbf{D}^0(\mathbf{k}) \right] + i\boldsymbol{\psi}_{\text{-}\mathbf{k}} \cdot \left[\mathbf{u}_{\mathbf{k}} + \frac{iN_p}{\Omega^2} \phi_{\mathbf{k}}\, \mathbf{D}^0(\text{-}\mathbf{k}) \right] \right) \right] \\
\times \exp\left[\text{-}\boldsymbol{\psi}_0 \cdot \frac{N_p}{2\Omega^2} \mathbf{G}^0(0) \cdot \boldsymbol{\psi}_0 + i\boldsymbol{\psi}_0 \cdot \mathbf{u}_0 \right],
\end{aligned} \tag{3.26}$$

which after $\boldsymbol{\psi}_{\mathbf{k}}$ integration results in

$$\text{constant} \times \int \mathscr{D}\phi \, \exp\left[i \sum_{\mathbf{k}\neq 0} \phi_{\mathbf{k}} \, \rho_{\text{-}\mathbf{k}} - \frac{N_p}{2\Omega^2} \sum_{\mathbf{k}\neq 0} g^0(\mathbf{k}) \phi_{\mathbf{k}} \, \phi_{\text{-}\mathbf{k}} \right] \times$$
$$\exp\left[\sum_{\mathbf{k}>0} \left(- \left[\mathbf{u}_{\text{-}\mathbf{k}} + \frac{iN_p}{\Omega^2} \phi_{\text{-}\mathbf{k}} \, \mathbf{D}^0(\mathbf{k}) \right] \cdot \frac{\Omega^2}{N_p} \left[\mathbf{G}^0(\mathbf{k}) \right]^{\text{-}1} \cdot \left[\mathbf{u}_{\mathbf{k}} + \frac{iN_p}{\Omega^2} \phi_{\mathbf{k}} \, \mathbf{D}^0(\text{-}\mathbf{k}) \right] \right.$$
$$\left. \times \exp\left[\text{-}\mathbf{u}_0 \cdot \frac{\Omega^2}{2N_p} \left[\mathbf{G}^0(0) \right]^{\text{-}1} \cdot \mathbf{u}_0 \right] . \quad (3.27)$$

To facilitate integration over $\phi_{\mathbf{k}}$, we first rearrange the terms containing $\phi_{\mathbf{k}}$ to obtain

$$\text{constant} \times \exp\left[\text{-} \frac{\Omega^2}{2N_p} \sum_{\mathbf{k}} \mathbf{u}_{\mathbf{k}} \cdot \left[\mathbf{G}^0(\mathbf{k}) \right]^{\text{-}1} \cdot \mathbf{u}_{\text{-}\mathbf{k}} \right]$$
$$\times \int \mathscr{D}\phi \, \exp\left[\sum_{\mathbf{k}>0} \left(\text{-} \frac{N_p}{\Omega^2} \left\{ g^0(\mathbf{k}) - \mathbf{D}^0(\mathbf{k}) \cdot \left[\mathbf{G}^0(\mathbf{k}) \right]^{\text{-}1} \cdot \mathbf{D}^0(\text{-}\mathbf{k}) \right\} \phi_{\mathbf{k}} \, \phi_{\text{-}\mathbf{k}} \right. \right.$$
$$+ i\phi_{\mathbf{k}} \left\{ \rho_{\text{-}\mathbf{k}} - \mathbf{u}_{\text{-}\mathbf{k}} \cdot \left[\mathbf{G}^0(\mathbf{k}) \right]^{\text{-}1} \cdot \mathbf{D}^0(\text{-}\mathbf{k}) \right\}$$
$$\left. \left. + i\phi_{\text{-}\mathbf{k}} \left\{ \rho_{\mathbf{k}} - \mathbf{u}_{\mathbf{k}} \cdot \left[\mathbf{G}^0(\mathbf{k}) \right]^{\text{-}1} \cdot \mathbf{D}^0(\mathbf{k}) \right\} \right) \right] . \quad (3.28)$$

Let us define

$$A^0(\mathbf{k}) \equiv g^0(\mathbf{k}) - \mathbf{D}^0(\mathbf{k}) \cdot \left[\mathbf{G}^0(\mathbf{k}) \right]^{\text{-}1} \cdot \mathbf{D}^0(\text{-}\mathbf{k}) \quad (3.29)$$

as the coefficient of the $\phi_{\mathbf{k}}\phi_{\text{-}\mathbf{k}}$-term. Then the result after integrating over $\phi_{\mathbf{k}}$ is:

$$\text{constant} \times \exp\left[\text{-} \frac{\Omega^2}{2N_p} \sum_{\mathbf{k}} \mathbf{u}_{\mathbf{k}} \cdot \left[\mathbf{G}^0(\mathbf{k}) \right]^{\text{-}1} \cdot \mathbf{u}_{\text{-}\mathbf{k}} \right]$$
$$\times \exp\left[\sum_{\mathbf{k}>0} \text{-} \frac{\Omega^2}{A^0(\mathbf{k}) \, N_p} \left\{ \rho_{\text{-}\mathbf{k}} - \mathbf{u}_{\text{-}\mathbf{k}} \cdot \left[\mathbf{G}^0(\mathbf{k}) \right]^{\text{-}1} \cdot \mathbf{D}^0(\text{-}\mathbf{k}) \right\} \right.$$
$$\left. \times \left\{ \rho_{\mathbf{k}} - \mathbf{u}_{\mathbf{k}} \cdot \left[\mathbf{G}^0(\mathbf{k}) \right]^{\text{-}1} \cdot \mathbf{D}^0(\mathbf{k}) \right\} \right] , \quad (3.30)$$

which after regrouping terms yields

$$\text{constant} \times \exp\left[-\frac{\Omega^2}{2\,N_p}\mathbf{u}_0 \cdot \left[\mathbf{G}^0(\mathbf{k})\right]^{-1} \cdot \mathbf{u}_0 + \sum_{\mathbf{k}>0} -\frac{\Omega^2}{N_p}\left(\frac{1}{A^0(\mathbf{k})}\rho_{\mathbf{k}}\,\rho_{\text{-}\mathbf{k}}\right.\right.$$
$$+ \mathbf{u}_{\mathbf{k}} \cdot \left\{\left[\mathbf{G}^0(\mathbf{k})\right]^{-1} + \frac{1}{A^0(\mathbf{k})}\left[\mathbf{G}^0(\mathbf{k})\right]^{-1} \cdot \mathbf{D}^0(\mathbf{k})\,\mathbf{D}^0(\text{-}\mathbf{k}) \cdot \left[\mathbf{G}^0(\mathbf{k})\right]^{-1}\right\} \cdot \mathbf{u}_{\text{-}\mathbf{k}}$$
$$\left.\left. - \frac{1}{A^0(\mathbf{k})}\left\{\rho_{\text{-}\mathbf{k}}\,\mathbf{u}_{\mathbf{k}} \cdot \left[\mathbf{G}^0(\mathbf{k})\right]^{-1} \cdot \mathbf{D}^0(\mathbf{k}) + \rho_{\mathbf{k}}\,\mathbf{u}_{\text{-}\mathbf{k}} \cdot \left[\mathbf{G}^0(\mathbf{k})\right]^{-1} \cdot \mathbf{D}^0(\text{-}\mathbf{k})\right\}\right)\right]. \tag{3.31}$$

The result of Section 3.3 (equation (3.46)) gives

$$\mathbf{D}^0(\mathbf{k}) = -i\,D^0(k)\,\mathbf{k}, \tag{3.32}$$

while equation (2.69) gives

$$\mathbf{G}^0(\mathbf{k}) = G^0(k)\,\mathbb{1}, \tag{3.33}$$

so we may rewrite equation (3.29) as

$$A^0(\mathbf{k}) \;=\; A^0(k) \;=\; g^0(k) - \frac{\left[D^0(k)\right]^2 k^2}{G^0(k)}. \tag{3.34}$$

Let us further define

$$\Delta S^0(k) \;\equiv\; G^0(k)\,A^0(k) \;=\; G^0(k)\,g^0(k) - \left[D^0(k)\right]^2 k^2. \tag{3.35}$$

Then our final result for the transformation of $H_0(\{\mathbf{b}_n^\alpha\})$ to $H_0(\{\rho_{\mathbf{k}}, \mathbf{u}_{\mathbf{k}}\})$ is given by

$$e^{\text{-}\beta\,H_0(\{\rho_{\mathbf{k}},\,\mathbf{u}_{\mathbf{k}}\})} \approx \text{constant} \times \exp\left[-\frac{\Omega^2}{2\,N_p\,G^0(k)}\mathbf{u}_0 \cdot \mathbf{u}_0\right.$$
$$+ \sum_{\mathbf{k}>0} -\frac{\Omega^2}{N_p}\left(\frac{G^0(k)}{\Delta S^0(k)}\rho_{\mathbf{k}}\,\rho_{\text{-}\mathbf{k}} + \mathbf{u}_{\mathbf{k}} \cdot \left[\frac{A^0(k)\,\mathbb{1} + \mathbf{k}\,\mathbf{k}\left[D^0(k)\right]^2/G^0(k)}{\Delta S^0(k)}\right] \cdot \mathbf{u}_{\text{-}\mathbf{k}}\right)$$
$$\left. + \frac{D^0(k)}{\Delta S^0(k)} i\,\mathbf{k} \cdot (\mathbf{u}_{\mathbf{k}}\,\rho_{\text{-}\mathbf{k}} - \mathbf{u}_{\text{-}\mathbf{k}}\,\rho_{\mathbf{k}})\right)\Bigg] \tag{3.36}$$

We have already computed $\mathbf{G}^0(\mathbf{k})$ in Section 2.7. The next two sections will show how $g^0(\mathbf{k})$ and $\mathbf{D}^0(\mathbf{k})$ are calculated.

3.2 The Gaussian Chain's Structure Function

From equation (3.17) we have

$$\begin{aligned} g^0(\mathbf{k}) &= \sum_{n,\,m} \left\langle e^{-i\mathbf{k}\cdot(\mathbf{r}_n - \mathbf{r}_m)} \right\rangle_0 \\ &= \sum_{n,\,m} \left\langle e^{-i\mathbf{k}\cdot\left(\sum_{i=1}^{n}\mathbf{b}_i - \sum_{j=1}^{m}\mathbf{b}_j\right)} \right\rangle_0 \\ &= \left(\sum_{n>m} + \sum_{n<m} + \sum_{n=m}\right) \left\langle e^{-i\mathbf{k}\cdot\left(\sum_{i=1}^{n}\mathbf{b}_i - \sum_{j=1}^{m}\mathbf{b}_j\right)} \right\rangle_0 \\ &= \sum_{n>m} \left\langle e^{-i\mathbf{k}\cdot\sum_{i=m+1}^{n}\mathbf{b}_i} \right\rangle_0 + \sum_{n<m} \left\langle e^{i\mathbf{k}\cdot\sum_{i=n+1}^{m}\mathbf{b}_i} \right\rangle_0 + N. \end{aligned} \tag{3.37}$$

Since for the Gaussian chain, the $\mathbf{b}_i$'s are independent of each other, the terms of the first sum has such factors as given in

$$\sum_{n>m} \prod_{i=m+1}^{n} \left\langle e^{-i\mathbf{k}\cdot\mathbf{b}_i} \right\rangle_0. \tag{3.38}$$

Thus from the definition of $\langle \ldots \rangle_0$ given in equation (2.43)

$$\begin{aligned} g^0(\mathbf{k}) &= N + \sum_{n>m} \left\langle e^{-i\mathbf{k}\cdot\mathbf{b}} \right\rangle_0^{n-m} + \sum_{m>n} \left\langle e^{i\mathbf{k}\cdot\mathbf{b}} \right\rangle_0^{m-n} \\ &= N + \sum_{n>m} e^{-\frac{k^2(n-m)}{4\,a}} + \sum_{m>n} e^{-\frac{k^2(m-n)}{4\,a}} \\ &= \sum_{n,\,m} e^{-\frac{k^2|n-m|}{4\,a}} \;=\; \sum_{n,\,m} e^{-\frac{1}{6}k^2 l^2 |n-m|}. \end{aligned} \tag{3.39}$$

In order to evaluate the remaining sum, we use the following approximation which is well-known in literature:

$$g^0(\mathbf{k}) = g^0(k) \approx \int_0^N \mathrm{d}n \int_0^N \mathrm{d}m\, e^{-\frac{1}{6}k^2 l^2 |n-m|} \;=\; N^2\, f_D\big(k^2\, {R_g}^2\big), \tag{3.40}$$

where

$$f_D(x) = \begin{cases} 1 & \text{if } x = 0 \\ \dfrac{2}{x^2}\big(e^{-x} - 1 + x\big) & \text{if } x > 0 \end{cases} \tag{3.41}$$

is called the *Debye function*, and

$${R_g}^2 = \frac{N\, l^2}{6} \tag{3.42}$$

is the *mean square radius of gyration* of the Gaussian chain.

3.3 The Gaussian Chain's Bond-Vector Structure Function

From equation (3.22) we have

$$\begin{aligned}
\mathbf{D}^0(\mathbf{k}) &= \sum_{n,\,m} \Big\langle \mathbf{b}_n \, e^{-i\mathbf{k}\cdot(\mathbf{r}_n - \mathbf{r}_m)} \Big\rangle_0 \\
&= \sum_{n,\,m} \Big\langle \mathbf{b}_n \, e^{-i\mathbf{k}\cdot\left(\sum_{i=1}^{n} \mathbf{b}_i - \sum_{j=1}^{m} \mathbf{b}_j\right)} \Big\rangle_0 \\
&= \left(\sum_{n>m} + \sum_{n<m} + \sum_{n=m} \right) \Big\langle \mathbf{b}_n \, e^{-i\mathbf{k}\cdot\left(\sum_{i=1}^{n} \mathbf{b}_i - \sum_{j=1}^{m} \mathbf{b}_j\right)} \Big\rangle_0 \\
&= \sum_{n>m} \Big\langle \mathbf{b}_n \, e^{-i\mathbf{k}\cdot\sum_{i=m+1}^{n} \mathbf{b}_i} \Big\rangle_0 \\
&\quad + \sum_{n<m} \Big\langle \mathbf{b}_n \, e^{i\mathbf{k}\cdot\sum_{i=n+1}^{m} \mathbf{b}_i} \Big\rangle_0 + \sum_{n=m} \langle \mathbf{b}_n \rangle_0
\end{aligned} \tag{3.43}$$

The second and third sums vanish because the factor $\langle \mathbf{b}_n \rangle_0 = 0$. Since for the Gaussian chain, the $\mathbf{b}_i$'s are independent of each other, the terms of the first sum has such factors as given in

$$\sum_{n>m} \Big\langle \mathbf{b}_n \, e^{-i\mathbf{k}\cdot\mathbf{b}_n} \Big\rangle_0 \prod_{i=m+1}^{n-1} \Big\langle e^{-i\mathbf{k}\cdot\mathbf{b}_i} \Big\rangle_0. \tag{3.44}$$

Thus from the definition of $\langle \ldots \rangle_0$ given in equation (2.43)

$$\begin{aligned}
\mathbf{D}^0(\mathbf{k}) &= \sum_{n>m} i \Big[\nabla_{\mathbf{k}} \Big\langle e^{-i\mathbf{k}\cdot\mathbf{b}_n} \Big\rangle_0 \Big] \Big\langle e^{-i\mathbf{k}\cdot\mathbf{b}} \Big\rangle_0^{\,n-m-1} \\
&= i \sum_{n>m} \Big[\nabla_{\mathbf{k}} e^{-\frac{k^2}{4\,a}} \Big] e^{-\frac{k^2 (n-m-1)}{4\,a}} \\
&= \frac{-i\,\mathbf{k}}{2\,a} \sum_{n>m} e^{-\frac{k^2 (n-m)}{4\,a}} \;=\; \frac{-i\,l^2\,\mathbf{k}}{3} \sum_{n>m} e^{-\frac{1}{6} k^2 l^2 (n-m)} \\
&= \frac{-i\,l^2\,\mathbf{k}}{6} \left(\sum_{n,\,m} e^{-\frac{1}{6} k^2 l^2 |n-m|} - N \right).
\end{aligned} \tag{3.45}$$

In order to evaluate the remaining sum, we use the approximation aforementioned in equation (3.40). Therefore, the bond-vector structure function is

$$\mathbf{D}^0(\mathbf{k}) = -i\, D^0(k)\, \mathbf{k}, \tag{3.46}$$

where

$$D^0(k) = \frac{1}{6}\, l^2\, N \big(N\, f_D\big(k^2\, {R_g}^2\big) - 1 \big). \tag{3.47}$$

3.4 The Collective Hamiltonian

Gathering the results obtained from equations (3.7), (2.26), (3.6), and (3.36), our partition function becomes

$$\begin{aligned}\mathscr{Z}_c &\propto \int\mathscr{D}\mathbf{u}\int\mathscr{D}\rho\, e^{-\beta[H_0(\{\rho_{\mathbf{k}},\,\mathbf{u}_{\mathbf{k}}\})+E(\{\rho_{\mathbf{k}}\})+U(\{\mathbf{u}_{\mathbf{k}}\})]}\\ &\propto \int\mathscr{D}\mathbf{u}\int\mathscr{D}\rho\, e^{-\beta H(\{\rho_{\mathbf{k}},\,\mathbf{u}_{\mathbf{k}}\})},\end{aligned} \tag{3.48}$$

where

$$\begin{aligned}\beta\, H(\{\rho_{\mathbf{k}},\,\mathbf{u}_{\mathbf{k}}\}) = \mathbf{u}_0\cdot\left[\frac{\Omega^2}{2\,N_p\,G^0(k)}+2\,\beta\,\mathbf{J}_0\right]\cdot\mathbf{u}_0+2\,\beta\,V_0\,{\rho_0}^2\\ +\Omega^2\sum_{\mathbf{k}>0}\Bigg(\mathbf{u}_{\mathbf{k}}\cdot\left[\frac{1}{N_p}\frac{A^0(k)\,\mathbb{1}+\mathbf{k}\,\mathbf{k}\left[D^0(k)\right]^2/G^0(k)}{\Delta S^0(k)}+2\,\beta\,\mathbf{J}_{\mathbf{k}}\right]\cdot\mathbf{u}_{\text{-}\mathbf{k}}\\ +\left[\frac{1}{N_p}\frac{G^0(k)}{\Delta S^0(k)}+2\,\beta\,V_{\mathbf{k}}\right]\rho_{\mathbf{k}}\,\rho_{\text{-}\mathbf{k}}+\frac{1}{N_p}\frac{D^0(k)}{\Delta S^0(k)}i\,\mathbf{k}\cdot\left[\mathbf{u}_{\mathbf{k}}\,\rho_{\text{-}\mathbf{k}}-\mathbf{u}_{\text{-}\mathbf{k}}\,\rho_{\mathbf{k}}\right]\\ +\mathrm{O}\big({\mathbf{u}_{\mathbf{k}}}^3,\ {\rho_{\mathbf{k}}}^3,\ {\mathbf{u}_{\mathbf{k}}}^2\rho_{\mathbf{k}},\ \mathbf{u}_{\mathbf{k}}\,{\rho_{\mathbf{k}}}^2\big)\Bigg).\end{aligned} \tag{3.49}$$

Observe that the Hamiltonian is quadratic in both $\rho_{\mathbf{k}}$ and $\mathbf{u}_{\mathbf{k}}$ as expected, but it also contains additional terms with the couplings: $\mathbf{u}_{\mathbf{k}}\rho_{\text{-}\mathbf{k}}$ and $\mathbf{u}_{\text{-}\mathbf{k}}\rho_{\mathbf{k}}$. Physically, these additional terms may be interpreted as a first approximation to the interaction between the fields (or, in the language of condensed matter physics, order parameters): $\rho(\mathbf{r})$ and $\mathbf{u}(\mathbf{r})$. Such additional couplings should be expected since $\rho(\mathbf{r})$ and $\mathbf{u}(\mathbf{r})$ are not independent of each other, that is, a change in $\rho(\mathbf{r})$ produces a change in $\mathbf{u}(\mathbf{r})$.

From this point, we may proceed in either of two directions: we may further integrate equation (3.48) over $\mathbf{u}_{\mathbf{k}}$ to obtain an effective Hamiltonian $H(\{\rho_{\mathbf{k}}\})$, or we may instead integrate over $\rho_{\text{-}\mathbf{k}}$ in equation (3.48) to obtain another effective Hamiltonian $H(\{\mathbf{u}_{\mathbf{k}}\})$. The first Hamiltonian is useful for studies in conventional elastic neutron-scattering experiments in which the polarization of the scattered beam is ignored. Such experiments detect density fluctuations as a function of the scattering wave-vector. The second Hamiltonian may be used to study the spatial fluctuations of the magnetization field.

Integrating equation (3.48) over $\mathbf{u}_{\mathbf{k}}$ (another Gaussian integral), we obtain

$$\mathscr{Z}_c \propto \int\mathscr{D}\rho\, e^{-\beta H(\{\rho_{\mathbf{k}}\})}, \tag{3.50}$$

where

$$\beta\, H(\{\rho_{\mathbf{k}}\}) = \Omega^2 \sum_{\mathbf{k}>0} \rho_{\mathbf{k}}\, \rho_{\text{-}\mathbf{k}} \Bigg\{ \frac{1}{N_p} \frac{G^0(k)}{\Delta S^0(k)} + 2\,\beta\, V_{\mathbf{k}} - \frac{1}{{N_p}^2} \frac{\left[D^0(k)\right]^2}{\left[\Delta S^0(k)\right]^2} \mathbf{k} \cdot \left[\frac{1}{N_p} \frac{A^0(k)\,\mathbb{1} + \mathbf{k}\,\mathbf{k}\left[D^0(k)\right]^2 / G^0(k)}{\Delta S^0(k)} + 2\,\beta\, \mathbf{J}_{\mathbf{k}} \right]^{-1} \cdot \mathbf{k} \Bigg\}. \tag{3.51}$$

After substituting the expression for $\mathbf{J}_{\mathbf{k}}$ (equation (2.88)) the matrix in equation (3.51) whose inverse is to be calculated becomes

$$\left[\frac{A^0(k)}{N_p\, \Delta S^0(k)} - \frac{4\pi\lambda_B\, C}{3\Omega} \right] + \left[\frac{\left[D^0(k)\right]^2 k^2}{N_p\, G^0(k)\, \Delta S^0(k)} + \frac{4\pi\lambda_B\, C}{\Omega} \right] \hat{\mathbf{k}}\,\hat{\mathbf{k}} \tag{3.52}$$

To evaluate the inverse of this matrix we will use the result: equation (B.6) in appendix B yielding

$$\frac{3\Omega\, N_p\, G^0(k)}{3\Omega - 4\pi\lambda_B\, C\, N_p\, G^0(k)} \times \left(\mathbb{1} - 3\hat{\mathbf{k}}\,\hat{\mathbf{k}} \frac{\Omega \left[D^0(k)\right]^2 k^2 / G^0(k) + 4\pi\lambda_B\, C\, N_p\, \Delta S^0(k)}{3\Omega\, g^0(k) + 8\pi\lambda_B\, C\, N_p\, \Delta S^0(k)} \right), \tag{3.53}$$

and after a bit of algebraic manipulation equation (3.51) simplifies to

$$\beta\, H(\{\rho_{\mathbf{k}}\}) = \Omega^2 \sum_{\mathbf{k}>0} \rho_{\mathbf{k}}\, \rho_{\text{-}\mathbf{k}} \left\{ 2\beta\, V_{\mathbf{k}} + \frac{1}{N_p} \frac{3\Omega + 8\pi\lambda_B\, C\, N_p\, G^0(k)}{3\Omega\, g^0(k) + 8\pi\lambda_B\, C\, N_p\, \Delta S^0(k)} \right\}. \tag{3.54}$$

Let us model the excluded volume interaction by

$$V(\mathbf{r}) = \frac{v}{2\beta} \delta(\mathbf{r}), \tag{3.55}$$

where v is the excluded volume and has the dimensions of volume. Then the Fourier transform of $V(\mathbf{r})$ is

$$V_{\mathbf{k}} \;=\; \int_{\Omega} \frac{\mathrm{d}^3 r}{\Omega}\, e^{i\mathbf{k}\cdot\mathbf{r}}\, V(\mathbf{r}) \;=\; \frac{v}{2\beta\,\Omega}. \tag{3.56}$$

so that

$$\boxed{\beta\, H(\{\rho_{\mathbf{k}}\}) = \Omega^2 \sum_{\mathbf{k}>0} \rho_{\mathbf{k}}\, \rho_{\text{-}\mathbf{k}} \left\{ \frac{v}{\Omega} + \frac{1}{N_p} \frac{3\Omega + 8\pi\lambda_B\, C\, N_p\, G^0(k)}{3\Omega\, g^0(k) + 8\pi\lambda_B\, C\, N_p\, \Delta S^0(k)} \right\}.} \tag{3.57}$$

If instead we integrate (3.48) with respect to $\rho_{\mathbf{k}}$ (also a Gaussian integral), then we obtain

$$\mathscr{Z}_c \propto \int \mathscr{D}\mathbf{u}\, e^{-\beta H(\{\mathbf{u_k}\})}, \tag{3.58}$$

where the Hamiltonian $H(\{\mathbf{u_k}\})$ is given by

$$\begin{aligned}\beta\, H(\{\mathbf{u_k}\}) = \mathbf{u}_0 \cdot \left[\frac{\Omega^2}{2\, N_p\, G^0(k)} + 2\,\beta\,\mathbf{J}_0\right] \cdot \mathbf{u}_0 + 2\,\beta\, V_0\, {\rho_0}^2 \\ + \Omega^2 \sum_{\mathbf{k}>0}\Bigg(\mathbf{u_k} \cdot \left[\frac{1}{N_p}\frac{A^0(k)\,\mathbb{1} + \hat{\mathbf{k}}\,\hat{\mathbf{k}}\,k^2\big[D^0(k)\big]^2/G^0(k)}{\Delta S^0(k)} + 2\,\beta\,\mathbf{J_k}\right] \cdot \mathbf{u_{-k}} \\ - \left[\frac{1}{N_p}\frac{G^0(k)}{\Delta S^0(k)} + 2\,\beta\, V_{\mathbf{k}}\right]^{-1} \frac{1}{{N_p}^2}\frac{k^2\big[D^0(k)\big]^2}{\big[\Delta S^0(k)\big]^2}\mathbf{u_k}\cdot\hat{\mathbf{k}}\,\hat{\mathbf{k}}\cdot\mathbf{u_{-k}}.\end{aligned} \tag{3.59}$$

After substituting the expressions for $\mathbf{J_k}$ (equation (2.88)) and $V_{\mathbf{k}}$ (equation (3.56)) the above equation gets to be of the form:

$$\boxed{\beta\, H(\{\mathbf{u_k}\}) = \frac{\Omega^2}{2\, N_p\, G^0(k)}\mathbf{u}_0\cdot\mathbf{u}_0 + \Omega^2 \sum_{\mathbf{k}>0}\mathbf{u_k}\cdot\left[a\mathbb{1} + b\hat{\mathbf{k}}\,\hat{\mathbf{k}}\right]\cdot\mathbf{u_{-k}}}, \tag{3.60}$$

where

$$\begin{aligned} a &= \frac{3\Omega - 4\pi\lambda_B\, C\, N_p\, G^0(k)}{3\Omega\, N_p\, G^0(k)}, \quad \text{and} \\ b &= \frac{1}{N_p}\frac{k^2\big[D^0(k)\big]^2}{\Delta S^0(k)}\left(\frac{1}{G^0(k)} - \frac{1}{G^0(k) + (v/\Omega)\,\Delta S^0(k)}\right) + \frac{4\pi\,\lambda_B\, C}{\Omega}. \end{aligned} \tag{3.61}$$

4. RESULTS

4.1 Asymptotic Behaviour of Gaussian Chain Structure Functions

It will be useful in the pending analysis of our results to first sketch the behaviour of certain functions we have defined in the preceding chapters. To facilitate our calculations, let

$$x = k^2 \, {R_g}^2. \tag{4.1}$$

In scattering experiments, $k = 2\pi/\lambda$ is the magnitude of the *scattering wave-vector* and λ provides a length-scale of observation which we may think of roughly as the distance between planes of atoms. We are interested in length-scales ranging from $\sim l$ to $\sim R_g$. Therefore we shall be considering functions of x defined over the domain $0 \leq x \lesssim 6N$. The functions that we shall consider are,

1. $G^0(k)$:

$$G^0(k) = 2{R_g}^2 \;=\; Nl^2/3, \tag{4.2}$$

   which is a constant function of k.

2. $g^0(k)$:

$$\begin{aligned} g^0(k) = N^2 f_D(x) \;&=\; \frac{2N^2}{x^2}(e^{-x} - 1 + x) \\ &\sim \begin{cases} N^2(1 - x/3) & \text{for } x \ll 1 \\ 2N^2/x & \text{for } x \gg 1 \end{cases}. \end{aligned} \tag{4.3}$$

   A graph of $f_D(x)$ is shown in Figure 4.1: $f_D(x)$ is a positive monotonically decreasing function less than or equal to unity.

3. $k^2\big[D^0(k)\big]^2/G^0(k)$:

$$\begin{aligned} k^2\big[D^0(k)\big]^2/G^0(k) = \frac{1}{2}x(Nf_D(x) - 1)^2 \;&=\; N^2 f_D(x) F_N(x) \\ &\sim \begin{cases} \frac{1}{2}x(N-1)^2 \;\approx\; \frac{1}{2}xN^2 & \text{for } x \ll 1 \\ \frac{1}{2}\big(4N^2/x - 4N + x\big) & \text{for } x \gg 1 \end{cases}, \end{aligned} \tag{4.4}$$

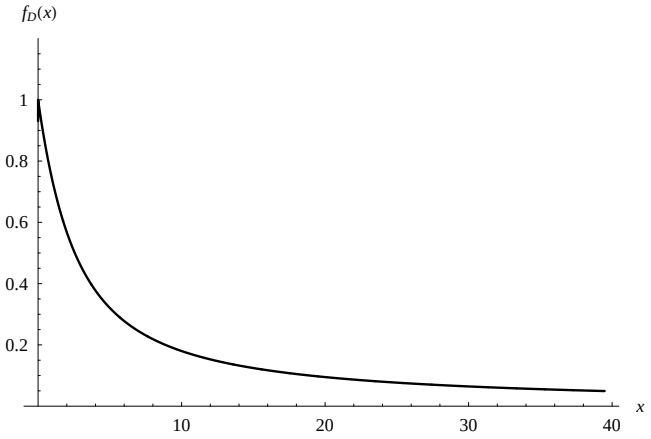

Fig. 4.1: Graph of the Debye function: $f_D(x) = \frac{2}{x^2}\big(e^{-x} - 1 + x\big)$.

where

$$\begin{aligned} F_N(x) &= \frac{1}{2}x\, f_D(x) + \frac{x}{N}\left[\frac{1}{2N\, f_D(x)} - 1\right] \\ &\sim \begin{cases} \frac{x(N-1)^2}{2N^2} \approx \frac{x}{2} & \text{for } x \ll 1 \\ 1 - \left(\frac{x}{N}\right) + \left(\frac{x}{2N}\right)^2 = \left(\frac{x}{2N} - 1\right)^2 & \text{for } x \gg 1 \end{cases}, \end{aligned} \tag{4.5}$$

A graph of $F_N(x)$ for $N = 10^4$ is shown in Figure 4.2: $F_N(x)$ is a function greater than or equal to zero and less than unity up to $x \gtrsim 4N$. That is,

$$k^2\, {R_g}^2 \gtrsim 4N \implies \lambda \lesssim 1.28255\, l. \tag{4.6}$$

4. $\Delta S^0(k)$:

$$\begin{aligned} \Delta S^0(k) &= G^0(k)\, g^0(k) - k^2\big[D^0(k)\big]^2 \;=\; 2{R_g}^2 N^2 f_D(x)\big(1 - F_N(x)\big) \\ &\sim \begin{cases} 2{R_g}^2 N^2(1 - 5x/6) & \text{for } x \ll 1 \\ {R_g}^2(4N - x) & \text{for } x \gg 1 \end{cases}, \end{aligned} \tag{4.7}$$

4.2 Bond-vector density fluctuations

We may obtain information about the dipole-dipole correlations in our system if we compute the average, $\langle \mathbf{u_k}\, \mathbf{u_{-k}} \rangle$. We have already obtained in equation (3.58) the following result:

$$\mathscr{Z}_c \propto \int \mathscr{D}\mathbf{u}\, e^{-\beta H(\{\mathbf{u_k}\})}, \tag{4.8}$$

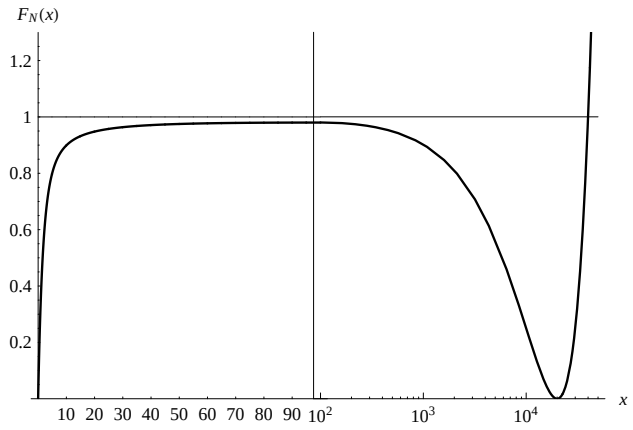

Fig. 4.2: Graph of the function: $F_N(x) = \frac{1}{2} x\, f_D(x) + \frac{x}{N}\left[\frac{1}{2N\, f_D(x)} - 1\right]$ for $N = 10^4$. Note that the abscissa has a linear scale for $0 \leq x \leq 100$ and a logarithmic scale for $100 \leq x \leq 5 \times 10^4$.

where the Hamiltonian $H(\{\mathbf{u_k}\})$ is given by

$$\beta\, H(\{\mathbf{u_k}\}) = \frac{\Omega^2}{2\, N_p\, G^0(k)}\, \mathbf{u}_0 \cdot \mathbf{u}_0 + \Omega^2 \sum_{\mathbf{k}>0} \mathbf{u_k} \cdot \Big[a\mathbb{1} + b\hat{\mathbf{k}}\,\hat{\mathbf{k}}\Big] \cdot \mathbf{u_{-k}}, \tag{4.9}$$

and

$$\begin{aligned} a &= \frac{3\Omega - 4\pi\lambda_B\, C\, N_p\, G^0(k)}{3\Omega\, N_p\, G^0(k)}, \\ b &= \frac{1}{N_p}\frac{k^2\big[D^0(k)\big]^2}{\Delta S^0(k)}\left(\frac{1}{G^0(k)} - \frac{1}{G^0(k) + (v/\Omega)\,\Delta S^0(k)}\right) + \frac{4\pi\,\lambda_B\, C}{\Omega}. \end{aligned} \tag{4.10}$$

Since equation (4.8) is a Gaussian integral, we can immediately write down the expressions for the averages

$$\langle \mathbf{u}_0\, \mathbf{u}_0 \rangle = \frac{N_p\, G^0(k)}{\Omega^2}\, \mathbb{1} \quad \text{and} \quad \langle \mathbf{u_k}\, \mathbf{u_{-k}} \rangle = \frac{1}{\Omega^2}\frac{1}{a}\left(\mathbb{1} - \frac{b}{a+b}\hat{\mathbf{k}}\,\hat{\mathbf{k}}\right). \tag{4.11}$$

To enable us obtain the expressions above, we have employed the result of Appendix B to find the inverse of the matrix $\Big(a\mathbb{1} + b\hat{\mathbf{k}}\,\hat{\mathbf{k}}\Big)$ in equation (4.9). Moreover, we require that $\Big(a\mathbb{1} + b\hat{\mathbf{k}}\,\hat{\mathbf{k}}\Big)$ be a *positive-definite* matrix, otherwise the Gaussian integrals that need to be performed to obtain the average diverge. This required property is also inherited by the average $\langle \mathbf{u_k}\, \mathbf{u_{-k}} \rangle$ which is merely the inverse of $\Omega^2\Big(a\mathbb{1} + b\hat{\mathbf{k}}\,\hat{\mathbf{k}}\Big)$.

In the orthonormal basis, $\Big\{\hat{\mathbf{k}},\, \hat{\mathbf{k}}_\perp^{(1)},\, \hat{\mathbf{k}}_\perp^{(2)}\Big\}$, first introduced in Section 2.8,

$\langle \mathbf{u_k}\, \mathbf{u_{-k}} \rangle$ is a diagonal matrix

$$\langle \mathbf{u_k}\, \mathbf{u_{-k}} \rangle = \frac{1}{\Omega^2} \begin{pmatrix} (a+b)^{-1} & 0 & 0 \\ 0 & a^{-1} & 0 \\ 0 & 0 & a^{-1} \end{pmatrix} \tag{4.12}$$

where, using equations (4.10),

$$\begin{aligned} (a+b)^{-1} &= \frac{3\Omega\, N_p \big(G^0(k) + (v/\Omega)\, \Delta S^0(k)\big)}{3\Omega + 3v\, g^0(k) + 8\pi\, \lambda_B\, C\, N_p \big(G^0(k) + (v/\Omega)\, \Delta S^0(k)\big)} \\ a^{-1} &= \frac{3\Omega\, N_p\, G^0(k)}{3\Omega - 4\pi \lambda_B\, C\, N_p\, G^0(k)}. \end{aligned} \tag{4.13}$$

The positive definite property requires that each of the eigenvalues of $\langle \mathbf{u_k u_{-k}} \rangle$ be positive. But

$$a^{-1} > 0 \quad \Longleftrightarrow \quad 3\Omega - 4\pi \lambda_B\, C\, N_p\, G^0(k) > 0. \tag{4.14}$$

Since $G^0(k) = 2{R_g}^2 = Nl^2/3$, the above inequality specifies an upper limit for the average concentration of monomers, $\rho_0 = NN_p/\Omega$, at a temperature given by the Bjerrum length λ_B:

$$\rho_0 < \frac{9}{4\pi(\lambda_B\, C\, l^2)} = \rho_*. \tag{4.15}$$

We may regard ρ_* as a *critical concentration* above which the melt has a different phase which is not described by our model. Alternatively, given the average concentration of monomers, ρ_0, we can specify a critical temperature given by

$$\lambda_{B*} = \frac{9}{4\pi(\rho_0\, C\, l^2)}, \tag{4.16}$$

below which the phase of the melt described by our model breaks down. (Remember that λ_B is inversely proportional to the temperature of the melt. See Appendix A.)

As for the eigenvalue $(a+b)^{-1}$, all its constituent quantities are positive except for $\Delta S^0(k)$, which is negative when $k^2{R_g}^2 > 4N$ (see equation (4.7)), and which appears in both the numerator and denominator. Therefore, even at temperatures greater than that given by λ_{B*}, our model breaks down for length-scales given by $k^2{R_g}^2$ between the numbers

$$2\left(\frac{\Omega + 2Nv}{v}\right) \quad \text{and} \quad \frac{V + \sqrt{V^2 + 32\,\pi\lambda_B\, C\, l^2\, N^2\, \rho_0\, v^2}}{(8/3)\pi\lambda_B\, C\, l^2\, \rho_0\, v^2}. \tag{4.17}$$

where

$$V = \frac{1}{3}\big[\Omega\big(9 + 8\pi\lambda_B\, C\, l^2\, \rho_0\big) + 16\pi\lambda_B\, C\, l^2\, N\, \rho_0\, v\big], \tag{4.18}$$

which is well beyond the range of k for which we are interested.

The trace of the matrix $\langle \mathbf{u_k}\, \mathbf{u_{-k}} \rangle$ is the Fourier transform of the dipole-dipole correlation function [17]:

$$\mathscr{F}[\langle \mathbf{u}(\mathbf{r}_1) \cdot \mathbf{u}(\mathbf{r}_2) \rangle] = \int \mathrm{d}r_1 \int \mathrm{d}r_2\, e^{-i\mathbf{k}\cdot(\mathbf{r}_1 - \mathbf{r}_2)} \langle \mathbf{u}(\mathbf{r}_1) \cdot \mathbf{u}(\mathbf{r}_2) \rangle \;=\; \langle \mathbf{u_k} \cdot \mathbf{u_{-k}} \rangle. \tag{4.19}$$

Therefore the magnetic structure function, or dipole-dipole structure function, is

$$g_m(k) \equiv \langle \mathbf{u_k} \cdot \mathbf{u_{-k}} \rangle = \mathrm{Tr}\, \langle \mathbf{u_k}\, \mathbf{u_{-k}} \rangle \;=\; \frac{1}{\Omega^2} \left(\frac{1}{a+b} + \frac{2}{a} \right). \tag{4.20}$$

Graphs of the dipole-dipole structure function $g_m(k)$ versus the scattering wave vector k for various temperatures are shown in Figure 4.3 on page 60. The graphs show that as temperature is decreased from infinity (that is, as the Bjerrum length is increased from zero) correlations in general diverge at all values of k in the range of interest. We again attribute this to the long-range character of the dipole interaction potential. Also curious is the shape of $g_m(k)$ for small values of k, as seen in Figure 4.4 on page 61: the function shows a dip for small values of k.

Care should be taken when interpreting the magnetization structure function: this is because the dipole-dipole correlation function inherently contains undesirable self-correlation terms that are not easy to remove:

$$\begin{aligned} \langle \mathbf{u}(\mathbf{r}_1) \cdot \mathbf{u}(\mathbf{r}_2) \rangle &= \sum_{\substack{\alpha,\, n \\ \beta,\, m}} \left\langle \delta^{(3)}(\mathbf{r}_1 - \mathbf{r}_n^{\alpha}) \delta^{(3)}\big(\mathbf{r}_2 - \mathbf{r}_m^{\beta}\big) \mathbf{b}_n^{\alpha} \cdot \mathbf{b}_m^{\beta} \right\rangle \\ &= \sum_{\alpha,\, n} \left\langle \left[\delta^{(3)}(\mathbf{r}_1 - \mathbf{r}_n^{\alpha})\right]^2 \mathbf{b}_n^{\alpha} \cdot \mathbf{b}_n^{\alpha} \right\rangle \\ &\quad + \sum_{\substack{\alpha \neq \beta \\ n \neq m}} \left\langle \delta^{(3)}(\mathbf{r}_1 - \mathbf{r}_n^{\alpha}) \delta^{(3)}\big(\mathbf{r}_2 - \mathbf{r}_m^{\beta}\big) \mathbf{b}_n^{\alpha} \cdot \mathbf{b}_m^{\beta} \right\rangle. \end{aligned} \tag{4.21}$$

The first term in the equation above is the self-correlation term.

Experimentally, the (apparent) correlation length for magnetization fluctuations, ξ_m, can be determined from the behaviour of $g(k)$ in the small k region:

$$\frac{g_m(0)}{g_m(k)} = 1 + k^2 {\xi_m}^2 \quad \text{for} \quad k \to 0. \tag{4.22}$$

After a bit of algebraic manipulation we discover that

$$\left(\frac{\xi_m}{R_g} \right)^2 \sim \frac{3}{2} \left(\frac{f}{1+f} \right) \left(\frac{9 - 4W_\beta}{81 + 108W_\beta + 32{W_\beta}^2} \right) \tag{4.23}$$

for large N, where

$$\begin{aligned} f &= \frac{N^2}{\Omega/v}, \\ W_\beta &= \rho_0 \left(\pi\, l^2\, \lambda_B\, C \right). \end{aligned} \tag{4.24}$$

A graph of ξ_m versus N^2 for increasing values of β is shown in Figure 4.5 on page 63. As $\lambda_B \to \lambda_{B*}$ from below, we see that ξ_m decreases to zero. Also, when the temperature is very high ($\lambda_B \to 0$), that is, when the thermal agitations overwhelm the dipolar interactions rendering them negligible, the apparent correlation length is dependent on the excluded volume (through f) as follows:

$$\left(\frac{\xi_m}{R_g}\right)^2 \sim \frac{1}{6}\left(\frac{f}{1+f}\right). \tag{4.25}$$

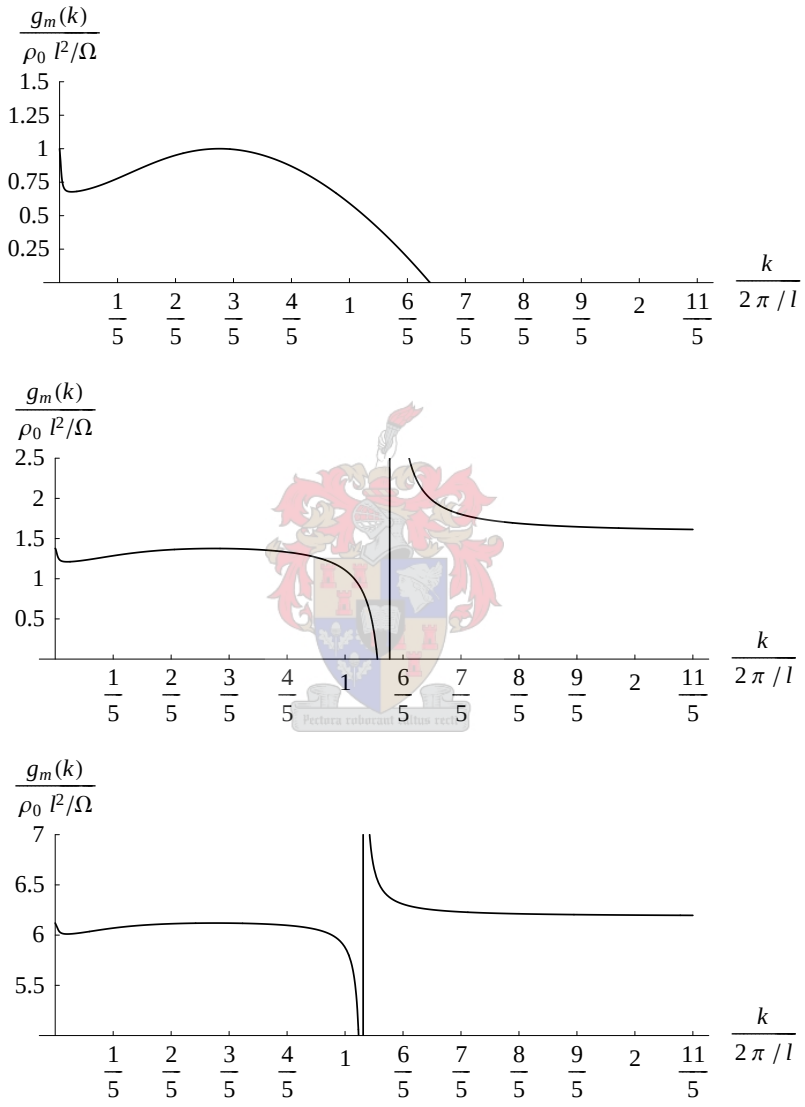

Fig. 4.3: Graphs of the dipole-dipole structure function $g_m(k)$ versus the scattering wave vector k for a melt of polymers with number of monomers per chain $N = 10^4$. The curves are for values of $W_\beta = \rho_0 \left(\pi\, l^2\, \lambda_B\, C\right) = 0,\ 1,\ 2$ respectively, from top to bottom. The excluded volume parameter is $v = \Omega/10^4$ where Ω is the volume of the melt.

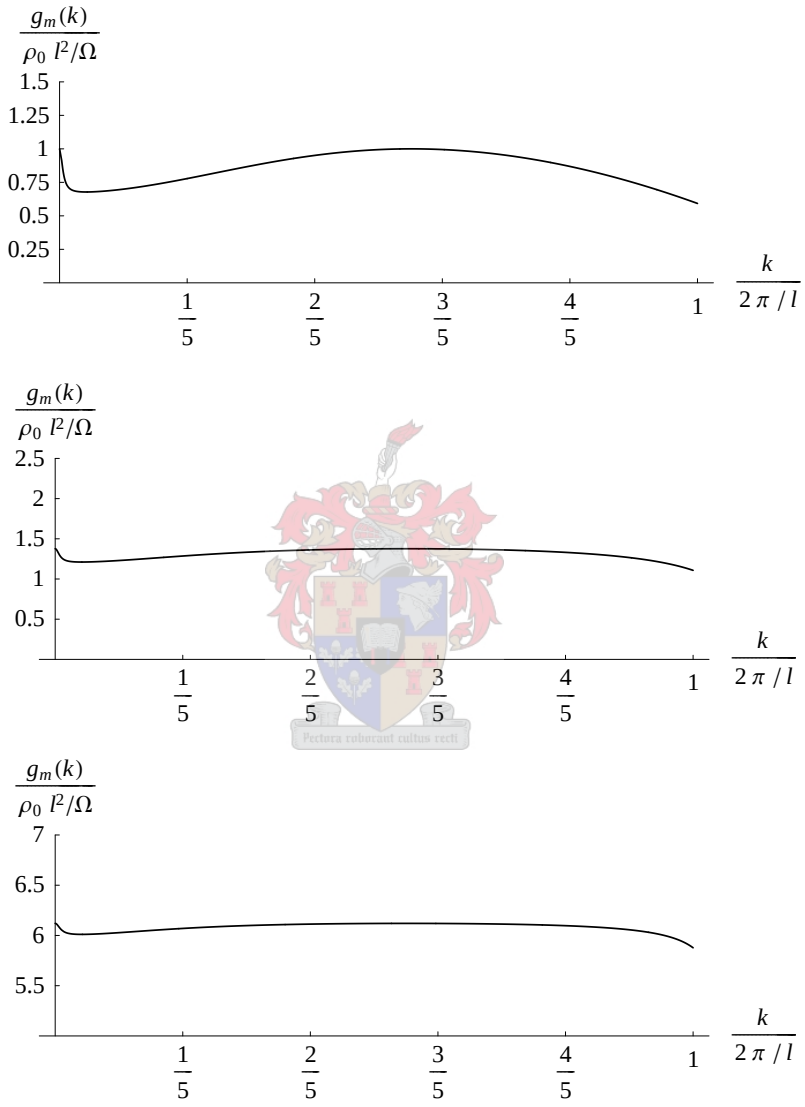

Fig. 4.4: Graphs of the dipole-dipole structure function $g_m(k)$ versus the scattering wave vector k near $k = 0$ for a melt of polymers with number of monomers per chain $N = 10^4$. The curves are for values of $W_\beta = \rho_0 \left(\pi\, l^2\, \lambda_B\, C\right) = 0,\ 1,\ 2$ respectively, from top to bottom. It is the curvature of the bulge near $k = 0$ that gives a sense of the magnetization correlation length. The excluded volume parameter is $v = \Omega/10^4$ where Ω is the volume of the melt.

4.3 Density fluctuations

We can also obtain the density structure function of our system by performing the integral in equation (3.50):

$$\mathscr{Z}_c \propto \int \mathscr{D}\rho \, e^{-\beta H(\{\rho_{\mathbf{k}}\})}, \tag{4.26}$$

where the Hamiltonian $H(\{\rho_{\mathbf{k}}\})$ is given by

$$\beta H(\{\rho_{\mathbf{k}}\}) = \Omega^2 \sum_{\mathbf{k}>0} \rho_{\mathbf{k}} \, \rho_{\text{-}\mathbf{k}} \left\{ \frac{v}{\Omega} + \frac{1}{N_p} \frac{3\Omega + 8\pi\lambda_B \, C \, N_p \, G^0(k)}{3\Omega \, g^0(k) + 8\pi\lambda_B \, C \, N_p \, \Delta S^0(k)} \right\}. \tag{4.27}$$

Therefore,

$$\begin{aligned} g_d(k) = \langle \rho_{\mathbf{k}} \, \rho_{\text{-}\mathbf{k}} \rangle &= \frac{1}{\Omega^2} \left\{ \frac{v}{\Omega} + \frac{1}{N_p} \frac{3\Omega + 8\pi\lambda_B \, C \, N_p \, G^0(k)}{3\Omega \, g^0(k) + 8\pi\lambda_B \, C \, N_p \, \Delta S^0(k)} \right\}^{\text{-}1} \\ &= \frac{1}{\Omega} \frac{N_p \, Q(k)}{\big(v \, N_p \, Q(k) + \Omega \, P(k)\big)} \end{aligned} \tag{4.28}$$

where

$$\begin{aligned} P(k) &= 3\Omega + 8\pi\lambda_B \, C \, N_p \, G^0(k) \\ \text{and} \quad Q(k) &= 3\Omega \, g^0(k) + 8\pi\lambda_B \, C \, N_p \, \Delta S^0(k). \end{aligned} \tag{4.29}$$

At very high temperatures, that is, when $\lambda_B \to 0$, then

$$g_d(k) = \frac{N_p}{\Omega} \frac{g^0(k)}{\big(v \, N_p \, g^0(k) + \Omega\big)}. \tag{4.30}$$

This result agrees with Edwards' result [10, 4] for polymer chains with only excluded-volume interactions.

We also note that, unlike the dipole structure function $g_m(k)$, $g_d(k)$ remains positive at all temperatures and for the greater part of the domain of interest of k because all the quantities making up $g_d(k)$ are positive except for $\Delta S^0(k)$ (appearing in both the numerator and the denominator of $g_d(k)$) which is negative when $k^2 {R_g}^2 > 4N$.

Graphs of the density-density structure function $g_d(k)$ versus the scattering wave vector k for various temperatures are shown in Figure 4.6 on page 64. The graphs show that as the temperature is decreased from infinity correlations in the positions of the monomers remain fairly the same decreasing only slightly on the lower length scales. Also as we expect, the structure function becomes negative (which is unphysical) at very low scales, signifying the breakdown of isotropy due to the anisotropic nature of the dipolar potential which should be more dominant at small scale separation of dipoles and govern the relative placement of neighbouring monomers.

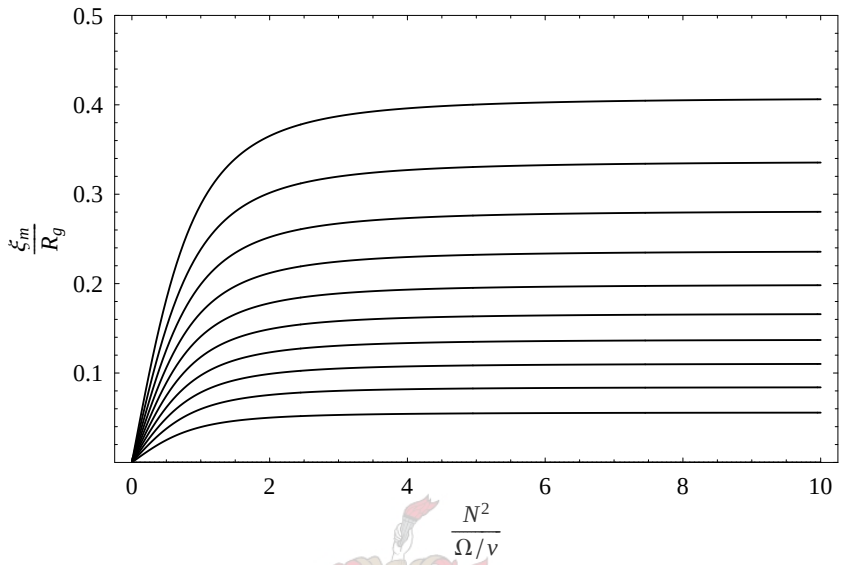

Fig. 4.5: Graph of the (apparent) magnetization correlation length ξ_m versus the square number of monomers per polymer N^2. The curves are for values of $W_\beta = \rho_0 \left(\pi\, l^2\, \lambda_B\, C\right)$ increasing in steps of 9/40 from 0 to 9/4 respectively, from top to bottom. Notice that the $W_\beta = 9/4$ curve is $\xi_m = 0$.

Experimentally, the correlation length ξ_d for density fluctuations can be calculated in a manner analogous to equation (4.22):

$$\frac{g_d(0)}{g_d(k)} = 1 + k^2 {\xi_d}^2 \quad \text{for} \quad k \to 0. \tag{4.31}$$

We obtain

$$\left(\frac{\xi_d}{l^2}\right)^2 \sim \left(\frac{N}{18(1 + N\, v\, \rho_0)}\right)\left(\frac{9 + 40W_\beta}{9 + 8W_\beta}\right) \tag{4.32}$$

for large N. Thus at high temperatures (that is, for $W_\beta \to 0$) and for $Nv\rho_0 \gg 1$ we recover the well known RPA result for polymers with excluded volume interaction:

$$\left(\frac{\xi_d}{l^2}\right)^2 \sim \frac{1}{18v\, \rho_0}. \tag{4.33}$$

Thus, unlike the magnetization correlation length, the density correlation length at high temperatures (λ_B very small), is of the order of the bond-length and remains fairly constant as the temperature is decreased (as illustrated in Figure 4.7). (In fact, as $W_\beta \to \infty$, ξ_d increases by a factor of only $\sqrt{5}$.) These results indicate that as far the monomer concentration of the melt is concerned, the melt remains homogeneous and isotropic at all temperatures and at all observation length-scales except at length-scales comparable to the Kuhn-length, l, of a polymer chain.

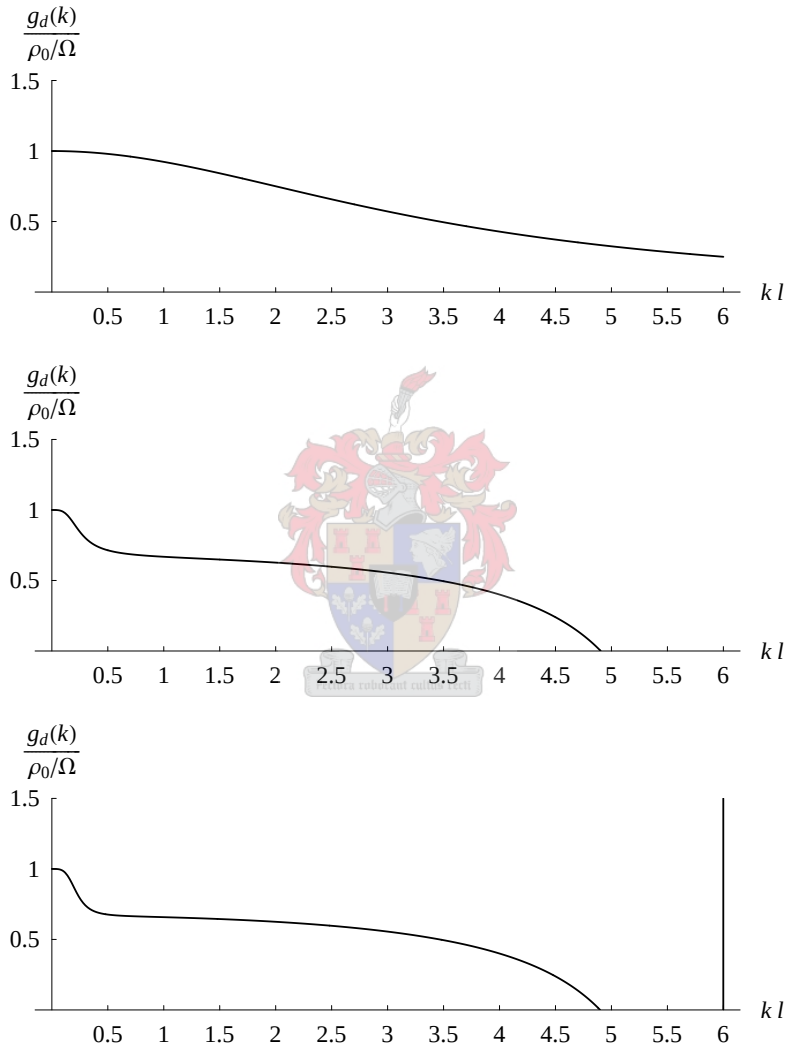

Fig. 4.6: Graphs of the density-density structure function $g_d(k)$ versus the scattering wave vector k for a melt of polymers with number of monomers per chain $N = 10^4$ and with excluded volume $v = 1/\rho_0$. The curves are for values of $W_\beta = \rho_0 \left(\pi\, l^2\, \lambda_B\, C\right) = 0,\ 10^3,\ 10^6$ respectively, from top to bottom.

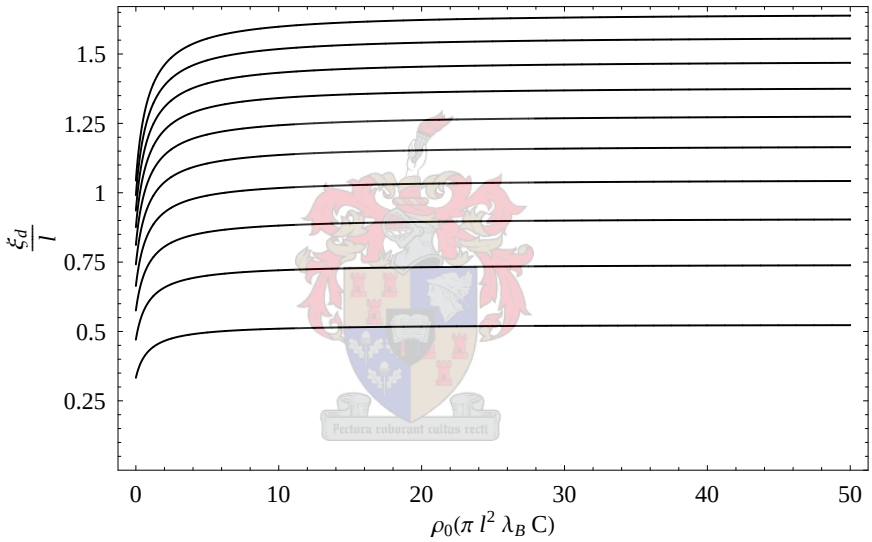

Fig. 4.7: Graph of the (apparent) density correlation length ξ_d versus inverse temperature for a melt of polymers with number of monomers per chain $N = 10^4$. The curves are for values of $\rho_0\, v = 1/20,\ 1/18,\ 1/16, 1, \ldots, 1/2$ respectively, from top to bottom.

5. EFFECT OF DEBYE-HÜCKEL SCREENING

The long range character (the r^{-3} falloff) of the dipolar potential implies that each dipole 'feels' the field of all other dipoles, not only of those nearby but even of those far away. Zhang and Widom [27, 28] have shown that the mean field experienced by any particular dipole in a system with a uniform distribution of dipoles depends on the shape of the outer boundary of the system under investigation. Thus with proper treatment of the boundary effects this problem might be resolved. However, to avoid any such complications let us introduce the phenomenon of screening which removes the long-range character of the dipole-dipole potential so that by varying a parameter known as the *screening length*, we might limit the influence of a dipole to only a finite region around the dipole.

Fortunately, screening is applicable in the case of polyampholytes [7] dissolved in solutions that have mobile ions, because it is these ions that are responsible for the screening.

5.1 Screened Dipolar Interaction

The Debye-Hückel theory [17] is often applied to electrolytes in which there are various mobile ions in solution. It is essentially a mean-field theory in which fixed numbers of mobile charged ions of each type are assumed to be in thermodynamic equilibrium at constant temperature. The main result of the theory which we shall use in this work is that the potential due to a point charge in the electrolyte is attenuated by means of a phenomenon known as *screening*: the mobile charges in the electrolyte collect around the point charge to reduce the total charge in the vicinity of the point charge. Thus the potential due to a point charge, Q, in an electrolyte is given by

$$V_{\mathrm{scr}}(r) = \frac{Q}{4\pi\varepsilon\varepsilon_0\, r} e^{-\kappa\, r} \tag{5.1}$$

where r is the distance from the charge, and $\kappa = \ell_D^{-1}$ is the inverse of the *screening length* (or the *Debye length*), ℓ_D, which depends on the concentration of ions and may thus be varied. As a consequence of Coulombic screening, the dipolar interaction is accordingly affected. The screened dipolar interaction follows straight forwardly from the second order multipole expansion of the

screened Coulomb interaction (see Appendix C) and is given by [7]

$$U_{\rm scr}(\mathbf{p}_1,\,\mathbf{p}_2,\,\mathbf{r}) = \mathbf{p}_1 \cdot \frac{\lambda_B\, e^{-\kappa\, r}}{\beta} \left\{ \frac{\mathbb{1} - 3\,\hat{\mathbf{r}}\,\hat{\mathbf{r}}}{r^3} \left[1 + \kappa\, r + \frac{1}{3}\kappa^2 r^2 \right] - \frac{\kappa^2 \mathbb{1}}{3r} \right\} \cdot \mathbf{p}_2 \quad (5.2)$$

Thus the screened exchange interaction analogous to the unscreened exchange interaction defined in equation (2.24) between two dipolar monomers is

$$\mathbf{M}_{\rm scr}(\mathbf{r}) = \frac{\lambda_B C e^{-\kappa\, r}}{2\beta} \left\{ \frac{\mathbb{1} - 3\,\hat{\mathbf{r}}\,\hat{\mathbf{r}}}{r^3} \left[1 + \kappa\, r + \frac{1}{3}\kappa^2 r^2 \right] - \frac{\kappa^2 \mathbb{1}}{3r} \right\}, \quad (5.3)$$

and its Fourier transform, which may be computed in much the same way as we did for the unscreened exchange interaction in Section 2.8, turns out to be

$$\mathbf{M}_{\mathbf{k}} = \frac{\pi \lambda_B C}{6\,\beta\,\Omega} \left(\frac{1 - 2\,(k/\kappa)^2}{1 + (k/\kappa)^2} \right) \left(\mathbb{1} - 3\,\hat{\mathbf{k}}\,\hat{\mathbf{k}} \right). \quad (5.4)$$

Comparison of this equation with the Fourier transform of the unscreened dipolar interaction in equation (2.88) shows that the corresponding results for the magnetic structure factor and the density structure factor may be obtained from the unscreened structure factors by effecting the replacement:

$$C \rightarrow \frac{\text{-}C}{2} \left(\frac{1 - 2\,(k/\kappa)^2}{1 + (k/\kappa)^2} \right) \quad (5.5)$$

in equations (4.20) and (4.28). Note from the above expression that as the screening length $\ell_D = \kappa^{\text{-}1}$ approaches infinity we get back to the case of the unscreened Coulomb potential as we would expect.

An interesting case occurs when the screening length $\ell_D = \kappa^{\text{-}1}$ approaches zero, that is, when the screened dipolar interactions are infinitesimally short-ranged. Then the replacement mentioned above should instead be

$$C \rightarrow \frac{\text{-}C}{2}. \quad (5.6)$$

The presence of the minus sign in this replacement gives rise to a structure function that is significantly different from that encountered in the case of the unscreened dipolar interaction potential.

5.2 Screening without Excluded Volume Interactions

After applying the replacement in equation (5.5) to the structure function for our previous model which had no excluded volume interaction (see equation (2.94)) we obtain

$$\langle \mathbf{u}_{\mathbf{k}}\, \mathbf{u}_{\text{-}\mathbf{k}} \rangle = \begin{pmatrix} (a+b)^{\text{-}1} & 0 & 0 \\ 0 & a^{\text{-}1} & 0 \\ 0 & 0 & a^{\text{-}1} \end{pmatrix} \quad (5.7)$$

where, using equations (2.93),

$$\begin{aligned}(a+b)^{-1} &= \frac{3NN_pl^2\left(1+(k/\kappa)^2\right)}{\Omega\Big(9\Omega\Big(1+(k/\kappa)^2\Big)-4\pi\lambda_BCNN_pl^2\Big(1-2\,(k/\kappa)^2\Big)\Big)}\\ a^{-1} &= \frac{3NN_pl^2\left(1+(k/\kappa)^2\right)}{\Omega\Big(9\Omega\Big(1+(k/\kappa)^2\Big)+2\pi\lambda_BCNN_pl^2\Big(1-2\,(k/\kappa)^2\Big)\Big)}.\end{aligned} \tag{5.8}$$

The positive definite property of $\langle \mathbf{u_{-k}u_k}\rangle$ requires that each of the eigenvalues of $\langle \mathbf{u_k u_{-k}}\rangle$ be positive for all k. Once again we obtain the condition:

$$9\Omega - 4\pi\lambda_B\, C\, N_pNl^2 > 0. \tag{5.9}$$

Thus the critical temperature is no different from that which was obtained in the unscreened case.

However the magnetic structure function is no longer a constant function of k but has a minimum at

$$k = \sqrt{\frac{1}{2}}\kappa. \tag{5.10}$$

Graphs of the magnetic structure function are shown in Figure 5.1.

5.3 Screening and Excluded Volume Interaction

This replacement yields a magnetic structure function matrix $\langle \mathbf{u_k}\,\mathbf{u_{-k}}\rangle$ (in the same orthonormal basis, $\left\{\hat{\mathbf{k}},\,\hat{\mathbf{k}}_\perp^{(1)},\,\hat{\mathbf{k}}_\perp^{(2)}\right\}$, first introduced in Section 2.8):

$$\langle \mathbf{u_k}\,\mathbf{u_{-k}}\rangle = \frac{1}{\Omega^2}\begin{pmatrix}(a+b)^{-1} & 0 & 0\\ 0 & a^{-1} & 0\\ 0 & 0 & a^{-1}\end{pmatrix} \tag{5.11}$$

where,

$$\begin{aligned}(a+b)^{-1} &= \frac{3\Omega\,N_p\big(G^0(k)+(v/\Omega)\,\Delta S^0(k)\big)}{3\Omega+3v\,g^0(k)-4\pi\,\lambda_B\,C\,N_p\big(G^0(k)+(v/\Omega)\,\Delta S^0(k)\big)}\\ a^{-1} &= \frac{3\Omega\,N_p\,G^0(k)}{3\Omega+2\pi\lambda_B\,C\,N_p\,G^0(k)}.\end{aligned} \tag{5.12}$$

As before, the positive definite property of the magnetic structure function matrix requires that each of the eigenvalues of $\langle \mathbf{u_k u_{-k}}\rangle$ be positive. But since the eigenvalue a^{-1} is always positive this property is satisfied for those solution parameters that make the eigenvalue $(a+b)^{-1}$ positive for all values of k. In spite of this, the temperature at which our model breaks down turns out to be the same as obtained for the unscreened dipoles:

$$\lambda_{B*} = \frac{9}{4\pi(\rho_0\,C\,l^2)}. \tag{5.13}$$

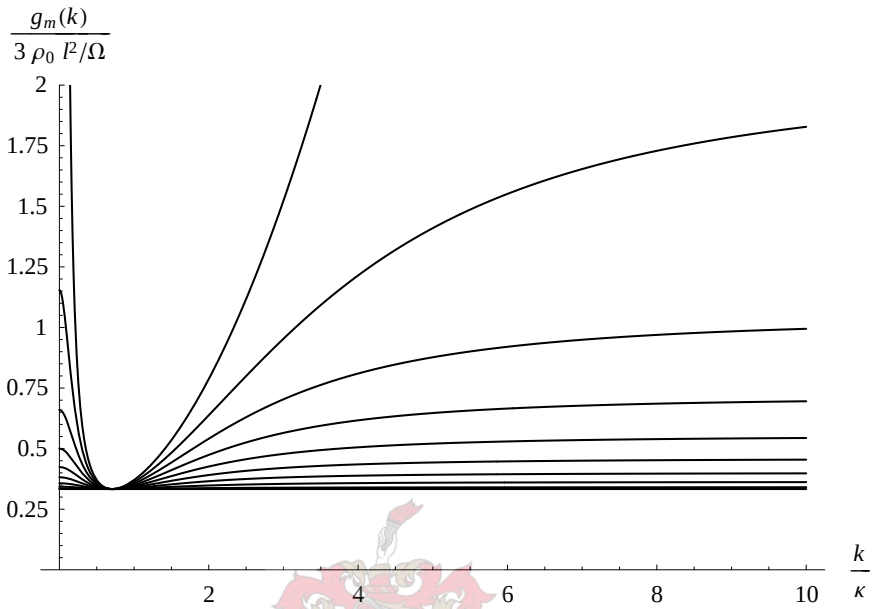

Fig. 5.1: Graph of the magnetization structure function $g_m(k)$ versus the ratio of scattering wave vector k to the inverse screening length κ^{-1} for a melt of polymers with number of monomers per chain $N = 10^4$. The curves are for values of $W_\beta = \rho_0 \left(\pi\, l^2\, \lambda_B\, C\right) = 0, \frac{1}{4}, \frac{1}{2}, \ldots, \frac{9}{4}$ respectively, from top to bottom. It is the curvature of the bulge near $k = 0$ that gives a sense of the magnetization correlation length.

Thus for infinitesimally short-ranged screened interactions the 'critical temperature' of our system is the same as that for unscreened dipoles.

5.4 Dipole-dipole Structure Function for non-zero Screening Length

Graphs for the dipole-dipole structure factor at different temperatures and screening lengths are shown in Figures 5.2, 5.3 and 5.4. Various observations of these graphs can be made. First of all, comparing these graphs with those for the unscreened dipolar interaction in Figure 4.3 on page 60 we notice that as the temperature decreases from infinity towards the 'critical temperature' the correlations remain finite everywhere except for a particular value of k which is of the order of a few Kuhn lengths.

Secondly, if the screening length is held constant and as the temperature of the random phase is lowered from infinity ($\lambda_B = 0$) the correlation in the magnetization fluctuations increases at large length-scales ($k \approx 0$) comparable to the radius of gyration of an ideal polymer. These small-k correlations continue to peak with decreasing temperature until the 'critical temperature' computed

above is reached where our RPA model breaks down. We note furthermore that for nonzero κ these small-k correlations are independent of the screening length $\ell_D = \kappa^{-1}$.

Thirdly, when the screening length ℓ_D is large, correlations of the magnetization fluctuations in the polymer melt are highest at a length-scale in the vicinity of $v^{1/3}$ where v is the excluded volume of the monomer. However, as the screening length is decreased to zero, a peak begins to arise in the vicinity of a length scale comaparable to the Kuhn length of a polymer chain, as observed in Figure 5.4. We also note that as the screening length increases from zero to infinity the width of this peak is broadened and its height is lowered until correlations at all length scales are nearly the same.

We also observe that if the screening length is held constant and the temperature is decreased from infinity to the 'critical temperature' at which our RPA model breaks down, then the height and width of this peak both increase, correlations increasing everywhere except at a length scale intermediate between the radius of gyration of the ideal polymer and the Kuhn length.

5.5 Structure Functions in the limit of zero Screening Length

The graphs of the dipole-dipole structure function and the density structure function in the limit of zero screening length are shown in Figures 5.5, 5.6, and 5.7. Close to the critical temperature the magnetic structure function exhibits a broad peak in the neighbourhood of a few Kuhn lengths and a very narrow peak at small k. On the other hand, the density structure factor shows a dip in the neighbourhood of a few Kuhn lengths otherwise it remains fairly constant over the entire range length scales of interest.

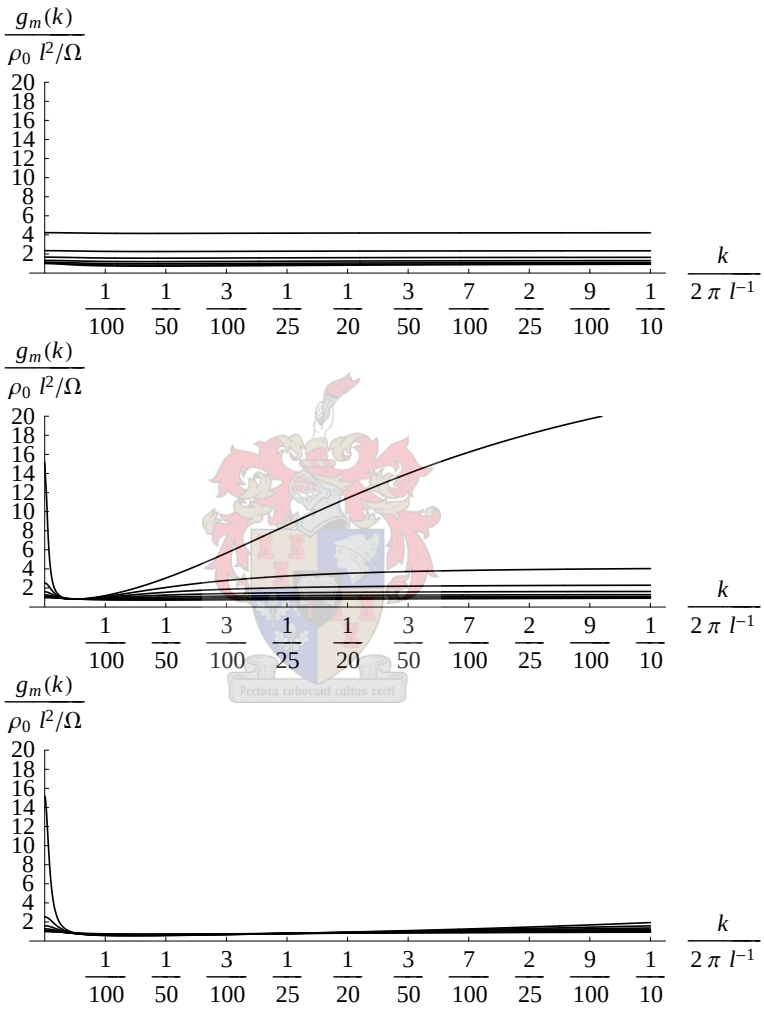

Fig. 5.2: Graphs of the magnetization structure function $g_m(k)$ versus small scattering wave vector k for different temperatures and screening lengths $\ell_D = \kappa^{-1}$ for a melt of polymers with number of monomers per chain $N = 10^4$. In each graph, the different curves are for decreasing values (increasing temperature) of $W_\beta = \rho_0 \left(\pi\, l^2\, \lambda_B\, C\right) = 0,\ \frac{1}{4},\ \frac{1}{2},\ \ldots,\ \frac{9}{4}$ respectively, from bottom to top. Each set of curves is for different values of $\kappa = 0,\ (0.05l)^{-1}\,,\ (0.5l)^{-1}$

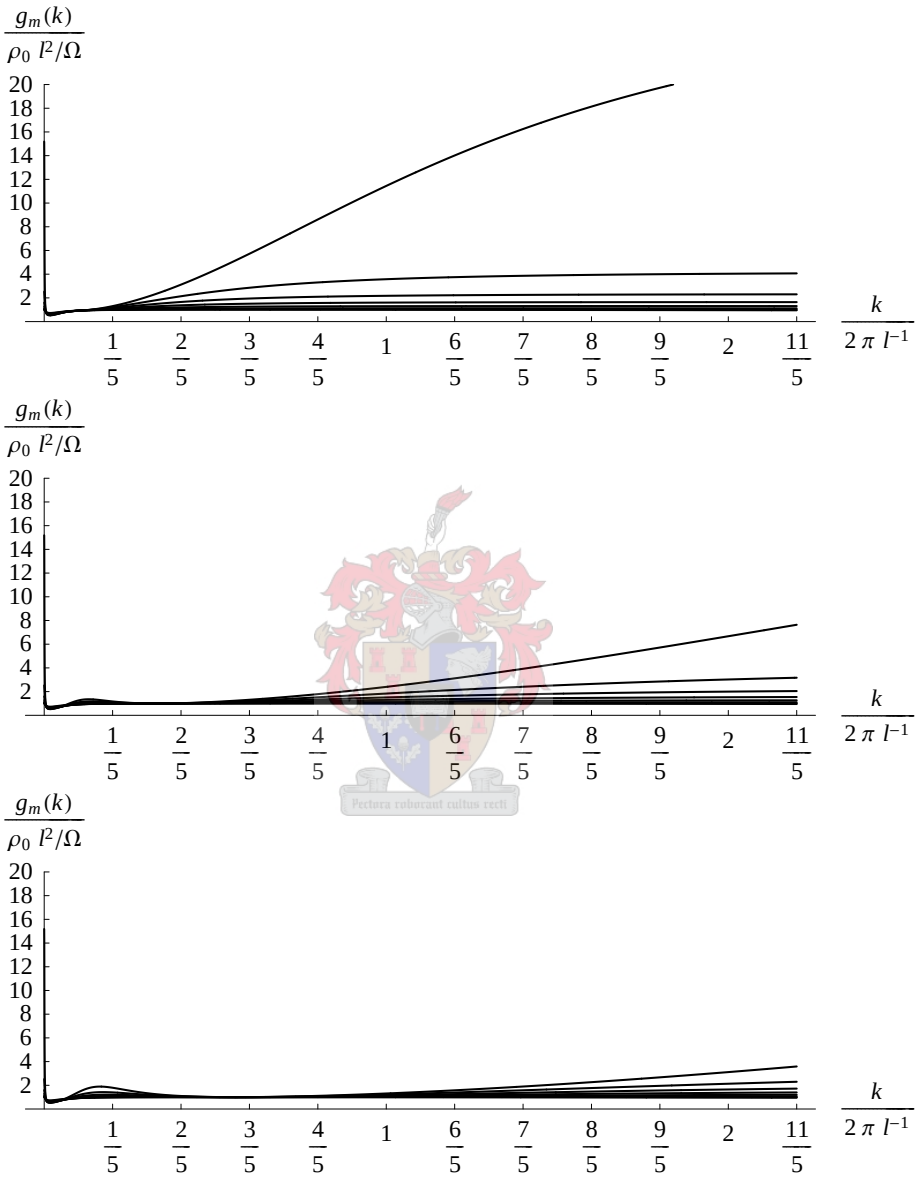

Fig. 5.3: Graphs of the magnetization structure function $g_m(k)$ versus the scattering wave vector k for different temperatures and screening lengths $\ell_D = \kappa^{-1}$ for a melt of polymers with number of monomers per chain $N = 10^4$. In each graph, the different curves are for decreasing values (increasing temperature) of $W_\beta = \rho_0 \left(\pi\, l^2\, \lambda_B\, C\right) = 0, \frac{1}{4}, \frac{1}{2}, \ldots, \frac{9}{4}$ respectively, from bottom to top. Each set of curves is for different values of $\kappa = l^{-1}, (3l)^{-1}, (5l)^{-1}$

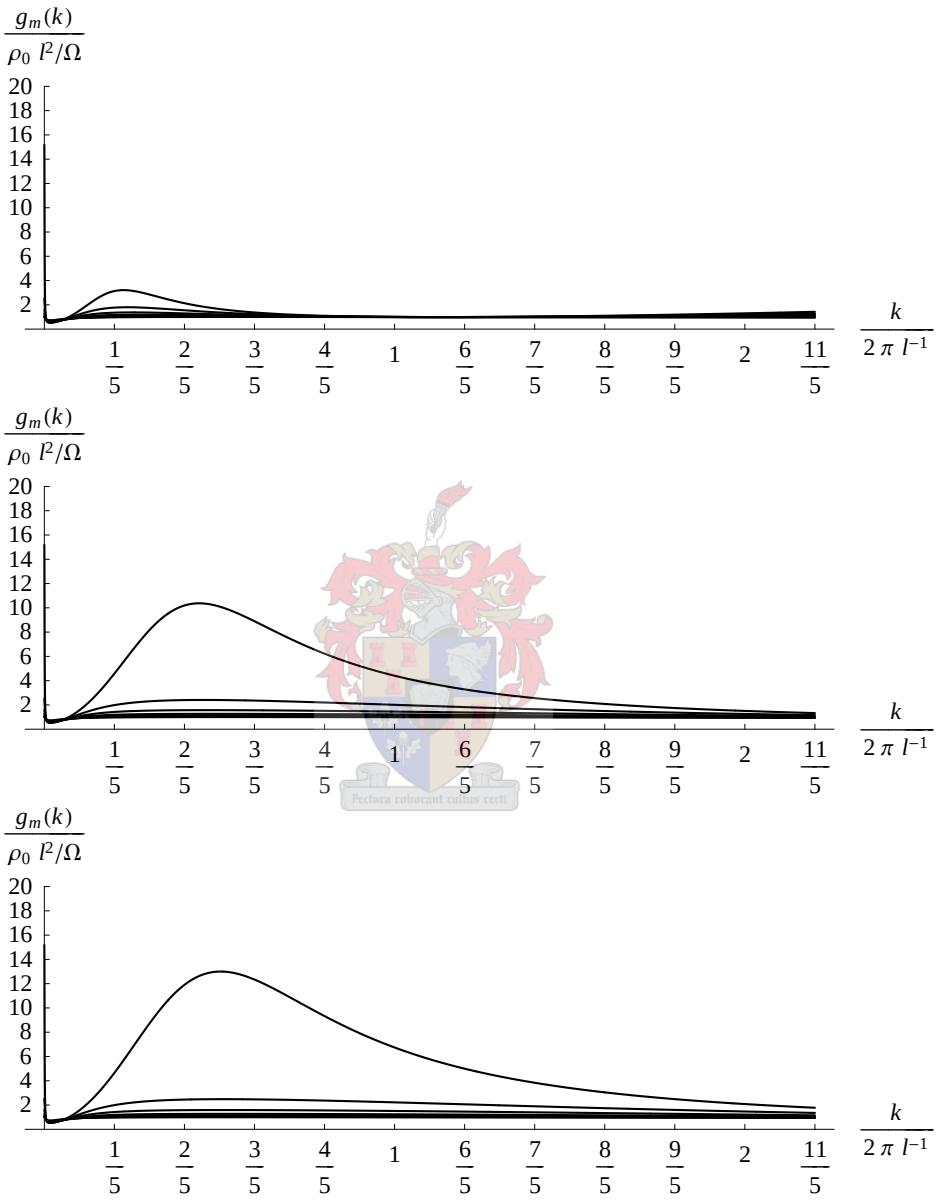

Fig. 5.4: Graphs of the magnetization structure function $g_m(k)$ versus the scattering wave vector k for different temperatures and screening lengths $\ell_D = \kappa^{-1}$ for a melt of polymers with number of monomers per chain $N = 10^4$. In each graph, the different curves are for increasing values (decreasing temperature) of $W_\beta = \rho_0 \left(\pi\, l^2\, \lambda_B\, C\right) = 0, \frac{1}{4}, \frac{1}{2}, \ldots, \frac{9}{4}$ respectively, from bottom to top. Each set of curves is for a different value of $\kappa = (10l)^{-1}, (50l)^{-1}, (90l)^{-1}$

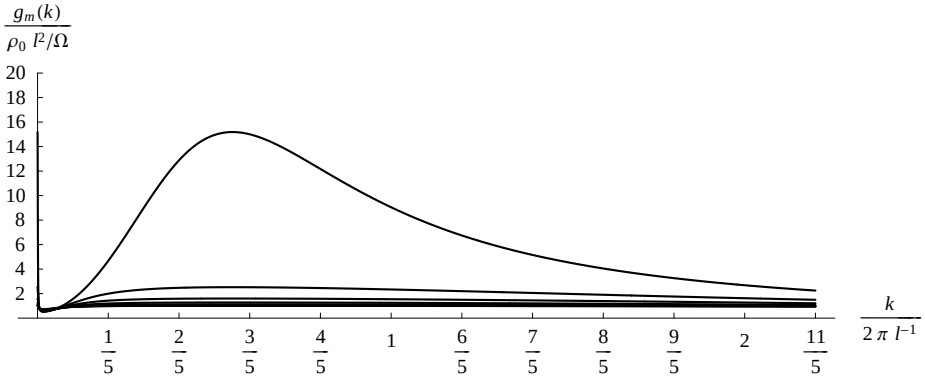

Fig. 5.5: The magnetization structure function $g_m(k)$ versus the scattering wave vector k for screening lengths $\ell_D = 0$ for a melt of polymers with number of monomers per chain $N = 10^4$. In this graph, the different curves are for increasing values (decreasing temperature) of $W_\beta = \rho_0 \left(\pi\, l^2\, \lambda_B\, C\right) = 0,\ \frac{1}{4},\ \frac{1}{2},\ \ldots,\ \frac{9}{4}$ respectively, from bottom to top.

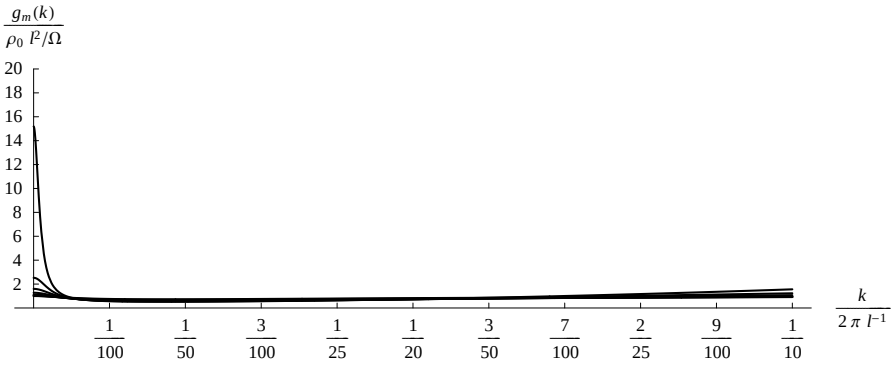

Fig. 5.6: The magnetization structure function $g_m(k)$ versus small scattering wave vector ($k \approx 0$) for screening lengths $\ell_D = 0$ for a melt of polymers with number of monomers per chain $N = 10^4$. In this graph, the different curves are for increasing values (decreasing temperature) of $W_\beta = \rho_0 \left(\pi\, l^2\, \lambda_B\, C\right) = 0,\ \frac{1}{4},\ \frac{1}{2},\ \ldots,\ \frac{9}{4}$ respectively, from bottom to top.

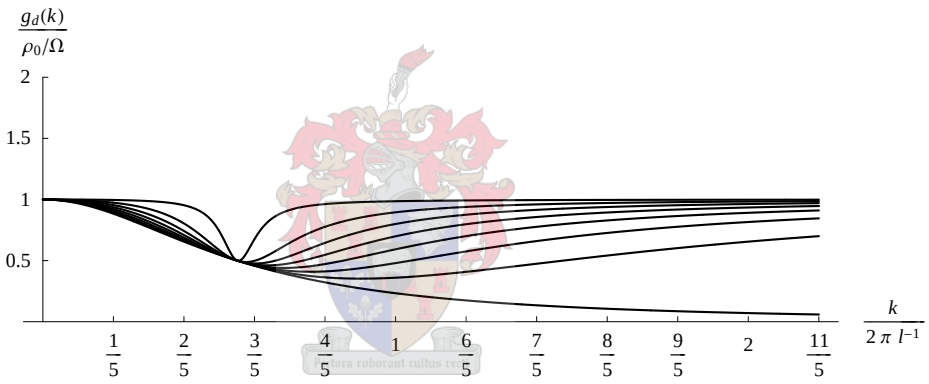

Fig. 5.7: The density structure function $g_d(k)$ versus the scattering wave vector k for screening lengths $\ell_D = 0$ for a melt of polymers with number of monomers per chain $N = 10^4$. In this graph, the different curves are for increasing values (decreasing temperature) of $W_\beta = \rho_0 \left(\pi\, l^2\, \lambda_B\, C\right) = 0, \frac{1}{4}, \frac{1}{2}, \ldots, \frac{9}{4}$ respectively, from bottom to top.

6. CONCLUSION

We presented an analysis of the unscreened and screened dipolar interactions between bond-directed dipolar monomers of a melt of flexible polymers without excluded volume interactions and also with excluded volume interactions. The formal context of our analysis is provided by the Random Phase Approximation (RPA) method that has already been successfully applied to different problems of polymer physics ([11, 12, 4]). In all these cases we investigated the structure of the melt via the density and magnetization structure functions. In the case of the unscreened dipolar interactions no structure is observed on any observable length scale within the melt, that is, no peak or divergence was observed in any of these structure functions at any length scale of interest. The type of screening investigated was that of Debye-Hückel screening which is applicable to polyampholytes in ionic solutions. Results show that structure begins to appear as the screening length is decreased from infinity to zero. Indeed in the case of screened dipolar interactions together with excluded volume interactions, a peak of finite width and height develops in the magnetization structure function over length scales which are of the order of a few Kuhn lengths. Another peak also appears at very large length scales (that is at small scattering angles) which indicates the presence of the formerly discovered fluctuation-induced orientational correlations [11]. On the other hand, the density structure function is fairly constant over all length scales but shows a significant dip within a band of length scales that is of the order of a few Kuhn lengths.

Of course this approach is inadequate to describe the full behaviour of the correlations in the fluctuations of magnetization and density, since the model breaks down at a particular temperature which we called the 'critical temperature'. This temperature is of a magnitude that is independent of whether steric interactions or screening is present or not. This 'critical temperature' may be checked by comparing it with the results of a variational mean field theory treatment of the problem [17], a task we postpone for later research. A more accurate mean-field theory than this will require computation of higher order terms in the perturbation expansion of the Hamiltonian. Such computations are considerably more arduous and are beyond the scope of the present work.

Moreover, the theory presented in this work is valid only at rather high concentration or at small excluded volume, that is near the Θ condition [10]. At both these limits there are additional difficulties. At very high concentrations the precise form of the excluded volume potential matters. Improvements can be made by considering the third and higher virial coefficients of a cluster expansion of the steric interaction. Furthermore, in order to determine the lower limit of

high concentration (that is, the threshold between concentrated and semidilute solutions or melts) below which the theory here presented will lose its validity, we could calculate the osmotic pressure of the melt as has been done in other polymer physics problems [10] and subsequently determine where the osmotic pressure becomes negative.

Eventually, the conclusions arrived at in this work would have to be tested against extensive simulations (such as Monte Carlo simulations) and experimental results. These are left to separate research.

In spite of all that has been mentioned above we expect that the present predictions show the main effects for systems below the critical point.

APPENDIX

A. LIST OF SYMBOLS

Symbol	**Description**
k_B	The Boltzmann constant
T	The absolute temperature
Ω	The volume of the melt
β	$\dfrac{1}{k_B T}$
ℓ_D	The Debye-Hückel screening length
κ	$\dfrac{1}{\ell_D}$
$\mathbf{k}$	The scattering wave-vector
$\mathbf{b}_n^\alpha$	The n-th bond on polymer chain α
$\mathbf{p}_n^\alpha$	The dipole-moment of the n-th bond on polymer chain α
c	A dimensionful constant defined so that $\mathbf{p}_n^\alpha = c\mathbf{b}_n^\alpha$
C	$\dfrac{c^2}{e_0^2}$
λ_B	$\dfrac{1}{k_B T}\dfrac{e^2}{4\pi\varepsilon_0\varepsilon_r}$ is the Bjerrum length.
$f_D(x)$	$\dfrac{2}{x}\left(e^{-x} - 1 + x\right)$ is the Debye function
R_g	$\dfrac{Nl^2}{6}$ is the radius of gyration of an ideal polymer
$\mathbf{G}^0(\mathbf{k})$	The bond-matrix structure function of an ideal polymer

B. INVERSE OF A SPECIAL FORM OF A MATRIX

Here we intend to find the inverse of any matrix of the form

$$a\,\mathbb{1} + b\,\hat{\mathbf{k}}\,\hat{\mathbf{k}}, \tag{B.1}$$

which was often encountered in this dissertation. Let

$$c\,\mathbb{1} + d\,\hat{\mathbf{k}}\,\hat{\mathbf{k}} = \left(a\,\mathbb{1} + b\,\hat{\mathbf{k}}\,\hat{\mathbf{k}}\right)^{-1}. \tag{B.2}$$

Then

$$\left(a\,\mathbb{1} + b\,\hat{\mathbf{k}}\,\hat{\mathbf{k}}\right)\left(c\,\mathbb{1} + d\,\hat{\mathbf{k}}\,\hat{\mathbf{k}}\right) = \mathbb{1}, \tag{B.3}$$

that is

$$a\,c\,\mathbb{1} + (a\,d + b\,c + b\,d)\hat{\mathbf{k}}\,\hat{\mathbf{k}} = \mathbb{1}, \tag{B.4}$$

Therefore

$$a\,c \;=\; 1 \quad \text{and} \quad a\,d + b\,c + b\,d \;=\; 0, \tag{B.5}$$

yielding $c = 1/a$ and $d = -b/a(a+b)$, that is,

$$\left(a\,\mathbb{1} + b\,\hat{\mathbf{k}}\,\hat{\mathbf{k}}\right)^{-1} = \frac{1}{a}\left(\mathbb{1} - \frac{b}{a+b}\hat{\mathbf{k}}\,\hat{\mathbf{k}}\right). \tag{B.6}$$

C. DEBYE-HÜCKEL SCREENED DIPOLAR INTERACTION

In this appendix we present calculations that lead from the Debye-Hückel screened Coulomb interaction to the expression obtained for the screened dipolar interaction in equation (5.2).

The screened Coulomb potential due to a given charge distribution, $\rho(\mathbf{r}')$, outside of that distribution is given by

$$\phi(\mathbf{r}) = \int \mathrm{d}^3 r \, \frac{\rho(\mathbf{r}') e^{-\kappa|\mathbf{r}-\mathbf{r}'|}}{|\mathbf{r}-\mathbf{r}'|}, \tag{C.1}$$

where, for convenience, we will choose the origin to lie within the charge distribution. If $\mathbf{r}$ is large compared to the characteristic dimensions of the charge distribution, we may expand Coulomb's potential as follows:

$$\frac{e^{-\kappa|\mathbf{r}-\mathbf{r}'|}}{|\mathbf{r}-\mathbf{r}'|} = \frac{e^{-\kappa r}}{r} - \mathbf{r}' \cdot \nabla \frac{e^{-\kappa r}}{r} + \ldots \tag{C.2}$$

so that the potential, in its leading behaviour for large distances, has the form

$$\phi(\mathbf{r}) = \frac{q e^{-\kappa r}}{r} - \mathbf{p} \cdot \nabla \frac{e^{-\kappa r}}{r} + \ldots \, . \tag{C.3}$$

Occurring here are the first two moments of the charge distribution:

$$q = \int \mathrm{d}^3 r \; \rho(\mathbf{r}'), \tag{C.4}$$

$$\mathbf{p} = \int \mathrm{d}^3 r \; \mathbf{r}' \rho(\mathbf{r}') \tag{C.5}$$

which are the total charge and the dipole moment vector respectively.

Let us now suppose that the charge distribution has only a dipole moment vector $\mathbf{p}_1$. Then the potential due to the charge distribution becomes

$$\phi(\mathbf{p}_1, \mathbf{r}) = -\mathbf{p}_1 \cdot \nabla \frac{e^{-\kappa r}}{r}. \tag{C.6}$$

Now let us place another dipole $\mathbf{p}_2$ at the point $\mathbf{r}$ lying outside the charge distribution, then the energy of interaction of the two dipoles is

$$\begin{aligned} E &= \mathbf{p}_2 \cdot [\nabla \phi(\mathbf{p}_1, \mathbf{r})] \\ &= \mathbf{p}_2 \cdot \left[-\nabla \mathbf{p}_1 \cdot \nabla \frac{e^{-\kappa r}}{r} \right] \; = \; -\mathbf{p}_1 \cdot \left[\nabla \, \nabla \frac{e^{-\kappa r}}{r} \right] \cdot \mathbf{p}_2. \end{aligned} \tag{C.7}$$

As the reader may verify for himself or herself the quantity in brackets is

$$-\left[\nabla\nabla\frac{e^{-\kappa r}}{r}\right]=\frac{\lambda_B\,e^{-\kappa\,r}}{\beta}\left\{\frac{\mathbb{1}-3\,\hat{\mathbf{r}}\,\hat{\mathbf{r}}}{r^3}\left[1+\kappa\,r+\frac{1}{3}\kappa^2r^2\right]-\frac{\kappa^2\mathbb{1}}{3r}\right\}. \tag{C.8}$$

Thus the energy of interaction of the two dipoles $\mathbf{p}_1$ and $\mathbf{p}_2$ is

$$U_{\rm scr}(\mathbf{p}_1,\,\mathbf{p}_2,\,\mathbf{r})=\mathbf{p}_1\cdot\frac{\lambda_B\,e^{-\kappa\,r}}{\beta}\left\{\frac{\mathbb{1}-3\,\hat{\mathbf{r}}\,\hat{\mathbf{r}}}{r^3}\left[1+\kappa\,r+\frac{1}{3}\kappa^2r^2\right]-\frac{\kappa^2\mathbb{1}}{3r}\right\}\cdot\mathbf{p}_2. \tag{C.9}$$

BIBLIOGRAPHY

[1] P. G. de Gennes. *Scaling Concepts in Polymer Physics*. Cornell University Press, Ithaca and London, 5 edition, 1996.

[2] R. D. Kamien. The geometry of soft materials: a primer. *Rev. Mod. Phys.*, 72:953, October 2002.

[3] A. M. Gupta and S. F. Edwards. Mean-field theory of phase transitions in liquid-crystalline polymers. *Journal of Chemical Physics*, 98:1588–1596, 1993.

[4] T. Shimada, M. Doi, and K. Okano. Concentration fluctuation of stiff polymers. I. Static structure factor. *Journal of Chemical Physics*, 88(4):2815–2821, 1988.

[5] P. L. Hansen, D. Svensek, V. A. Parsegian, and R. Podgornik. Buckling, fluctuations, and collapse in semiflexible polyelectrolytes. *Phys. Rev. E*, 60(2):1956, August 1999.

[6] P. L. Hansen and R. Podgornik. Wormlike chains in the large-d limit. *J. Chem. Phys.*, 114:8637, May 2001.

[7] R. Podgornik. Electrostatic contribution to the persistence length of a semiflexible dipolar chain. *Phys. Rev. E*, 70(031801):031801–1, September 2004.

[8] R. Podgornik, P. L. Hansen, and V. A. Parsegian. Elastic moduli renormalization in self interacting stretchable polyelectrolytes. *Journal of Chemical Physics*, 113(2):9343, August 2000.

[9] S. F. Edwards. The theory of polymer solutions at intermediate concentration. *Proceedings of the Physical Society, London*, 1966(2):265–280, June 1966.

[10] M. Doi and S. F. Edwards. *The Theory of Polymer Dynamics*. Oxford University Press Inc., New York, 1999.

[11] T. A. Vilgis, A. Weyersberg, and M. G. Brereton. Fluctuation-induced correlations in polymer blends and diblock copolymer melts. *Physical Review E*, 49(4):3031–3037, April 1994.

[12] T. A. Vilgis and M. G. Brereton. Statistical Mechanics of polymers with directed bond vectors: Collective behaviour of melts and mixtures. *Phys. Rev. A*, 45(10):7413, May 1992.

[13] E. Jarkova and T. A. Vilgis. Scattering from ferrogels. *Macromolecular Theory and Simulations*, 13:592–602, 2004.

[14] R. Holyst and T. A. Vilgis. Critical temperature and concentration versus molecular weight in polymer blends: Conformations, fluctuations, and the Ginzburg criterion. *Journal of Chemical Physics*, 99:4835–4844, 1993.

[15] S. F. Edwards. The statistical mechanics of polymers with excluded volume. *Proceedings of the Physical Society, London*, 88(4):613–624, April 1965.

[16] P. G. Gennes. Qualitative features of polymer demixtion. *J. Phys. Lett.*, 38:441, 1977.

[17] P. M. Chaikin and T. C. Lubensky. *Principles of condensed matter physics*. Cambridge University Press, Cambridge, 1995.

[18] K. Binder. Nucleation barriers, spinodals, and the ginzburg criterion. *Physical Review A*, 29:341, 1984.

[19] J. Schwinger, L. L. DeRaad Jr., K. A. Milton, and W. Tsai. *Classical Electrodynamics*. Perseus Books, Reading, Massachusetts, 1998.

[20] L. Leibler. Theory of microphase separation in block copolymers. *Macromolecules*, 13(6):1602–1617, November-December 1980.

[21] M. Muthukumar. Localized structures of polymers with long-range interactions. *Journal of Chemical Physics*, 104(2):691–700, January 1996.

[22] M. Zrnyi and F. Horkay. On the thermodynamics of mechanochemical energy conversion realised by neutral polymer gels. *Journal of Intelligent Material Systems and Structures*, 4(2):190–201, 1993.

[23] M. Zrnyi, L. Barsi, and A. Bki. Deformation of ferrogels induced by nonuniform magnetic fields. *Journal of Chemical Physics*, 104:8750–8756, 1996.

[24] M. Zrnyi, L. Barsi, and A. Bki. Ferrogel: a new magnetocontrolled elastic medium. *Polymer Gels and Networks*, 5:415–427, 1997.

[25] D. Lacoste and T. C. Lubensky. Phase Transitions in a ferrofluid at magnetic-field-induced microphase separation. *Physical Review E*, 64:041506, 2001.

[26] M. Rubinstein and R. H. Colby. *Polymer Physics*. Oxford University Press Inc., New York, 2003.

[27] H. Zhang and M. Widom. Global phase diagrams for dipolar fluids. *Physical Review E*, 49:R3591, 1994.

[28] H. Zhang and M. Widom. Spontaneous magnetic order in random dipolar solids. *Physical Review B*, 51:8951–8957, 1995.